



# Kent Academic Repository

Froebrich, D., Schmeja, S., Samuel, D. and Lucas, P.W. (2010) *Old star clusters in the FSR catalogue*. *Monthly Notices of the Royal Astronomical Society*, 409 (3). pp. 1281-1288. ISSN 00358711 (ISSN).

## Downloaded from

<https://kar.kent.ac.uk/49566/> The University of Kent's Academic Repository KAR

## The version of record is available from

<https://doi.org/10.1111/j.1365-2966.2010.17390.x>

## This document version

UNSPECIFIED

## DOI for this version

## Licence for this version

UNSPECIFIED

## Additional information

Unmapped bibliographic data:LA - English [Field not mapped to EPrints]J2 - Mon. Not. R. Astron. Soc. [Field not mapped to EPrints]AD - Centre for Astrophysics and Planetary Science, University of Kent, Canterbury CT2 7NH, United Kingdom [Field not mapped to EPrints]AD - Zentrum für Astronomie der Universität Heidelberg, Institut für Theoretische Astrophysik, Albert-Ueberle-Str 2, 69120 Heidelberg, Germany [Field not mapped to EPrints]AD - Centre for Astrophysics Research, University of Hertfordshire, College Lane, Hatfield AL10 9AB, United Kingdom [Field not mapped to EPrints]DB - Scopus [Field not mapped to EPrints]

## Versions of research works

### Versions of Record

If this version is the version of record, it is the same as the published version available on the publisher's web site. Cite as the published version.

### Author Accepted Manuscripts

If this document is identified as the Author Accepted Manuscript it is the version after peer review but before type setting, copy editing or publisher branding. Cite as Surname, Initial. (Year) 'Title of article'. To be published in *Title of Journal*, Volume and issue numbers [peer-reviewed accepted version]. Available at: DOI or URL (Accessed: date).

## Enquiries

If you have questions about this document contact [ResearchSupport@kent.ac.uk](mailto:ResearchSupport@kent.ac.uk). Please include the URL of the record in KAR. If you believe that your, or a third party's rights have been compromised through this document please see our [Take Down policy](https://www.kent.ac.uk/guides/kar-the-kent-academic-repository#policies) (available from <https://www.kent.ac.uk/guides/kar-the-kent-academic-repository#policies>).

# Old Star Clusters in the FSR catalogue

D. Froebrich<sup>1\*</sup>, S. Schmeja<sup>2</sup>, D. Samuel<sup>3</sup>, P.W. Lucas<sup>3</sup>

<sup>1</sup> *Centre for Astrophysics and Planetary Science, University of Kent, Canterbury, CT2 7NH, UK*

<sup>2</sup> *Zentrum für Astronomie der Universität Heidelberg, Institut für Theoretische Astrophysik, Albert-Ueberle-Str. 2, 69120 Heidelberg, Germany*

<sup>3</sup> *Centre for Astrophysics Research, University of Hertfordshire, College Lane, Hatfield, AL10 9AB, UK*

Received sooner; accepted later

## ABSTRACT

We investigate the old star clusters in the sample of cluster candidates from Froebrich, Scholz & Raftery 2007 – the FSR list. Based on photometry from the 2 Micron All Sky Survey we generated decontaminated colour-magnitude and colour-colour diagrams to select a sample of 269 old stellar clusters. This sample contains 63 known globular clusters, 174 known open clusters and 32 so far unclassified objects. Isochrone fitting has been used to homogeneously calculate the age, distance and reddening to all clusters. The mean age of the open clusters in our sample is 1 Gyr. The positions of these clusters in the Galactic Plane show that 80 % of open clusters older than 1 Gyr have a Galactocentric distance of more than 7 kpc. The scale height for the old open clusters above the Plane is 375 pc, more than three times as large as the 115 pc which we obtain for the younger open clusters in our sample. We find that the mean optical extinction towards the open clusters in the disk of the Galaxy is 0.70 mag/kpc. The FSR sample has a strong selection bias towards objects with an apparent core radius of 30'' to 50'' and there is an unexplained paucity of old open clusters in the Galactic Longitude range of  $120^\circ < l < 180^\circ$ .

**Key words:** Galaxy: globular clusters: individual; Galaxy: open clusters, individual

## 1 INTRODUCTION

As birthplaces for the majority of stars (e.g. Lada & Lada (2003)) stellar clusters can be considered the building blocks of galaxies. The vast majority of them only reaches ages of a few Myrs after which their member stars dissolve into the general field star population. The disruption timescales are dependent e.g. on the local tidal gravitational field (interaction with nearby giant molecular clouds), the star formation efficiency in the cluster, the mass of the cluster and the efficiency of the feedback from the young stars in the cluster (jets, winds, supernova explosions). There is evidence that the disruption timescales are increasing with distance from the Galactic Center (e.g. Lamers & Gieles (2006), Goodwin & Bastian (2006), Piskunov et al. (2007)). A number of clusters, however, survive this initial infant mortality phase and become open clusters, which then can reach ages of up to several Gyrs.

These old stellar systems, including both, open and globular clusters, provide us with laboratory like conditions. All stars within such a cluster can be considered as being situated at the same distance, having the same age and metallicity. Due to their age, they are usually not associated with giant molecular clouds, thus there is a constant reddening towards all cluster members. Hence, one can fit theoretical isochrones to the cluster colour-magnitude dia-

gram to determine the age, distance and reddening simultaneously, provided the metallicity is known.

As current catalogues of old open clusters are rather incomplete (e.g. Bonatto & Bica (2007b)), our aim is to establish a large, well defined sample of such old stellar systems and to determine its properties in a homogeneous way. This will then be used to investigate the distribution of these old clusters in the Galaxy which will improve our understanding not just of the old stellar systems, but also on issues such as the interstellar extinction law, disruption timescales of clusters, and ultimately the chemical evolution and enrichment history of the Galactic Disk.

To obtain a large sample of old clusters and analyse its properties homogeneously, we utilise the 2 Micron All Sky Survey (2MASS, Skrutskie et al. (2006)) point source catalogue and the star cluster candidate list provided by Froebrich et al. (2007a). We identify the old systems amongst their catalogue by investigation of decontaminated colour-magnitude and colour-colour diagrams and determine their parameters by fitting theoretical isochrones from Girardi et al. (2002) to the 2MASS photometry.

Our paper is structured as follows. In Sect. 2 we describe the selection of our cluster sample and the determination of its properties. This includes the automatic decontamination of foreground stars in the cluster fields, the selection and identification of the old stellar systems and the determination of their ages, distances and reddening via isochrone fits. In Sect. 3 we present our main results and discussion. We characterise the cluster sample, discuss the dis-

\* E-mail: df@star.kent.ac.uk

tribution of clusters in the Galactic Plane and identify selection effects. Finally we present our conclusions in Sect. 4.

## 2 DATA ANALYSIS

### 2.1 The FSR sample

The sample of clusters analysed in this work is based on the FSR catalogue by Froebrich et al. (2007a). They determined a star density map based on 2MASS data (Skrutskie et al. (2006)) along the entire Galactic Plane with  $|b| < 20^\circ$ . Star cluster candidates were selected as local star density enhancements and a total of 1788 objects were found. These candidates were cross referenced with the SIMBAD database. This uncovered that the FSR list contained 86 known globular clusters, 681 known open clusters and 1021, so far unknown cluster candidates. An estimate of the contamination suggested that about half of these new candidates are real star clusters. A number of these have been confirmed as real clusters since then. See Froebrich et al. (2008b) for a recent summary of FSR cluster candidates investigated so far.

### 2.2 Accurate cluster positions and radii

Our first aim was to determine more accurate cluster coordinates and the radius for each FSR cluster candidate. We hence extracted the 2MASS photometry for all stars in a  $0.5^\circ \times 0.5^\circ$  sized field around each cluster. Only stars with reliable photometry (quality flag A to C in each of the JHK bands; Skrutskie et al. (2006)) were used. We then modelled the cluster candidates by two-dimensional angular Gaussian distributions applying an expectation-maximization algorithm (Dempster, Laird & Rubin (1977)) and evaluating the best fit using the Bayesian information criterion (BIC; Schwarz (1978)) by means of a code developed for the cluster search in UKIDSS GPS data (Samuel & Lucas, in preparation). This procedure provides us with the cluster centre and the size of the best-fit Gaussian and the BIC value – essentially a description of how probable it is that a given cluster candidate is a real star cluster. Objects with a BIC value less than zero are generally considered real, and a smaller BIC value indicates a higher probability to be a real cluster. The obtained central coordinates, and BIC values for each of the investigated clusters are listed in Table A1.

With the more accurate central positions for each cluster candidate we calculated radially averaged star density profiles  $\rho(r)$ . Those profiles were fit automatically to the function:

$$\rho(r) = \rho_{bgr} + \frac{\rho_{cen}}{1 + \left(\frac{r}{r_{core}}\right)^2}, \quad (1)$$

where  $\rho_{cen}$  and  $\rho_{bgr}$  are the central cluster and background star densities and  $r_{core}$  the radius of the cluster. Using the distances to the clusters, we later convert these radii into real sizes in parsec.

### 2.3 Membership probabilities

To determine the cluster properties via isochrone fitting we need to identify the most likely cluster member stars. This is in particular important in the high star density fields near the Galactic Plane, where field star contamination is important. We used the position and radius of each cluster to define a cluster region and a control field in the  $0.5^\circ \times 0.5^\circ$  area around the cluster coordinates. Stars which were closer than three times the cluster radius to the centre

are considered part of the cluster area, all stars further away than five times the cluster radius are part of the control field.

We then applied a variation of the colour-colour-magnitude (CCM) decontamination procedure from Bonatto & Bica (2007a) to the stars in the cluster area. For each star  $i$  with the apparent 2MASS magnitudes  $J^i$ ,  $H^i$ ,  $K^i$  and colours  $J^i - H^i = JH^i$ ,  $J^i - K^i = JK^i$  we calculate the CCM distance  $r_{ccm}$  to every other star  $j \neq i$  in the following way:

$$r_{ccm} = \sqrt{\frac{1}{2} [J^i - J^j]^2 + [JK^i - JK^j]^2 + [JH^i - JH^j]^2} \quad (2)$$

The factor of 0.5 in front of the differences in the J-band magnitudes accounts for the generally larger spread of the magnitudes compared to the colours. We determine  $r_{ccm}^{10}$  as the 10<sup>th</sup> smallest value over all stars  $j \neq i$  and count the number  $N_{ccm}$  of stars in the control area that are within the CCM distance  $r_{ccm}^{10}$  around the values  $J^i$ ,  $JK^i$  and  $JH^i$ . The probability  $P_{ccm}$  of star  $i$  to be a member of the cluster is then given by:

$$P_{ccm} = 1.0 - \frac{N_{ccm}}{10} \frac{A_{cl}}{A_{con}} \quad (3)$$

where  $A_{cl}$  and  $A_{con}$  are the areas of the cluster and control field, respectively. If  $P_{ccm}$  for a particular star is negative, then its membership probability is zero. This approach, instead of a fixed CCM cell size as in Bonatto & Bica (2007a) gives better results for the probabilities in regions of the CCM space with only a few stars, i.e. at bright magnitudes.

Alternatively one could determine the probability  $P_{pos}$  for each star to be a cluster member based on its distance from the cluster centre by assuming that the projected cluster star density profile has a given distribution  $\rho_{cl}(r)$  (e.g. a Gaussian or similar to Eq. 1), overlaid on a constant background star density  $\rho_{bgr}$ . Stars outside five times the cluster radius could be used to determine the background star density  $\rho_{bgr}$ . Based on the distance  $r$  of each individual star to the cluster centre, one could estimate its probability  $P_{pos}(r)$  to be a cluster member based of the star density at this position via:

$$P_{pos}(r) = \rho_{cl}(r)/\rho_{bgr}. \quad (4)$$

Both probabilities  $P_{ccm}$  and  $P_{pos}$  could be combined to a total membership probability  $P = \sqrt{P_{ccm} \cdot P_{pos}}$ . However, we find that using the position does not give reliable results in many cases. In particular in dense (globular) clusters, where no stars are detected in 2MASS in the cluster centres, the probabilities are not reliable. Furthermore, for clusters in regions of high background star density the membership probability for most stars will drop below 20 %, despite the fact that their colours are clearly different from the field. Hence, for the purpose of this paper we solely use the membership probabilities of stars determined from the CCM considerations.

### 2.4 Selection of old star clusters

Utilising the individual membership probabilities for all stars in each cluster we plotted J-K vs. K colour-magnitude (CMD) and H-K vs J-H colour-colour (CCD) diagrams for each FSR cluster candidate. In Fig. 1 we show the diagrams, including the best fitting isochrone (see below) of the so far uninvestigated cluster FSR 0412 (Pfleiderer 3) as an example. One can nicely see that the cluster

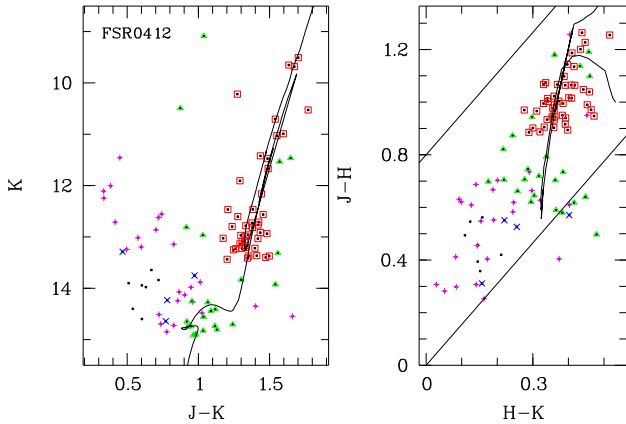


**Figure 1.** Example of our colour-magnitude (left) and colour-colour diagrams for the cluster FSR 0412 (Pfeleiderer 3) which has so far not been investigated in detail. Red squares are stars with  $P > 80\%$ , green triangles are stars with  $60\% < P < 80\%$ , pink + - signs are stars with  $40\% < P < 60\%$ , blue crosses are stars with  $20\% < P < 40\%$  and black dots are stars with  $P < 20\%$ . Overplotted in black is the best fitting isochrone ( $d = 6.1$  kpc,  $\log(\text{age}/\text{yr}) = 9.1$ ,  $A_K = 0.46$  mag and solar metallicity). The two solid lines in the right panel enclose the reddening band for stellar atmospheres.

red giant stars are the most likely members ( $P_{cem} > 80\%$ ). Stars possessing colours in agreement with foreground dwarf stars are much less likely to be cluster members. In Appendix C we show the CMDs and CCDs for all clusters investigated in this paper.

We then inspected the 1788 CMDs and CCDs generated for the entire FSR catalogue, to decide if the high probability members are consistent with a sequence representing an old stellar cluster. In other words, we manually selected all FSR objects that either showed a Red Giant Branch (RGB) or the top of the Main Sequence (MS) and a number of giant stars. Note that this selection has been performed ‘blind’, without the knowledge of which object is which cluster (known or unknown) in order to ensure an unbiased selection. In total 269 of the 1788 objects were selected as candidates for old clusters and analysed in more detail for this paper.

## 2.5 Identification of known old star clusters

We cross-identified the list of 269 clusters with the SIMBAD<sup>1</sup> database. In total 63 known globular clusters are in the list, 174 known open clusters (including some already confirmed FSR objects) and 32 so far unclassified FSR cluster candidates. Some obviously old clusters, in particular some of the known globular clusters (e.g. FSR 0005 or NGC 6569, vdB-Hagen 260), are missing in our sample of old FSR clusters. This is mainly caused by the fact that they do not contain a large enough number of high probability cluster members, representing an old stellar sequence.

We obtained the distances, metallicities and reddening for the known globular clusters from the list of Harris (1996). The parameters for FSR 0040 (2MASS GC 1) are obtained from Ivanov et al. (2000) and the values for FSR 1735 are taken from Froebrich et al. (2008b). The cluster FSR 1762 (Pismis 26, vdB-Hagen 71, Tonantzintla 2) is listed as globular or cluster of stars in SIMBAD and we used its parameters from the list of Harris (1996). The clusters

FSR 0190, 0584 and 1716 are also listed as globular or open cluster. In those cases we used the literature data from Froebrich et al. (2008a), Bica et al. (2007) and Froebrich et al. (2008b) and Bonatto & Bica (2008), respectively.

The open cluster parameters were obtained (as first choice) from the WEBDA<sup>2</sup> database for galactic open clusters. If no data was available for an open cluster we searched the literature. The main Table A1 with the cluster parameters indicates the papers used in those cases. In total we obtained data for 147 of the known open clusters. For 27 open clusters no data was available and their properties have hence been determined here, together with the parameters for the 32 so far unclassified FSR cluster candidates.

## 2.6 Cluster parameter determination

From our analysis so far we only determined the cluster position and radius, as well as the BIC value. In order to determine the cluster parameters such as distance, reddening and age, we need to fit an appropriate isochrone to the CMD and CCD for each cluster. We used the isochrone models from Girardi et al. (2002) for 2MASS data to perform this task. The Figures containing the CMDs and CCDs for all selected old FSR clusters in Appendix C show in general two isochrones: One with the literature values for the cluster and our best fitting isochrone. The literature isochrone is shown as dashed blue line, the best fitting isochrone from this paper is shown as a solid black line. The parameters used for our best isochrone fit for all clusters are listed in Table A1. The uncertainties of the determined parameters are discussed in Sect. 3.3.

The reddening to each cluster used in our best fitting isochrone is given as the K-band extinction in Table A1. To overplot the isochrones on the CMDs and CCDs we need to convert the K-band into the J and H-band extinction using  $A_J = C_{JK} * A_K$  and  $A_H = C_{HK} * A_K$ . We use a conversion factor  $C_{JK} = 2.618$  following Mathis (1990). In order to fit the isochrone data in the CCD as well, in general the conversion factor  $C_{HK} = 1.529$  from Mathis (1990) seems too low. For the majority of clusters we hence use  $C_{HK} = 1.67$ . However, in some cases those values do not provide a satisfying fit, and we hence adjusted the value for  $C_{HK}$  for each cluster separately. The used values for each cluster are listed in Table A1.

## 3 RESULTS AND DISCUSSION

### 3.1 General

We have identified 269 old stellar clusters in the FSR catalogue of possible cluster candidates. For the 63 known globular clusters and 147 known open clusters we extracted parameters (distance, reddening, age) from the literature. For the remaining 27 known open clusters and 32 so far unclassified FSR cluster candidates we determine parameters here using isochrone fitting. Additionally, we determine the parameters of all clusters homogeneously by the same set of data (2MASS JHK photometry), the same data analysis method and the same set of isochrones (Girardi et al. (2002)). This will allow us, in particular for the open clusters, to analyse and compare the distribution of the parameters of our sample of old stellar clusters along the entire Galactic Plane. We will in the following only discuss the open cluster parameters, if not stated otherwise.

<sup>1</sup> <http://simbad.u-strasbg.fr/simbad/sim-fid>

<sup>2</sup> <http://www.univie.ac.at/webda/>

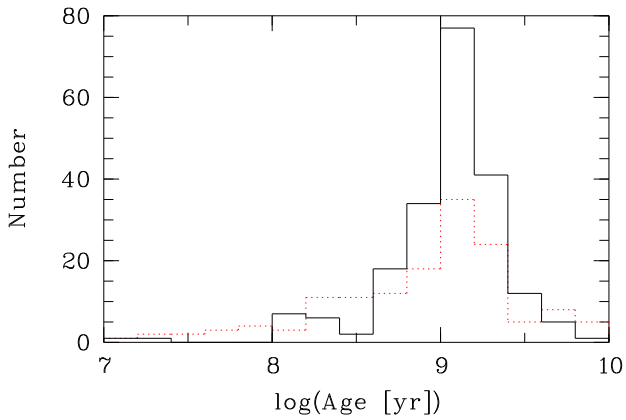


**Figure 2.** Distribution of the ages of the open clusters in our sample. The red dotted histogram shows the distribution of ages (from the literature) for the known open clusters. The black solid histogram shows the distribution for the ages (determined in this paper) of all open clusters in our sample. Typical age uncertainties are within the bin width of the histogram (see also Sect. 3.3).

In Appendix B we provide some notes for all newly identified old open clusters and for the known ones when their parameters differ significantly from the literature values. Here we will briefly mention some of the notable discoveries and their properties. FSR 0039 is a 1 Gyr old, highly reddened cluster. With just 4.6 kpc from the Galactic Centre it is one of the rare old inner Galaxy clusters. FSR 0313 (Kronberger 81) shows a large number of giants but no main sequence. This indicates that it might be an old, massive cluster about 10 kpc from the Galactic Centre. Both, FSR 0412 (Pfleiderer 3) and FSR 0460 are very distant (6.1 kpc) and old (1.2 Gyr) clusters. Very nice examples of newly discovered clusters (or objects with parameters determined for the first time) are FSR 0134, 0177 (Kronberger 52), 0275, 0342, 0972 (NGC 2429), 1404 (vdB-Hagen 55), 1463, 1565 (Trumpler 19), 1670 (Loden 1101) which show a number of red giants and main sequence stars, while for FSR 0170, 0329 (Berkeley 92), 1521, 1559 (Teutsch 106) only red giants are detected.

### 3.2 Age distribution

Since we aim to investigate the old clusters in the FSR catalogue, we have to analyse the age distribution of our sample. This is shown in Fig. 2. There the red dotted histogram shows the age distribution as obtained for the known open clusters using the literature values. The black solid histogram shows the distribution of the ages determined in the paper for all open clusters. In both cases there is a clear peak at about 1 Gyr (which is also the average of the distribution), and more than 80% of the clusters are older than 500 Myrs. This shows that our selection of clusters with a clear RGB or a main sequence and red giants, was successful in picking out old stellar systems. However, it still selects a few younger clusters. Most likely these are more massive, hence showing a larger, and thus observable number of red (super) giants earlier in their evolution. Some of the clusters with lower ages (based on the literature) have, according to our isochrone fits, an older age. This is caused by the fact that we try to include potential giant stars in the fit of the cluster isochrone, generally leading to a slightly larger age.

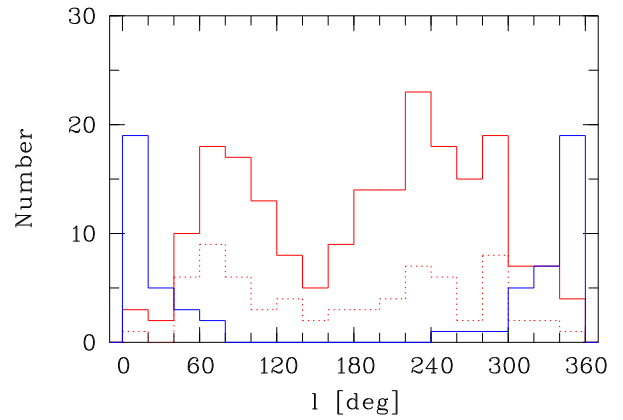


**Figure 4.** Histogram showing the distribution of the clusters in our sample along the Galactic Plane. In blue we show the globular clusters and in red (solid line) all open clusters, while the dotted red line shows only clusters with ages below one Gyr. The paucity of open clusters near the Galactic Centre direction is a simple selection effect caused by the high star density and thus low detection probability. The paucity between  $120^\circ < l < 180^\circ$  is not explained.

### 3.3 Comparison with literature data

For a large fraction of clusters we can compare our determined parameters with the values obtained from the literature. This will allow us to estimate the uncertainties of the isochrone fitting for the clusters without known parameters.

At first we check the position accuracy of the cluster candidates. We determine the difference of our coordinates and the literature coordinates for the known clusters. For the generally highly concentrated globular clusters the average difference is  $0.5'$ , while for the open clusters we find an average positional difference of  $2'$ . This rather large value seems to be caused by erroneous coordinates of some not well investigated clusters in SIMBAD. See Table A1 to check the differences for each individual cluster.

Except in some cases the distance, age and reddening estimates from the literature and our isochrone fitting are in agreement. In the Appendix B we will discuss in detail the clusters with large differences in the parameters. On average the cluster distances show a scatter of about 30% between the literature values and our estimates. For the  $\log(\text{age})$  values an agreement of about 10% is found. The reddening values also agree to within 30%. The 2MASS photometry does not allow the determination of the metallicity. Hence, we generally used solar values, except if a different value was available from the literature. In some cases it was, however, only possible to obtain a fit to the CMDs and CCDs with non-solar values. See Table A1 for the metallicities used for our best fitting isochrone. Please note that if the cluster has a lower metallicity than used here, the estimated reddening would be higher and the distances lower. Similarly the cluster age would be influenced systematically. However, if the metallicity is changed by less than a few tenth of a dex, then the parameters will stay within the above mentioned uncertainties. It is much more important to identify the cluster red giants and main sequence turn off with high accuracy.

### 3.4 Distribution in the Galactic Plane

Using the positions and determined distances to the clusters in our sample, we can investigate their distribution in the Galactic Plane.

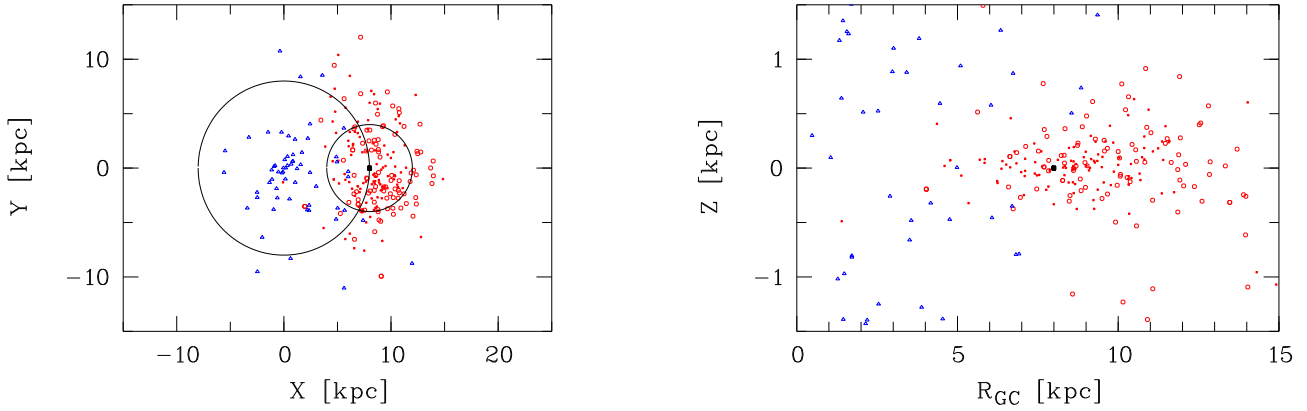


**Figure 3. Left:** Distribution of the clusters in the Galactic Plane based on the distances determined in this paper. Known globular clusters are shown as blue triangles, old open clusters (age above one Gyr) as red circles and younger open clusters as red dots. The distance of the Sun to the Galactic Centre is assumed to be 8 kpc and the Sun's position is indicated by the black square. The two circles indicate a distance of 8 kpc (large circle) from the Galactic Centre and 4 kpc (small circle) from the Sun. Note that the three globular clusters FSR 0021 (M 54), FSR 0164 (NGC 7006) and FSR 1745 (Terzan 3) are outside the plotted area. **Right:** Distribution of the clusters perpendicular to the Galactic Plane of the Galaxy. Shown is the height  $Z$  above the Plane against the Galactocentric distance. The same symbols as in the left panel are used and for clarity only the region containing the open clusters is shown.

In the left panel of Fig. 3 we show the distribution of all clusters in the X-Y plane. As blue triangles we plot the known globular clusters, while the open clusters are plotted as red symbols (large circles for clusters with ages above 1 Gyr, small dots for clusters with ages below 1 Gyr). The plot assumes a distance of the Sun to the Galactic Centre of 8 kpc. As expected one finds most of the globular clusters concentrated towards the Galactic Centre. The open clusters are mostly found near the Sun's position. This is, however, a simple selection effect, as the sample contains naturally only clusters near enough to be visible in 2MASS data.

Two details of the spatial distribution of the open clusters are, however, worth discussing in a bit more detail:

i) A histogram of the distribution of Galactic Longitude values of the open clusters in our sample (see Fig. 4) reveals two regions with a smaller than average number of clusters. This is a) the region near the Galactic Centre ( $\pm 60^\circ$  away) and b) the Galactic Longitude range  $120^\circ < l < 180^\circ$ . In the case of a) there are two reasons for this. Firstly, the high star density towards the Galactic Centre prevents the detection and identification of stellar clusters in this area (a selection effect when establishing the sample) and secondly the fact that there are indeed fewer old stellar clusters closer than the Sun to the Galactic Centre (see below). In the case of b), there seems to be no obvious reason for the paucity of old open clusters in this region compared to the same longitude range on the opposite side of the Galactic Anticentre (i.e. the region  $180^\circ < l < 240^\circ$ ). One explanation could be one or several large, high extinction molecular clouds in this direction, preventing the detection of clusters. However, in the all sky extinction maps from Rowles & Froebrich (2009) there is no indication of such clouds. Furthermore, the clusters which are detected in this longitude range, cover all distances between 1 and 7 kpc homogeneously, as well as extinction values between 0.0 and 0.4 mag  $A_K$ . Finally, as can be seen in Fig. 4, the effect is more pronounced for clusters with ages above 1 Gyr. Hence, this region either suffers from an unknown selection effect, or indeed there are fewer than normal old open clusters present in this part of the Galaxy.

ii) While our sample clearly contains a large number of clusters within 4 kpc from the Sun, there is a clear paucity of objects

with distances to the Galactic Centre less than that of the Sun. This is a fact already noticed by Friel (1995) and replicated since then. In our sample only 3% of the open clusters with ages above 1 Gyr are closer than 5 kpc to the Galactic Centre (only 10% are closer than 7 kpc). In total 80% of the old open clusters are further away than the Sun from the Galactic Centre. This clearly indicates that survival times of open clusters at smaller Galactocentric distances than the one of the Sun are significantly shortened due to the stronger tidal forces and the more frequent encounters with giant molecular clouds (e.g. van den Bergh & McClure (1980), Gieles et al. (2006; 2008)).

We also analysed the distribution of clusters below and above the Galactic Plane by fitting a Gaussian to the distribution. While the distribution of Galactic Latitudes is slightly off-centre with the peak of the distribution at  $b = -0.6^\circ$  and a width of  $7^\circ$ , the distribution of distances  $Z$  to the Galactic Plane is almost centred ( $Z = -33$  pc). In the right panel of Fig. 3 we show the distribution of all clusters perpendicular to the Galactic Plane. For clarity we zoom into the region where the open clusters are situated. The older clusters seem to be much more widely distributed perpendicular to the Galactic Plane than the younger objects. We hence analyse the full width half maximum of the distributions for clusters older and younger than 1 Gyr. We find that the 137 clusters with ages equal to or above 1 Gyr have a scale height of 375 pc. This agrees with earlier findings from e.g. Janes & Phelps (1994) utilising a much smaller sample of clusters. In contrast, the clusters in our sample which are younger than 1 Gyr have a scale height of only 115 pc. Even if our sample is inhomogeneous (see below), this is a clear indication that the older clusters have either survived longer due to their more inclined orbits, have been scattered into those, or have been formed there as part of the thick disk. The different scale heights are not caused by selecting older clusters further away from the Galactic Centre than the younger clusters. The average distance to the Galactic Centre is 8.9 and 9.4 kpc for the younger and older clusters, respectively. Given the scatter in these distances of about 2 kpc, this difference is not enough to explain the different scale heights.

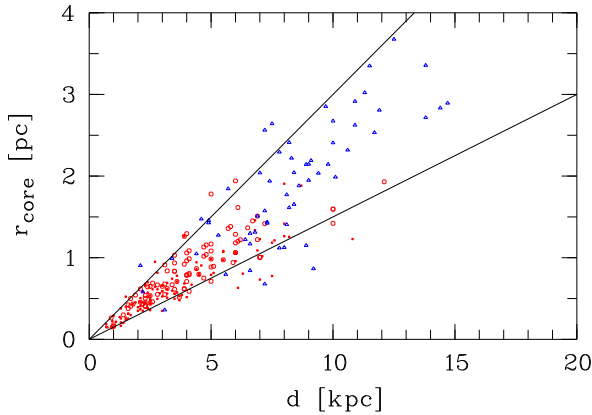


**Figure 5.** The apparent correlation of distance and core radius of our cluster sample, identified as one major selection effect in the FSR list. Blue triangles are the globular clusters, while large and small red circles are old (above one Gyr) and younger (less than one Gyr) open clusters. The two black lines indicate the range for the correlation as given in Eq. 5.

### 3.5 Reddening

The extinction towards the clusters ranges from zero to more than 0.8 mag  $A_K$ , in a handful of cases. Generally there is a trend of the extinction values with Galactic Longitude. Near to the Galactic Anticentre generally values of 0.3 mag  $A_K$  are not exceeded and away from the Anticentre region we detect more distant and reddened clusters. To account for the different distances we investigated the distribution of the reddening per kiloparsec values of our clusters. There are a handful of objects with more than 0.2 mag  $A_K$  per kiloparsec distance, which are most likely clusters behind nearby giant molecular clouds. The remaining clusters more or less show a homogeneous distribution between zero and 0.1 mag  $A_K$ /kpc. If we exclude clusters below or above the scale height (outside the main disk) of the entire sample, we find an average extinction for the entire sample of old open clusters of 0.70 mag/kpc of optical extinction (conversion of  $A_K$  into  $A_V$  following Mathis (1990)).

### 3.6 Selection effects and Cluster Radii

One so far not investigated issue of the FSR cluster candidate list is selection effects. The cluster selection is of course influenced by the local background star density and 2MASS completeness limit, as well as the distance to the cluster and the extinction along the line of sight.

However, we seem to have found one further important selection bias in the FSR sample. We investigate the core radius (in pc) of all clusters, determined from the fit of the radial star density profile and the estimated distance from the isochrone fitting (see Table A1 for the values of the individual clusters). We find that there is a clear correlation of the cluster core radius and its distance from the Sun (see Fig. 5). In particular, if we exclude the known globular clusters, the cluster core radii seem to follow the relation

$$r_{core}[pc] = (0.225 \pm 0.075) \cdot d[kpc] \quad (5)$$

Hence, the FSR sample does neither contain compact distant clusters nor more extended nearby objects. Both these effects are understandable when one looks back at the cluster candidate selection procedure (see Sect. 2). Stars in compact distant clusters are

simply not resolved in the 2MASS data and hence might not have been picked up as local star density enhancements, and/or the number of detectable cluster members is too small to be identified as an old evolutionary sequence in the CMDs and CCDs. Similarly, nearby clusters are more extended in the sky and are hence also not picked up. Note that the average apparent cluster core radius of the old open clusters in our sample is about  $40''$ , with a scatter of just  $\pm 10''$ .

The identification of this selection effect in our cluster sample, also does not allow us to study the evolution of cluster radius with age and/or position in the Galaxy, as any trend might simply be caused by selection bias. If we try to account for the selection effect, we can still obtain some tentative trends for the cluster radii. i) more extended clusters seem to be found generally more often at larger Galactocentric distance; ii) larger clusters seem to be found generally at larger distances  $Z$  from the Galactic Plane. This trend has already been found by other authors (e.g. Janes et al. (1988), Tadross et al. (2002), Schilbach et al. (2006)).

## 4 CONCLUSIONS

We have analysed the entire list of cluster candidates from Froeblich et al. (2007a) by means of 2MASS photometry. We calculate more accurate cluster positions and radii. For stars within each cluster we calculate the membership probability based on a modified version of the colour-colour-magnitude approach by Bonatto & Bica (2007a). A by eye inspection of 2MASS colour-magnitude and colour-colour diagrams of high probability members has been used to identify 269 candidates for old clusters in the FSR sample.

Our sample of clusters contains 63 known globular clusters, 147 known open clusters with literature parameters, 27 known open clusters without known parameters and 32 previously unknown objects. We use isochrones from Girardi et al. (2002) to determine the age, distance and reddening for each cluster homogeneously from the 2MASS photometry. Our sample has a mean age of 1 Gyr and 80 % of the clusters are older than 500 Myrs.

The distribution of open clusters in the Galaxy shows that 80 % of the clusters with ages above 1 Gyr are further away than 7 kpc from the Galactic Centre, strengthening earlier findings e.g. from Friel (1995). Furthermore, the scale height of these old clusters is with 375 pc more than three times as large as the scale height of the younger (less than 1 Gyr) fraction in our sample, which we found to be 115 pc. This is still about twice as large as the scale height of young star clusters which is about 55 pc (Friel (1995)).

The large sample of clusters also allows us to investigate the general interstellar extinction for objects mostly not associated with Giant Molecular Clouds. For our sample of old clusters we find an average interstellar optical extinction of 0.70 mag/kpc.

We also identify a main selection effect in the FSR cluster sample, besides distance and reddening. An investigation of the cluster radii shows that the sample contains mostly clusters which have a distance to radius ratio in the range  $3.3$  to  $6.7 \cdot 10^3$ . This is caused by the fact that the sample seems to be biased towards clusters with an apparent projected core radius of  $40'' \pm 10''$ .

Finally we find that there seems to be a significantly smaller than average number of old open clusters in the longitude range  $120^\circ < l < 180^\circ$ , which cannot be explained by any of the sample selection effects. The reason for this paucity is unknown.

Large improvements can be expected in the near future for this kind of work, as the UKIDSS GPS and Vista VVV surveys can be utilised. Their increase in limiting magnitude and in particular spa-

tial resolution compared to 2MASS will allow us to improve on the parameter determinations, as well as to build up a cluster sample with less selection effects, e.g. circumventing the core radius selection effect.

## ACKNOWLEDGMENTS

S.Schmeja acknowledges funding by the Deutsche Forschungsgemeinschaft (DFG) through grant SCHM 2490/1-1. This publication makes use of data products from the Two Micron All Sky Survey, which is a joint project of the University of Massachusetts and the Infrared Processing and Analysis Center/California Institute of Technology, funded by the National Aeronautics and Space Administration and the National Science Foundation. This research has made use of the SIMBAD database, operated at CDS, Strasbourg, France. This research has made use of the WEBDA database, operated at the Institute for Astronomy of the University of Vienna.

## REFERENCES

- Bica, E., Bonatto, C., 2008, MNRAS, 384, 1733  
 Bica, E., Bonatto, C., Camargo, D. 2008, MNRAS, 384, 349  
 Bica, E., Bonatto, C., Ortolani, S., Barbuy, B. 2007, A&A, 472, 483  
 Bica, E., Dutra, C.M., Soares, J., Barbuy, B., 2003, A&A, 404, 223  
 Bonatto, C., Bica, E. 2007, MNRAS, 377, 1301  
 Bonatto, C., Bica, E. 2007, A&A, 473, 445  
 Bonatto, C., Bica, E., 2008, A&A, 491, 767  
 Bonatto, C., Bica, E. 2008, A&A, 485, 81  
 Bonatto, C., Bica, E., MNRAS, 392, 483  
 Camargo, D., Bonatto, C., Bica, E., 2009, A&A, 508, 211  
 Dempster, A.P., Laird, N.M., Rubin, D.B., 1977, J. R. Stat. Soc. Ser. B, 39, 1  
 Friel, E.D., 1995, ARA&A, 33, 381  
 Froebrich, D., Meusinger, H., Davis, C.J., Schmeja, S., 2009, MNRAS, 395, 1768  
 Froebrich, D., Meusinger, H., Scholz, A. 2007, MNRAS, 377, 54L  
 Froebrich, D., Meusinger, H., Davis, C.J. 2008, MNRAS, 383, 45  
 Froebrich, D., Meusinger, H., Scholz, A., 2008, MNRAS, 390, 1598  
 Froebrich, D., Scholz, A., Raftery, C.L. 2007, MNRAS, 374, 399  
 Gieles, M., Lamers, H.J.G.L.M., Baumgardt, H., 2008, in Dynamical Evolution of Dense Stellar Systems, Proceedings of the International Astronomical Union, IAU Symposium, Volume 246, 171  
 Gieles, M., Portegies Zwart, S.F., Baumgardt, H., Athanassoula, E., Lamers, H.J.G.L.M., Sipiør, M., Leenaarts, J., 2006, MNRAS, 371, 793  
 Girardi, L., Bertelli, G., Bressan, A., et al. 2002, A&A, 391, 195  
 Glushkova, E.V., Koposov, S.E., Zolotukhin, I.Y., Beletsky, Y.V., Vlasov, A.D., Leonova, S.I., 2010, AstL, 36, 75  
 Goodwin, S.P., Bastian, N., 2006, 373, 752  
 Harris, W.E. 1996, AJ, 112, 1487  
 Ivanov, V. D., Borissova, J., Vanzi, L., 2000, A&A, 362, 1  
 Janes, K.A., Phelps, R.L., 1994, AJ, 108, 1773  
 Janes, K.A., Tilley, C., Lynga, G., 1988, 95, 771  
 Koposov, S.E., Glushkova, E.V., Zolotukhin, I.Y., 2008, A&A, 486, 771  
 Lamers, H.J.G.L.M., Gieles, M., 2006, A&A, 455, 17  
 Lada, C.J., Lada, E.A., 2003, ARA&A, 41, 57  
 Lata, S., Pandey, A.K., Kumar, B., Bhatt, H., Pace, G., Sharma, S., 2010, AJ, 139, 378  
 Mathis, J.S. 1990, ARA&A, 28, 37  
 Momany, Y., Ortolani, S., Bonatto, C., Bica, E., Barbuy, B., 2008, MNRAS, 391, 1650  
 Ortolani, S., Bica, E., Barbuy, B., 2005, A&A, 437, 531  
 Piskunov, A.E., Schilbach, E., Kharchenko, N.V., Röser, S., Scholz, R.-D., 2007, A&A, 468, 151  
 Rowles, J. & Froebrich, D. 2009, MNRAS, 395, 1640  
 Schilbach, E., Kharchenko, N.V., Piskunov, A.E., Röser, S., Scholz, R.-D., 2006, A&A, 456, 523  
 Schwarz G., 1978, Ann. Stat., 6, 461  
 Skrutskie, M.F., Cutri, R.M., Stiening, R., et al. 2006, AJ, 131, 1163  
 Tadross, A.L., Werner, P., Osman, A., Marie, M., 2002, NewA, 7, 553  
 van den Bergh, S. & McClure, R. D., A&A, 88, 360

## APPENDIX A: MAIN TABLE

Table A1: Summary table of the properties of the old stellar clusters analysed in this paper. We list the FSR catalogue ID, the coordinates, BIC value and core radius, the cluster properties as used in the isochrone fit in this work, the WEBDA or literature cluster parameter, the separation and classification of the known clusters in SIMBAD, and finally other common names for the clusters. The parameters for the isochrone fit used in this paper include the distance to the cluster, its age, the K-band extinction, the metallicity and the reddening law. The WEBDA and literature values are the distance of the cluster, its age, the reddening and metallicity. To plot the literature isochrone for the known globular clusters we use an age of 12 Gyrs. For clusters marked with a \*, please read the notes in Appendix B for details on the isochrone fits.

| FSR ID            | Coordinates |            | BIC    | $r_{core}$<br>[pc] | this paper |                  |                |                |          | Literature <sup>1</sup> |                  |                 |                | SIMBAD   |       | other Names                     |
|-------------------|-------------|------------|--------|--------------------|------------|------------------|----------------|----------------|----------|-------------------------|------------------|-----------------|----------------|----------|-------|---------------------------------|
|                   | l<br>[deg]  | b<br>[deg] |        |                    | d<br>[kpc] | log(age)<br>[yr] | $A_K$<br>[mag] | [M/H]<br>[dex] | $C_{HK}$ | d<br>[kpc]              | log(age)<br>[yr] | E(B-V)<br>[mag] | [M/H]<br>[dex] | r<br>['] | Class |                                 |
| 0003              | 0.069       | -17.2926   | -289.4 | 2.4                | 8.20       | 10.00            | 0.05           | -1.28          | 1.97     | 8.2                     | —                | 0.04            | -1.12          | 23       | GIC   | NGC 6723                        |
| 0004              | 0.130       | +11.0276   | -146.6 | 1.6                | 8.20       | 10.20            | 0.23           | -2.28          | 1.63     | 8.2                     | —                | 0.59            | -2.05          | 17       | GIC   | NGC 6287                        |
| 0006              | 0.982       | +8.0110    | -2.5   | 2.1                | 9.00       | 10.20            | 0.30           | -1.28          | 1.74     | 9.0                     | —                | 0.89            | -1.17          | 43       | GIC   | NGC 6325                        |
| 0007              | 1.541       | -11.3652   | -40.3  | 1.9                | 9.00       | 10.20            | 0.03           | -0.68          | 1.67     | 9.0                     | —                | 0.09            | -0.96          | 39       | GIC   | NGC 6652                        |
| 0008              | 1.729       | -10.2619   | -36.5  | 2.3                | 7.80       | 10.20            | 0.06           | -0.68          | 1.67     | 7.8                     | —                | 0.17            | -0.71          | 35       | GIC   | M 69,<br>NGC 6637               |
| 0011              | 2.796       | -7.9082    | 19.1   | 1.9                | 7.40       | 10.20            | 0.08           | -0.38          | 1.67     | 7.4                     | —                | 0.27            | -0.42          | 34       | GIC   | NGC 6624,<br>vdB-Hagen 262      |
| 0012              | 2.863       | -12.5030   | -37.7  | 0.8                | 6.60       | 10.10            | 0.06           | -1.28          | 1.67     | 8.6                     | —                | 0.07            | -1.51          | 42       | GIC   | M 70,<br>NGC 6681               |
| 0015              | 4.909       | +9.7260    | -62.1  | 1.4                | 7.30       | 10.20            | 0.19           | -0.68          | 1.78     | 8.6                     | —                | 0.44            | -0.65          | 35       | GIC   | NGC 6342                        |
| 0016              | 5.126       | +0.7720    | 17.2   | 0.7                | 7.20       | 10.20            | 1.10           | -1.28          | 1.55     | 7.2                     | —                | 2.93            | -1.20          | 30       | GIC   | UKS 1                           |
| 0020              | 5.552       | +10.7114   | -65.6  | 1.8                | 8.10       | 10.10            | 0.12           | -1.68          | 1.67     | 8.1                     | —                | 0.36            | -1.78          | 34       | GIC   | M 9,<br>NGC 6333,<br>Faust 4082 |
| 0021              | 5.615       | -14.0769   | -87.9  | 8.2                | 25.40      | 10.10            | 0.05           | -1.68          | 1.67     | 25.4                    | —                | 0.15            | -1.59          | 41       | GIC   | M 54,<br>NGC 6715               |
| 0024              | 6.730       | +10.2202   | -65.5  | 3.4                | 13.80      | 10.10            | 0.08           | -0.38          | 2.05     | 13.8                    | —                | 0.29            | -0.50          | 22       | GIC   | NGC 6356                        |
| 0029              | 7.905       | -7.1422    | 3.6    | 1.1                | 7.80       | 10.20            | 0.20           | -1.28          | 1.67     | 7.8                     | —                | 0.40            | -0.99          | 47       | GIC   | NGC 6638                        |
| 0036              | 9.818       | -6.4370    | 10.7   | 1.4                | 7.30       | 10.10            | 0.15           | -1.28          | 1.67     | 7.3                     | —                | 0.40            | -1.35          | 18       | GIC   | NGC 6642                        |
| 0039*             | 10.249      | +0.3198    | 16.3   | 0.5                | 3.50       | 9.00             | 1.22           | 0.00           | 1.60     | —                       | —                | —               | —              | —        | —     | —                               |
| 0040 <sup>2</sup> | 10.480      | +0.0967    | 9.7    | 0.4                | 3.10       | 10.20            | 2.30           | -1.28          | 1.58     | 3.1                     | —                | 6.45            | —              | 36       | GIC   | 2MASS GC 01                     |
| 0044              | 12.868      | -10.9084   | -0.9   | 1.3                | 6.60       | 10.20            | 0.10           | -1.28          | 1.67     | 6.6                     | —                | 0.21            | -1.32          | 42       | GIC   | NGC 6717,<br>Pal 9              |

Continued on next page

Table A1 – continued from previous page

| FSR ID              | Coordinates |          | BIC    | $r_{core}$ [pc] | this paper |               |             |             |          | Literature <sup>1</sup> |               |              |             | SIMBAD |       | other Names  |
|---------------------|-------------|----------|--------|-----------------|------------|---------------|-------------|-------------|----------|-------------------------|---------------|--------------|-------------|--------|-------|--|
|                     | l [deg]     | b [deg]  |        |                 | d [kpc]    | log(age) [yr] | $A_K$ [mag] | [M/H] [dex] | $C_{HK}$ | d [kpc]                 | log(age) [yr] | E(B-V) [mag] | [M/H] [dex] | r ["]  | Class |  |
| 0045                | 12.870      | -1.3182  | 18.0   | 0.5             | 3.00       | 8.40          | 0.22        | 0.00        | 1.62     | 3.6                     | 8.30          | 0.79         | —           | 137    | OpC   | M 24,<br>NGC 6603,<br>Melotte 197,<br>Collinder 374,<br>Raab 129 |
| 0048                | 14.103      | -6.8006  | -20.2  | 2.5             | 11.70      | 10.20         | 0.08        | -0.38       | 1.96     | 11.7                    | —             | 0.33         | -0.48       | 13     | GIC   | Pal 8  |
| 0050*               | 16.388      | +11.4136 | 14.4   | 0.5             | 2.60       | 9.70          | 0.25        | 0.00        | 1.67     | —                       | —             | —            | —           | —      | —     |  |
| 0056                | 18.413      | +16.0388 | -122.2 | 1.0             | 3.40       | 10.20         | 0.20        | -0.68       | 1.54     | 3.4                     | —             | 0.69         | -0.82       | 9      | GIC   | NGC 6366   |
| 0058                | 19.223      | +6.7695  | -60.4  | 2.0             | 10.10      | 10.20         | 0.33        | -1.28       | 1.57     | 10.1                    | —             | 1.08         | -1.37       | 26     | GIC   | NGC 6517   |
| 0061                | 20.799      | +6.7836  | -25.4  | 2.6             | 7.50       | 10.20         | 0.31        | -0.68       | 1.67     | 7.5                     | —             | 1.00         | -0.66       | 32     | GIC   | NGC 6539   |
| 0064                | 21.325      | +14.8146 | -414.5 | 2.0             | 8.40       | 10.10         | 0.14        | -0.68       | 1.86     | 8.4                     | —             | 0.60         | -1.39       | 38     | GIC   | M 14,<br>NGC 6402  |
| 0066                | 21.839      | +5.6724  | -18.8  | 2.1             | 8.90       | 10.20         | 0.27        | -0.68       | 1.67     | 8.9                     | —             | 0.92         | —           | 31     | GIC   | IC 1276, Pal 7   |
| 0074                | 25.359      | -4.3113  | 6.4    | 1.2             | 6.40       | 10.20         | 0.20        | -1.28       | 1.50     | 6.4                     | —             | 0.46         | -1.01       | 31     | GIC   | NGC 6712   |
| 0076*               | 25.558      | +5.0780  | 13.5   | 0.9             | 4.60       | 9.00          | 0.35        | 0.00        | 1.55     | —                       | —             | —            | —           | —      | —     |  |
| 0101 <sup>3</sup>   | 35.147      | +1.7487  | 12.6   | 0.4             | 2.10       | 9.00          | 0.67        | 0.00        | 1.62     | 1.9                     | 8.95          | 2.37         | —           | —      | OpC   |  |
| 0104                | 36.110      | -3.9213  | -12.1  | 1.5             | 6.90       | 10.20         | 0.23        | -0.68       | 1.67     | 6.9                     | —             | 0.78         | -0.52       | 15     | GIC   | NGC 6760   |
| 0119 <sup>4,*</sup> | 44.100      | +13.2947 | 12.5   | 1.4             | 6.50       | 9.40          | 0.13        | -1.68       | 1.67     | —                       | —             | —            | —           | —      | —     |  |
| 0122                | 45.700      | -0.1220  | 8.4    | 0.8             | 2.80       | 8.35          | 0.51        | 0.00        | 1.60     | 1.4                     | 8.60          | 1.50         | —           | 276    | Cl*   | Berkeley 43  |
| 0123*               | 45.948      | +1.0507  | 17.6   | 0.8             | 4.50       | 8.70          | 0.32        | 0.00        | 1.54     | —                       | —             | —            | —           | —      | —     |  |
| 0124 <sup>5</sup>   | 46.477      | +2.6500  | 2.6    | 0.4             | 2.30       | 9.10          | 0.32        | 0.00        | 1.67     | 2.0                     | 9.10          | 0.98         | —           | —      | OpC   |  |
|                     |             |          |        |                 |            |               |             |             |          | 2.6                     | 9.00          | 1.10         | —           | —      | OpC   |  |
| 0131*               | 51.104      | -1.4282  | 19.8   | 1.1             | 5.50       | 8.80          | 0.53        | 0.00        | 1.59     | —                       | —             | —            | —           | —      | —     |  |
| 0134*               | 51.677      | +0.5755  | 17.3   | 0.5             | 3.20       | 8.90          | 0.63        | 0.00        | 1.67     | —                       | —             | —            | —           | —      | —     |  |
| 0135                | 52.104      | -18.8918 | -157.2 | 2.8             | 14.40      | 10.10         | 0.08        | -1.68       | 1.67     | 14.4                    | —             | 0.11         | -1.54       | 8      | GIC   | NGC 6934   |
| 0137                | 52.442      | +2.7299  | -15.5  | 2.3             | 10.60      | 10.10         | 0.43        | -0.68       | 1.63     | 10.6                    | —             | 1.15         | —           | 28     | GIC   | Pal 10   |
| 0138                | 53.217      | +3.3421  | 16.8   | 0.6             | 2.60       | 9.00          | 0.28        | 0.00        | 1.61     | 1.8                     | 9.11          | 1.40         | —           | 300    | Cl*   | Berkely 44   |
| 0141*               | 55.320      | +0.9176  | 2.3    | 0.6             | 2.70       | 8.70          | 0.23        | 0.00        | 1.67     | 1.1                     | 8.87          | 0.85         | —           | 41     | OpC   | NGC 6802,<br>Collinder 400                                       |
| 0147                | 56.747      | -4.5574  | -28.2  | 1.0             | 4.40       | 10.00         | 0.03        | -0.68       | 1.67     | 3.6                     | —             | 0.25         | -0.73       | 24     | GIC   | M 71,<br>NGC 6838  |
| 0152                | 58.267      | -2.3341  | 5.2    | 0.6             | 6.10       | 8.80          | 0.19        | 0.00        | 1.67     | 4.1                     | 8.90          | 1.05         | —           | 74     | OpC   | NGC 6827,<br>Berkeley 48   |
| 0155*               | 60.775      | -0.5552  | 9.3    | 0.5             | 3.80       | 8.80          | 0.42        | 0.00        | 1.67     | 0.9                     | 7.88          | 0.10         | —           | 74     | Cl*   | Teutsch 7  |
| 0156 <sup>6,*</sup> | 60.917      | -0.1084  | 13.4   | 0.8             | 7.50       | 8.60          | 0.76        | 0.00        | 1.57     | —                       | —             | —            | —           | 145    | Cl*   | BDS 2003 158   |
| 0159                | 62.666      | +8.3389  | -190.0 | 2.9             | 9.70       | 10.10         | 0.07        | -1.68       | 1.94     | 9.7                     | —             | 0.20         | -1.94       | 23     | GIC   | M 56,<br>NGC 6779  |
| 0164                | 63.779      | -19.3976 | -7.7   | 7.0             | 39.50      | 10.10         | 0.03        | -1.68       | 1.67     | 39.5                    | —             | 0.05         | -1.68       | 48     | GIC   | NGC 7006   |

Continued on next page

Table A1 – continued from previous page

| FSR ID             | Coordinates |            | BIC    | $r_{core}$<br>[pc] | this paper |                  |                |                |          | Literature <sup>1</sup> |                  |                 |                | SIMBAD        |         | other Names                |
|--------------------|-------------|------------|--------|--------------------|------------|------------------|----------------|----------------|----------|-------------------------|------------------|-----------------|----------------|---------------|---------|----------------------------|
|                    | l<br>[deg]  | b<br>[deg] |        |                    | d<br>[kpc] | log(age)<br>[yr] | $A_K$<br>[mag] | [M/H]<br>[dex] | $C_{HK}$ | d<br>[kpc]              | log(age)<br>[yr] | E(B-V)<br>[mag] | [M/H]<br>[dex] | r<br>[ $''$ ] | Class   |                            |
| 0167*              | 65.162      | -2.4057    | 19.8   | 0.3                | 1.60       | 9.00             | 0.20           | 0.00           | 1.80     | —                       | —                | —               | —              | —             | —       |                            |
| 0170*              | 65.929      | -2.6900    | 12.1   | 1.3                | 8.00       | 9.00             | 0.61           | 0.00           | 1.67     | —                       | —                | —               | —              | —             | —       |                            |
| 0177*              | 67.640      | +0.8548    | 15.2   | 0.6                | 3.60       | 8.90             | 0.23           | 0.00           | 1.61     | —                       | —                | —               | —              | 44            | OpC     | Kronberger 52              |
| 0178 <sup>7</sup>  | 67.876      | -2.8305    | 13.6   | 0.6                | 3.90       | 9.20             | 0.33           | 0.00           | 1.67     | 3.7                     | 9.30             | 1.34            | —              | —             | OpC     |                            |
| 0179               | 67.900      | -3.1769    | 5.2    | 1.1                | 6.00       | 9.00             | 0.38           | 0.00           | 1.59     | 4.9                     | 9.30             | 1.50            | —              | 173           | Cl*     | Berkeley 52                |
| 0184*              | 69.557      | -9.6561    | 98.0   | 1.2                | 6.90       | 9.20             | 0.02           | 0.00           | 4.58     | —                       | —                | —               | —              | —             | —       |                            |
| 0186               | 69.969      | +10.9141   | -43.4  | 1.1                | 4.10       | 9.55             | 0.07           | 0.00           | 2.34     | 4.1                     | 9.43             | 0.12            | 0.15           | 54            | OpC     | NGC 6791,<br>Berkeley 46   |
| 0190 <sup>8</sup>  | 70.729      | +0.9614    | 12.6   | 1.4                | 10.00      | 9.85             | 0.65           | 0.00           | 1.67     | 10.0                    | 9.85             | 2.37            | —              | —             | OpC/G1C |                            |
| 0191*              | 70.990      | +2.5840    | -2.7   | 0.6                | 3.40       | 8.50             | 0.38           | 0.00           | 1.67     | 2.0                     | 8.20             | 1.57            | —              | 372           | Cl*     | Berkeley 49                |
| 0197               | 72.155      | +0.2991    | 11.8   | 0.3                | 3.00       | 8.80             | 0.40           | 0.00           | 1.67     | 3.2                     | 8.18             | 1.66            | —              | 240           | Cl*     | Berkeley 51                |
| 0202*              | 73.990      | +8.4872    | -100.0 | 0.6                | 2.40       | 9.30             | 0.03           | 0.00           | 3.53     | 2.4                     | 9.17             | 0.24            | —              | 50            | OpC     | NGC 6819,<br>Melotte 223   |
| 0203*              | 74.312      | +1.2601    | 18.1   | 1.2                | 10.80      | 8.10             | 0.40           | 0.00           | 1.67     | —                       | —                | —               | —              | 22            | Cl*     | Kronberger 73              |
| 0208*              | 75.695      | +0.9893    | 2.1    | 0.9                | 4.40       | 8.10             | 0.36           | 0.00           | 1.56     | 1.8                     | 9.00             | 0.77            | —              | 88            | Cl*     | Berkeley 85                |
| 0214*              | 77.708      | +4.1767    | -2.9   | 1.9                | 8.70       | 8.70             | 0.13           | 0.00           | 1.87     | 5.3                     | 8.60             | 0.76            | —              | 374           | Cl*     | IC 1311                    |
| 0222*              | 78.395      | +2.5302    | 17.7   | 0.4                | 1.60       | 9.20             | 0.63           | 0.00           | 1.67     | —                       | —                | —               | —              | —             | —       |                            |
| 0233 <sup>9</sup>  | 79.869      | -0.9313    | 13.0   | 0.3                | 1.60       | 8.70             | 0.85           | 0.00           | 1.56     | 1.4                     | 9.00             | 2.74            | —              | —             | OpC     | [LK2002] Cl 10123          |
| 0256*              | 83.079      | -4.1254    | -6.7   | 1.5                | 6.90       | 9.60             | 0.22           | 0.00           | 1.88     | 2.3                     | 9.60             | 0.77            | —              | 187           | OpC     | Berkeley 54                |
| 0268               | 85.897      | -4.1416    | -144.2 | 1.0                | 3.50       | 9.15             | 0.20           | 0.00           | 1.84     | 3.2                     | 9.30             | 0.59            | —              | 125           | OpC     | NGC 7044,<br>Collinder 433 |
| 0269               | 85.995      | -5.1827    | -5.4   | 1.9                | 12.10      | 9.60             | 0.10           | 0.00           | 1.96     | 12.1                    | 9.60             | 0.40            | —              | 178           | OpC     | Berkeley 56                |
| 0275*              | 87.196      | +0.9740    | 15.3   | 0.6                | 3.60       | 9.00             | 0.25           | 0.00           | 1.67     | —                       | —                | —               | —              | —             | —       |                            |
| 0280*              | 88.240      | +0.2626    | 13.6   | 0.9                | 4.40       | 8.90             | 0.32           | 0.00           | 1.67     | —                       | —                | —               | —              | 33            | Cl*     | Teutsch 156                |
| 0282*              | 88.753      | +1.0502    | 15.5   | 0.5                | 2.50       | 9.05             | 0.30           | 0.00           | 1.73     | —                       | —                | —               | —              | —             | —       |                            |
| 0287*              | 90.010      | +0.2846    | 13.7   | 1.0                | 6.00       | 8.60             | 0.40           | 0.00           | 1.64     | 2.4                     | 8.70             | 1.00            | —              | 37            | Cl*     | Berkeley 91                |
| 0289               | 90.306      | +3.7604    | 5.9    | 0.9                | 3.50       | 9.10             | 0.42           | 0.00           | 1.67     | 3.1                     | 9.10             | 1.52            | —              | 393           | Cl*     | Berkeley 53                |
| 0294*              | 91.274      | +2.3434    | 14.5   | 1.0                | 7.10       | 8.70             | 0.55           | 0.00           | 1.64     | 0.9                     | 8.14             | 0.85            | —              | 279           | OpC     | NGC 7031                   |
| 0304*              | 93.560      | +0.6703    | 18.6   | 1.5                | 6.80       | 8.60             | 0.47           | 0.00           | 1.67     | —                       | —                | —               | —              | —             | —       |                            |
| 0313*              | 95.278      | +2.0726    | 13.8   | 1.1                | 6.00       | 9.20             | 0.42           | 0.00           | 1.67     | —                       | —                | —               | —              | 43            | OpC     | Kronberger 81              |
| 0315               | 95.920      | +12.2942   | -35.8  | 0.5                | 1.70       | 9.20             | 0.07           | 0.00           | 1.96     | 1.2                     | 9.35             | 0.32            | 0.02           | 72            | OpC     | NGC 6939,<br>Melotte 231   |
| 0327*              | 97.338      | +0.4451    | 14.8   | 0.4                | 2.30       | 7.25             | 0.32           | 0.00           | 1.67     | 2.3                     | 7.25             | 1.00            | —              | 79            | OpC     | NGC 7128                   |
| 0329*              | 97.928      | +5.0672    | -5.4   | 1.0                | 5.50       | 9.00             | 0.27           | 0.00           | 1.67     | —                       | —                | —               | —              | 222           | Cl*     | Berkeley 92                |
| 0333*              | 98.488      | +1.0632    | 12.2   | 0.9                | 5.00       | 9.10             | 0.27           | 0.00           | 1.71     | —                       | —                | —               | —              | —             | —       |                            |
| 0338*              | 99.243      | +0.9490    | -7.3   | 1.1                | 6.00       | 8.60             | 0.76           | 0.00           | 1.62     | —                       | —                | —               | —              | —             | —       |                            |
| 0342*              | 99.763      | -2.2132    | 4.6    | 0.7                | 2.60       | 9.10             | 0.10           | 0.00           | 2.15     | —                       | —                | —               | —              | —             | —       |                            |
| 0358 <sup>10</sup> | 103.346     | +2.2085    | -40.9  | 1.4                | 7.20       | 9.70             | 0.57           | 0.00           | 1.67     | 7.2                     | 9.70             | 1.78            | -0.37          | —             | OpC     | Kirkpatrick 1              |

Continued on next page

Table A1 – continued from previous page

| FSR ID               | Coordinates |          | BIC    | $r_{core}$ [pc] | this paper |               |             |             |          | Literature <sup>1</sup> |               |              |             | SIMBAD |         | other Names                |
|----------------------|-------------|----------|--------|-----------------|------------|---------------|-------------|-------------|----------|-------------------------|---------------|--------------|-------------|--------|---------|----------------------------|
|                      | l [deg]     | b [deg]  |        |                 | d [kpc]    | log(age) [yr] | $A_K$ [mag] | [M/H] [dex] | $C_{HK}$ | d [kpc]                 | log(age) [yr] | E(B-V) [mag] | [M/H] [dex] | r ["]  | Class   |                            |
| 0373                 | 105.354     | +9.4978  | -41.2  | 0.4             | 2.30       | 9.30          | 0.12        | 0.00        | 1.67     | 1.7                     | 9.20          | 0.40         | 0.04        | 53     | OpC     | NGC 7142,<br>Collinder 442 |
| 0385*                | 106.960     | +0.1164  | 12.9   | 0.3             | 1.70       | 8.90          | 0.25        | 0.00        | 1.67     | —                       | —             | —            | —           | —      | —       |                            |
| 0386*                | 107.126     | +12.6129 | 19.9   | 0.6             | 2.80       | 9.10          | 0.24        | 0.00        | 1.67     | —                       | —             | —            | —           | —      | —       |                            |
| 0391                 | 107.620     | -2.2686  | -10.0  | 0.7             | 4.00       | 9.10          | 0.15        | 0.00        | 2.05     | 4.2                     | 9.15          | 0.75         | —           | 30     | OpC     | NGC 7423,<br>Berkeley 57   |
| 0394*                | 108.318     | -0.8075  | 18.9   | 0.6             | 4.10       | 9.10          | 0.36        | 0.00        | 1.67     | —                       | —             | —            | —           | —      | —       |                            |
| 0412*                | 110.703     | +0.4833  | -41.7  | 1.6             | 6.10       | 9.10          | 0.46        | 0.00        | 1.67     | —                       | —             | —            | —           | 33     | Cl*     | Pfeiderer 3                |
| 0450                 | 115.539     | -5.3639  | 12.5   | 0.5             | 1.90       | 9.20          | 0.06        | 0.00        | 2.09     | 2.3                     | 9.20          | 0.22         | -0.08       | 80     | OpC     | NGC 7789,<br>Melotte 245   |
| 0460*                | 116.576     | -1.5334  | 8.9    | 1.2             | 6.10       | 9.10          | 0.28        | 0.00        | 1.67     | —                       | —             | —            | —           | —      | —       |                            |
| 0478*                | 118.544     | -2.6126  | -1.3   | 0.8             | 5.10       | 8.90          | 0.31        | 0.00        | 1.67     | —                       | —             | —            | —           | 17     | OpC     | Juchert-<br>Saloranta 1    |
| 0480*                | 118.586     | -1.0902  | 13.4   | 1.4             | 5.80       | 9.10          | 0.32        | 0.00        | 1.75     | —                       | —             | —            | —           | —      | —       |                            |
| 0489                 | 119.712     | -2.3171  | -14.1  | 1.1             | 5.50       | 8.90          | 0.26        | 0.00        | 1.67     | 5.3                     | 8.90          | 0.80         | —           | 37     | Cl*     | Berkeley 2                 |
| 0490                 | 119.776     | +1.7034  | -38.9  | 0.4             | 1.70       | 9.20          | 0.24        | 0.00        | 1.67     | 1.9                     | 9.30          | 0.70         | —           | 70     | Cl*     | King 1                     |
| 0514*                | 122.620     | +4.3250  | 10.7   | 1.9             | 8.00       | 8.10          | 0.27        | 0.00        | 1.67     | 3.3                     | 8.30          | 1.10         | —           | 168    | Cl*     | Berkeley 61                |
| 0523                 | 123.591     | +5.6045  | 15.1   | 0.4             | 2.50       | 8.95          | 0.17        | 0.00        | 1.73     | 1.6                     | 9.08          | 0.85         | —           | 62     | OpC     | Skiff 1                    |
| 0527 <sup>11</sup>   | 124.669     | +2.8388  | 18.1   | 1.0             | 5.00       | 8.80          | 0.30        | 0.00        | 1.67     | 7.2                     | 9.00          | 0.94         | —           | 79     | Cl*     | Pfeiderer 1                |
| 0545                 | 127.356     | +13.2183 | -26.0  | 1.1             | 4.00       | 9.30          | 0.17        | 0.00        | 1.79     | 3.2                     | 9.50          | 0.75         | —           | 345    | OpC     | Berkeley 8                 |
| 0548*                | 127.749     | +2.0909  | -66.0  | 0.7             | 4.20       | 8.40          | 0.31        | 0.00        | 1.65     | 4.0                     | 9.23          | 0.35         | —           | 25     | Cl*     | NGC 609                    |
| 0563*                | 130.050     | -0.1575  | -110.1 | 1.8             | 5.00       | 9.15          | 0.22        | 0.00        | 1.85     | 4.0                     | 8.63          | 1.05         | -0.17       | 137    | OpC     | IC 166,<br>Tombaugh 1      |
| 0584 <sup>12,*</sup> | 134.051     | +0.8413  | -35.8  | 0.3             | 1.40       | 10.20         | 0.50        | 0.00        | 1.48     | 1.4                     | —             | 2.97         | —           | —      | Cl*/GIC |                            |
| 0624                 | 139.422     | +0.1812  | -27.5  | 1.2             | 6.20       | 9.20          | 0.36        | 0.00        | 1.67     | 5.2                     | 9.70          | 1.25         | —           | 141    | OpC     | Berkeley 66                |
| 0639                 | 143.775     | -4.2683  | -44.1  | 0.4             | 2.10       | 9.00          | 0.20        | 0.00        | 1.74     | 1.9                     | 9.00          | 0.76         | -0.38       | 124    | OpC     | King 5                     |
| 0648*                | 146.669     | -8.9229  | -37.2  | 1.0             | 2.70       | 9.00          | 0.04        | 0.00        | 2.89     | 2.9                     | 8.70          | 0.30         | 0.10        | 103    | OpC     | NGC 1245,<br>Melotte 18    |
| 0652*                | 147.518     | +5.6634  | -82.8  | 1.3             | 3.90       | 9.00          | 0.17        | 0.00        | 1.76     | 1.1                     | 7.70          | 1.12         | —           | 182    | Cl*     | IC 361                     |
| 0667*                | 151.144     | -0.6509  | 13.6   | 0.1             | 0.75       | 8.90          | 0.09        | 0.00        | 1.67     | —                       | —             | —            | —           | —      | —       |                            |
| 0677                 | 154.837     | +2.4894  | -5.9   | 0.6             | 2.20       | 8.95          | 0.26        | 0.00        | 1.67     | 2.5                     | 9.00          | 0.79         | —           | 155    | Cl*     | Berkeley 67                |
| 0705                 | 160.707     | +4.8608  | -20.0  | 1.0             | 4.70       | 9.10          | 0.11        | 0.00        | 1.90     | 3.6                     | 9.20          | 0.37         | —           | 249    | OpC     | NGC 1798,<br>Berkeley 16   |
| 0726                 | 162.808     | +0.6572  | 1.2    | 1.0             | 5.00       | 9.30          | 0.15        | 0.00        | 1.79     | 5.5                     | 9.20          | 0.52         | —           | 416    | Cl*     | Berkeley 14                |
| 0731*                | 163.581     | +5.0501  | 22.0   | 1.1             | 4.70       | 9.15          | 0.20        | 0.00        | 1.67     | 5.8                     | 9.60          | 0.46         | 0.02        | 217    | OpC     | Berkeley 18,<br>King 22    |
| 0774                 | 172.640     | +0.3262  | -25.6  | 0.3             | 1.50       | 8.80          | 0.13        | 0.00        | 1.79     | 1.6                     | 8.57          | 0.42         | —           | 91     | Cl*     | NGC 1907                   |
| 0790*                | 173.747     | -5.8707  | 9.4    | 1.2             | 6.00       | 9.30          | 0.11        | 0.00        | 1.91     | —                       | —             | —            | —           | —      | —       |                            |

Continued on next page

Table A1 – continued from previous page

| FSR ID               | Coordinates |          | BIC    | $r_{core}$ [pc] | this paper |               |             |             |          | Literature <sup>1</sup> |               |              |             | SIMBAD |       | other Names   |
|----------------------|-------------|----------|--------|-----------------|------------|---------------|-------------|-------------|----------|-------------------------|---------------|--------------|-------------|--------|-------|---|
|                      | l [deg]     | b [deg]  |        |                 | d [kpc]    | log(age) [yr] | $A_K$ [mag] | [M/H] [dex] | $C_{HK}$ | d [kpc]                 | log(age) [yr] | E(B-V) [mag] | [M/H] [dex] | r ["]  | Class |   |
| 0810                 | 176.635     | +0.8982  | -15.5  | 0.6             | 2.40       | 9.00          | 0.30        | 0.00        | 1.72     | 3.9                     | 8.80          | 0.85         | —           | 480    | Cl*   | Berkeley 71   |
| 0818                 | 177.644     | +3.0819  | 7.6    | 0.3             | 1.25       | 8.70          | 0.08        | 0.00        | 1.85     | 1.4                     | 8.54          | 0.30         | 0.08        | 51     | OpC   | M 37,<br>NGC 2099                                     |
| 0825                 | 179.317     | +1.2611  | -2.1   | 0.7             | 3.40       | 8.60          | 0.13        | 0.00        | 1.67     | 3.0                     | 8.30          | 0.45         | —           | 385    | OpC   | Basel 4, Czernik 22                                   |
| 0828 <sup>13,*</sup> | 179.919     | +1.7460  | 18.3   | 1.4             | 5.70       | 9.20          | 0.14        | 0.00        | 2.15     | 2.8                     | 9.30          | 0.38         | -9.00       | 69     | OpC   |   |
| 0847 <sup>14</sup>   | 182.739     | +0.4827  | -8.4   | 0.8             | 4.10       | 9.15          | 0.31        | 0.00        | 1.67     | 2.9                     | 8.95          | 1.03         | —           | 17     | OpC   | Teutsch 51  |
| 0872                 | 186.643     | +1.7965  | -265.1 | 1.3             | 3.90       | 9.20          | 0.12        | 0.00        | 1.90     | 5.1                     | 9.02          | 0.36         | -0.23       | 65     | OpC   | NGC 2158,<br>Melotte 40,<br>Lund 206                  |
| 0875                 | 186.836     | -2.4796  | -25.7  | 1.9             | 6.00       | 9.20          | 0.20        | 0.00        | 1.73     | 5.0                     | 9.34          | 0.76         | —           | 105    | OpC   | Berkeley 21   |
| 0877*                | 187.450     | -1.0998  | 11.0   | 0.2             | 1.10       | 8.80          | 0.11        | 0.00        | 1.67     | 1.7                     | 7.80          | 0.32         | —           | 58     | Cl*   | Basel 11b   |
| 0879*                | 187.794     | +10.3037 | -92.3  | 0.7             | 3.00       | 9.00          | 0.01        | 0.00        | 7.34     | 3.4                     | 8.80          | 0.10         | —           | 132    | OpC   | NGC 2266,<br>Melotte 50                               |
| 0881                 | 188.056     | -2.2158  | -11.7  | 0.9             | 4.40       | 9.30          | 0.17        | 0.00        | 1.91     | 4.1                     | 9.25          | 0.54         | -0.41       | 198    | OpC   | Czernik 24  |
| 0884 <sup>15,*</sup> | 188.403     | -8.7922  | 0.3    | 0.7             | 7.00       | 9.00          | 0.00        | 0.00        | 1.67     | —                       | —             | —            | —           | —      | —     |   |
| 0926*                | 193.672     | -2.3381  | 5.1    | 1.3             | 6.00       | 9.10          | 0.39        | 0.00        | 1.82     | —                       | —             | —            | —           | 52     | Cl*   | Teutsch 58  |
| 0942 <sup>16</sup>   | 195.582     | -3.5934  | -0.3   | 0.4             | 2.40       | 9.00          | 0.21        | 0.00        | 1.86     | 2.0                     | 9.00          | 0.59         | —           | —      | OpC   |   |
| 0961                 | 197.241     | -2.3375  | -43.4  | 0.7             | 2.40       | 8.80          | 0.13        | 0.00        | 1.82     | 3.1                     | 9.00          | 0.52         | —           | —      | OpC   |   |
| 0961                 | 197.241     | -2.3375  | -43.4  | 0.7             | 2.40       | 8.80          | 0.13        | 0.00        | 1.82     | 3.8                     | 8.50          | 0.38         | —           | 91     | OpC   | NGC 2194,<br>Melotte 43,<br>Collinder 87              |
| 0963*                | 197.333     | -2.0879  | -1.3   | 0.4             | 2.50       | 8.70          | 0.14        | 0.00        | 1.90     | —                       | —             | —            | —           | —      | —     |   |
| 0971                 | 198.044     | -5.7968  | -66.8  | 1.3             | 4.00       | 9.30          | 0.10        | 0.00        | 2.01     | 4.0                     | 9.20          | 0.25         | -0.26       | 141    | OpC   | NGC 2141,<br>Collinder 79                             |
| 0972*                | 198.111     | +19.6514 | -326.5 | 0.5             | 2.30       | 9.30          | 0.00        | 0.00        | 1.67     | —                       | —             | —            | —           | 63     | OpC   | NGC 2429,<br>Melotte 69,<br>Collinder 154,<br>Raab 56 |
| 0989                 | 202.817     | +1.0224  | -8.6   | 0.6             | 3.00       | 9.45          | 0.19        | 0.00        | 1.81     | 3.0                     | 9.60          | 0.58         | —           | 198    | OpC   | Collinder 105,<br>Trumpler 5                          |
| 0995*                | 203.380     | +11.8209 | -21.8  | 0.5             | 1.90       | 9.00          | 0.02        | 0.00        | 3.13     | 2.2                     | 8.85          | 0.12         | -0.07       | 68     | OpC   | NGC 2355,<br>Melotte 63                               |
| 1002                 | 204.368     | -1.6948  | -9.1   | 0.5             | 2.50       | 8.80          | 0.14        | 0.00        | 1.84     | 2.9                     | 8.50          | 0.48         | —           | 34     | OpC   | NGC 2236,<br>Collinder 94,<br>Ruprecht 501            |
| 1007                 | 205.878     | -12.6098 | 11.5   | 0.2             | 0.95       | 9.10          | 0.23        | 0.00        | 1.67     | 0.9                     | 9.30          | 0.63         | -0.11       | 26     | OpC   | NGC 2112,<br>Collinder 76                             |

Continued on next page

Table A1 – continued from previous page

| FSR ID               | Coordinates |          | BIC   | $r_{core}$ [pc] | this paper |               |             |             |          | Literature <sup>1</sup> |               |              |             | SIMBAD |       | other Names                  |
|----------------------|-------------|----------|-------|-----------------|------------|---------------|-------------|-------------|----------|-------------------------|---------------|--------------|-------------|--------|-------|------------------------------|
|                      | l [deg]     | b [deg]  |       |                 | d [kpc]    | log(age) [yr] | $A_K$ [mag] | [M/H] [dex] | $C_{HK}$ | d [kpc]                 | log(age) [yr] | E(B-V) [mag] | [M/H] [dex] | r ["]  | Class |                              |
| 1049                 | 209.636     | -1.8600  | 11.2  | 0.5             | 2.30       | 9.30          | 0.12        | 0.00        | 1.83     | 2.0                     | 9.15          | 0.50         | —           | 246    | OpC   | Collinder 110                |
| 1055                 | 210.571     | -2.1013  | -61.3 | 0.6             | 3.00       | 8.90          | 0.19        | 0.00        | 1.85     | 3.6                     | 9.00          | 0.55         | —           | 2      | Cl*   | NGC 2262,<br>Collinder 109   |
| 1058                 | 210.781     | +2.8825  | -13.7 | 0.7             | 3.60       | 8.80          | 0.11        | 0.00        | 1.99     | 4.8                     | 8.50          | 0.50         | —           | 87     | OpC   | Berkeley 30,<br>Biurakan 9   |
| 1070 <sup>17</sup>   | 212.162     | -3.4261  | -11.1 | 0.9             | 5.10       | 9.15          | 0.15        | 0.00        | 1.67     | 4.7                     | 9.30          | 0.40         | —           | 187    | Cl*   | Berkeley 24                  |
| 1089                 | 213.456     | +3.3003  | -9.5  | 0.6             | 3.20       | 8.80          | 0.03        | 0.00        | 1.67     | 3.8                     | 8.60          | 0.13         | -0.52       | 66     | OpC   | NGC 2324,<br>Melotte 59      |
| 1113*                | 216.303     | +3.2509  | 8.1   | 0.8             | 4.00       | 9.50          | 0.00        | 0.00        | 1.67     | —                       | —             | —            | —           | —      | —     | —                            |
| 1119*                | 217.123     | +5.9673  | 19.9  | 1.0             | 5.50       | 9.20          | 0.00        | -0.68       | 1.67     | 3.1                     | 8.95          | 0.16         | —           | 224    | OpC   | Czernik 28                   |
| 1121*                | 217.292     | +6.3119  | 5.5   | 0.7             | 3.40       | 9.30          | 0.01        | 0.00        | 6.23     | 3.1                     | 8.95          | 0.16         | —           | 48     | Cl*   | King 23                      |
| 1135                 | 218.787     | -9.8622  | -20.3 | 0.5             | 3.10       | 9.10          | 0.11        | 0.00        | 2.01     | 3.2                     | 9.10          | 0.35         | —           | 18     | OpC   | NGC 2225                     |
| 1138 <sup>18,*</sup> | 219.250     | +5.1768  | 1.4   | 0.7             | 3.60       | 9.40          | 0.00        | 0.00        | 1.67     | 4.6                     | 8.80          | 0.12         | —           | 392    | Cl*   | Berkeley 77                  |
| 1174                 | 223.540     | +10.0865 | -19.5 | 1.2             | 4.80       | 9.50          | 0.02        | 0.00        | 2.83     | 4.8                     | 9.90          | 0.12         | —           | 280    | OpC   | Berkeley 39                  |
| 1201*                | 226.019     | -16.0990 | -27.7 | 1.0             | 4.00       | 9.30          | 0.05        | -0.68       | 2.05     | 2.6                     | 8.90          | 0.09         | -0.33       | 383    | OpC   | NGC 2204,<br>Melotte 44      |
| 1214*                | 227.492     | -0.5626  | 8.1   | 1.1             | 6.00       | 9.50          | 0.13        | 0.00        | 2.17     | 6.1                     | 9.50          | 0.40         | —           | 32     | OpC   | Berkeley 36                  |
| 1215                 | 227.871     | +5.3783  | -35.5 | 0.5             | 2.50       | 9.00          | 0.03        | 0.00        | 1.67     | 3.0                     | 8.80          | 0.20         | 0.00        | 124    | OpC   | Melotte 72                   |
| 1217                 | 227.908     | +15.3836 | 12.3  | 0.2             | 0.70       | 8.70          | 0.00        | 0.00        | 1.67     | 0.8                     | 8.56          | 0.03         | 0.08        | 132    | Cl*   | M 48,<br>NGC 2548            |
| 1222*                | 228.948     | +4.5131  | -10.7 | 0.5             | 2.30       | 9.10          | 0.00        | 0.00        | 1.67     | 3.2                     | 8.40          | 0.11         | -0.30       | 237    | OpC   | Melotte 71,<br>Collinder 155 |
| 1225*                | 229.820     | -1.4077  | -2.2  | 0.3             | 0.90       | 9.10          | 0.02        | 0.00        | 3.19     | 1.9                     | 8.75          | 0.11         | -0.15       | 103    | OpC   | NGC 2360,<br>Melotte 64      |
| 1230                 | 230.577     | +9.9461  | -54.4 | 0.9             | 3.10       | 9.20          | 0.00        | 0.00        | 1.67     | 3.5                     | 9.05          | 0.08         | -0.37       | 61     | OpC   | NGC 2506,<br>Melotte 80      |
| 1231                 | 230.803     | +1.0129  | -34.1 | 0.6             | 3.50       | 9.50          | 0.14        | 0.00        | 1.89     | 3.7                     | 9.40          | 0.52         | —           | 57     | OpC   | Haffner 10                   |
| 1238*                | 231.515     | +3.3025  | -18.1 | 0.7             | 4.70       | 9.20          | 0.13        | -0.68       | 1.67     | 3.4                     | 9.40          | 0.31         | —           | 70     | Cl*   | NGC 2425                     |
| 1241*                | 231.891     | +4.0891  | 19.5  | 0.2             | 1.40       | 8.50          | 0.02        | 0.00        | 3.55     | 1.4                     | 8.40          | 0.15         | 0.05        | 197    | Cl*   | M 46,<br>NGC 2437            |
| 1244*                | 232.080     | +2.6929  | -4.3  | 0.4             | 2.20       | 8.70          | 0.10        | 0.00        | 1.67     | 1.4                     | 7.50          | 0.10         | —           | 103    | OpC   | Ruprecht 26                  |
| 1246                 | 232.347     | -7.2958  | -6.4  | 0.4             | 2.20       | 9.10          | 0.07        | 0.00        | 2.12     | 3.0                     | 9.00          | 0.40         | —           | 80     | OpC   | Haffner 1,<br>Tombaugh 1     |
| 1250*                | 232.844     | -6.8690  | -17.8 | 1.4             | 8.00       | 9.00          | 0.15        | -0.68       | 1.67     | 13.3                    | 9.00          | 0.08         | -0.36       | 234    | OpC   | Haffner 2,<br>Tombaugh 2     |
| 1256*                | 233.746     | +11.1047 | 9.8   | 0.3             | 1.00       | 9.00          | 0.02        | -0.68       | 2.77     | 1.4                     | 8.57          | 0.08         | 0.13        | 84     | OpC   | NGC 2539,<br>Melotte 83      |
| 1266*                | 235.379     | +0.1513  | 6.9   | 0.2             | 0.95       | 9.00          | 0.02        | 0.00        | 4.83     | —                       | —             | —            | —           | 26     | Cl*   | Teutsch 61                   |

Continued on next page

Table A1 – continued from previous page

| FSR ID | Coordinates |          | BIC    | $r_{core}$ [pc] | this paper |               |             |             |          | Literature <sup>1</sup> |               |              |             | SIMBAD |       | other Names  |
|--------|-------------|----------|--------|-----------------|------------|---------------|-------------|-------------|----------|-------------------------|---------------|--------------|-------------|--------|-------|--|
|        | l [deg]     | b [deg]  |        |                 | d [kpc]    | log(age) [yr] | $A_K$ [mag] | [M/H] [dex] | $C_{HK}$ | d [kpc]                 | log(age) [yr] | E(B-V) [mag] | [M/H] [dex] | r ["]  | Class |  |
| 1267*  | 235.477     | +1.7956  | 6.9    | 0.5             | 2.10       | 8.70          | 0.06        | 0.00        | 1.96     | 1.8                     | 8.20          | 0.12         | —           | 401    | Cl*   | NGC 2432   |
| 1271   | 235.991     | +5.3764  | 16.9   | 0.3             | 1.60       | 8.80          | 0.05        | 0.00        | 2.25     | 1.2                     | 9.00          | 0.10         | —           | 5      | OpC   | NGC 2479,<br>Trumpler 8                                    |
| 1274*  | 236.283     | +0.0702  | 1.4    | 0.4             | 1.80       | 8.80          | 0.02        | 0.00        | 3.28     | 2.2                     | 7.40          | 0.45         | —           | 44     | OpC   | NGC 2421   |
| 1282*  | 237.854     | +5.8572  | -27.9  | 0.6             | 2.50       | 9.10          | 0.01        | 0.00        | 5.09     | 0.9                     | 9.90          | 0.15         | —           | 142    | Cl*   | NGC 2509,<br>Melotte 81                                    |
| 1296*  | 239.485     | -18.0099 | -78.5  | 0.8             | 4.50       | 9.60          | 0.00        | -0.68       | 1.67     | 4.5                     | 9.65          | 0.05         | -0.44       | 28     | OpC   | NGC 2243,<br>Melotte 46                                    |
| 1298*  | 239.797     | +2.7191  | 13.7   | 0.6             | 3.20       | 9.20          | 0.11        | 0.00        | 1.67     | —                       | —             | —            | —           | —      | —     | —  |
| 1299*  | 239.928     | -4.9366  | -6.8   | 0.5             | 2.30       | 8.10          | 0.26        | 0.00        | 1.67     | 1.1                     | 7.65          | 0.70         | -0.01       | 106    | OpC   | Ruprecht 18  |
| 1301*  | 240.037     | +0.1531  | -11.1  | 0.2             | 0.70       | 9.00          | 0.00        | -0.68       | 1.67     | 1.0                     | 8.60          | 0.05         | —           | 80     | Cl*   | M 93,<br>NGC 2447,<br>Collinder 160                        |
| 1310   | 242.395     | -3.5267  | 6.3    | 1.0             | 4.80       | 9.10          | 0.12        | 0.00        | 2.05     | 6.1                     | 8.70          | 0.57         | —           | 113    | Cl*   | Haffner 11,<br>vdB-Hagen 3                                 |
| 1313*  | 243.067     | +1.2807  | -3.8   | 0.7             | 2.30       | 8.00          | 0.08        | 0.00        | 1.67     | 2.3                     | 8.00          | 0.25         | —           | 50     | OpC   | Trumpler 9   |
| 1322   | 245.634     | -15.9998 | -176.8 | 2.7             | 10.00      | 10.00         | 0.06        | -1.28       | 2.37     | 10.4                    | —             | 0.13         | -1.85       | 32     | GIC   | NGC 2298   |
| 1325   | 245.906     | -1.7415  | -13.8  | 0.8             | 4.10       | 9.10          | 0.20        | 0.00        | 1.78     | 4.1                     | 9.00          | 0.85         | —           | 150    | OpC   | King 24,<br>Czernik 32,<br>vdB-Hagen 17                    |
| 1330*  | 246.720     | -0.7697  | -16.7  | 0.4             | 1.30       | 8.80          | 0.07        | 0.00        | 2.29     | 4.0                     | 7.26          | 0.37         | 0.08        | 16     | OpC   | NGC 2489,<br>vdB-Hagen 15                                  |
| 1337*  | 247.708     | -2.5250  | -46.4  | 0.6             | 3.00       | 8.10          | 0.31        | 0.00        | 1.67     | 2.9                     | 7.70          | 1.26         | —           | 145    | Cl*   | Haffner 17,<br>vdB-Hagen 12                                |
| 1354*  | 249.833     | +2.9693  | 1.8    | 0.2             | 1.30       | 8.80          | 0.01        | 0.00        | 4.49     | 1.7                     | 8.50          | 0.13         | —           | 157    | OpC   | NGC 2567,<br>vdB-Hagen 26                                  |
| 1361*  | 251.562     | -5.0032  | 15.4   | 0.2             | 1.50       | 9.00          | 0.16        | 0.00        | 1.67     | —                       | —             | —            | —           | —      | —     | —  |
| 1362*  | 251.596     | +6.6499  | -4.9   | 0.4             | 1.80       | 9.20          | 0.01        | 0.00        | 4.74     | 2.0                     | 8.57          | 0.09         | —           | 84     | OpC   | NGC 2627,<br>Collinder 188,<br>Melotte 87,<br>vdB-Hagen 38 |
| 1369   | 253.575     | -5.8391  | -6.8   | 0.3             | 1.30       | 9.00          | 0.05        | 0.00        | 2.06     | 1.2                     | 8.85          | 0.28         | 0.01        | 69     | OpC   | NGC 2477,<br>Melotte 78,<br>vdB-Hagen 13                   |
| 1373   | 254.572     | +6.0758  | 1.5    | 0.6             | 2.80       | 8.80          | 0.09        | 0.00        | 1.67     | 2.2                     | 9.15          | 0.04         | —           | 111    | OpC   | NGC 2658,<br>vdB-Hagen 48                                  |
| 1385*  | 257.879     | +0.5044  | -7.1   | 0.6             | 2.10       | 9.50          | 0.24        | 0.00        | 1.76     | 1.4                     | 9.02          | 1.30         | —           | 296    | OpC   | Pismis 3, vdB-Hagen 33                                     |

Continued on next page

Table A1 – continued from previous page

| FSR ID               | Coordinates |            | BIC    | $r_{core}$<br>[pc] | this paper |                  |                |                |          | Literature <sup>1</sup> |                  |                 |                | SIMBAD        |       | other Names                               |
|----------------------|-------------|------------|--------|--------------------|------------|------------------|----------------|----------------|----------|-------------------------|------------------|-----------------|----------------|---------------|-------|---|
|                      | l<br>[deg]  | b<br>[deg] |        |                    | d<br>[kpc] | log(age)<br>[yr] | $A_K$<br>[mag] | [M/H]<br>[dex] | $C_{HK}$ | d<br>[kpc]              | log(age)<br>[yr] | E(B-V)<br>[mag] | [M/H]<br>[dex] | r<br>[ $''$ ] | Class |   |
| 1386*                | 257.994     | -0.9963    | -5.2   | 0.7                | 5.00       | 9.20             | 0.40           | 0.00           | 1.67     | 4.7                     | 9.40             | 1.24            | —              | 15            | OpC   | Saurer 2                                  |
| 1388*                | 258.496     | +2.2968    | 2.2    | 0.9                | 3.90       | 9.10             | 0.13           | 0.00           | 1.90     | —                       | —                | —               | —              | 108           | OpC   | Ruprecht 66,<br>vdB-Hagen 41              |
| 1392                 | 258.865     | -3.3346    | -122.3 | 1.0                | 4.10       | 9.20             | 0.34           | 0.00           | 1.70     | 3.3                     | 9.06             | 1.30            | —              | 31            | OpC   | Pismis 2, vdB-<br>Hagen 25                |
| 1393                 | 259.055     | +2.0041    | -8.0   | 0.8                | 3.60       | 9.00             | 0.16           | 0.00           | 1.95     | 4.9                     | 8.70             | 0.69            | —              | 74            | Cl*   | Pismis 7, vdB-<br>Hagen 43                |
| 1396*                | 259.579     | -14.2491   | 19.8   | 1.2                | 5.00       | 9.45             | 0.02           | 0.00           | 1.67     | 4.3                     | 9.45             | 0.14            | -0.35          | 72            | OpC   | Collinder 147,<br>Melotte 66              |
| 1399*                | 259.952     | +2.0556    | 6.0    | 1.3                | 6.80       | 8.40             | 0.36           | 0.00           | 1.58     | —                       | —                | —               | —              | —             | —     | —   |
| 1404*                | 261.528     | +3.7552    | 9.2    | 0.5                | 3.70       | 9.00             | 0.17           | 0.00           | 1.84     | —                       | —                | —               | —              | 106           | Cl*   | vdB-Hagen 55                              |
| 1408*                | 262.007     | +8.6030    | -3.7   | 0.8                | 3.20       | 9.10             | 0.01           | 0.00           | 1.67     | 1.9                     | 8.60             | 0.12            | -0.17          | 38            | OpC   | NGC 2818A,<br>Melotte 96,<br>vdB-Hagen 59 |
| 1409*                | 262.157     | +0.7894    | -28.7  | 0.4                | 1.50       | 8.40             | 0.33           | 0.00           | 1.59     | 1.7                     | 7.90             | 1.04            | —              | 28            | Cl*   | NGC 2671,<br>vdB-Hagen 51                 |
| 1415 <sup>19,*</sup> | 263.744     | -1.8061    | -36.0  | 1.6                | 10.00      | 9.40             | 0.45           | 0.00           | 1.67     | 3.5                     | 9.25             | 1.87            | —              | —             | OpC   | —   |
|                      |             |            |        |                    |            |                  |                |                |          | 8.6                     | 9.40             | 1.47            | 0.00           | —             | OpC   | —   |
| 1420*                | 264.094     | -5.5126    | 9.6    | 0.7                | 3.90       | 9.00             | 0.12           | 0.00           | 1.95     | —                       | —                | —               | —              | 73            | OpC   | Ruprecht 60,<br>vdB-Hagen 31              |
| 1439*                | 265.283     | +6.3723    | -14.4  | 0.9                | 5.90       | 9.10             | 0.06           | 0.00           | 2.56     | 6.4                     | 8.80             | 0.46            | —              | 161           | OpC   | NGC 2849,<br>vdB-Hagen 61                 |
| 1445                 | 265.939     | -3.0032    | -38.0  | 0.5                | 2.80       | 9.00             | 0.11           | 0.00           | 1.89     | 2.8                     | 9.03             | 0.31            | -0.18          | 50            | OpC   | NGC 2660,<br>Melotte 92,<br>vdB-Hagen 45  |
| 1458*                | 268.654     | +3.2100    | -23.1  | 0.5                | 2.10       | 9.10             | 0.15           | 0.00           | 1.83     | —                       | —                | —               | —              | 84            | Cl*   | Pismis 12, vdB-<br>Hagen 62               |
| 1463*                | 269.245     | -3.7475    | 15.5   | 0.8                | 4.50       | 9.00             | 0.30           | 0.00           | 1.76     | —                       | —                | —               | —              | —             | —     | —   |
| 1480*                | 272.500     | +2.8701    | -25.4  | 0.4                | 2.30       | 9.10             | 0.13           | 0.00           | 1.67     | 4.7                     | 8.90             | 0.53            | —              | 290           | Cl*   | Pismis 15                                 |
| 1483*                | 273.642     | +0.9465    | 7.4    | 0.8                | 5.00       | 9.00             | 0.23           | 0.00           | 1.84     | —                       | —                | —               | —              | 169           | Cl*   | vdB-Hagen 73                              |
| 1486*                | 273.774     | -0.3812    | 4.0    | 1.2                | 7.60       | 8.60             | 0.34           | 0.00           | 1.70     | 7.4                     | 9.08             | 0.95            | —              | 138           | Cl*   | vdB-Hagen 67                              |
| 1494*                | 275.492     | -1.1605    | 3.7    | 0.7                | 3.20       | 9.00             | 0.16           | 0.00           | 1.76     | —                       | —                | —               | —              | 284           | Cl*   | vdB-Hagen 72                              |
| 1499                 | 276.790     | -4.4763    | 7.2    | 0.6                | 3.90       | 9.10             | 0.09           | 0.00           | 1.85     | 4.3                     | 9.15             | 0.24            | —              | 167           | OpC   | Ruprecht 75,<br>vdB-Hagen 65              |
| 1503                 | 277.232     | +8.6459    | -230.2 | 1.5                | 4.90       | 10.00            | 0.09           | -1.68          | 1.67     | 4.9                     | —                | 0.21            | -1.45          | 22            | GIC   | NGC 3201                                  |
| 1520*                | 280.208     | +0.0730    | 6.6    | 0.5                | 4.00       | 8.60             | 0.28           | 0.00           | 1.67     | 1.4                     | 8.70             | 0.21            | —              | 367           | OpC   | Ruprecht 85,<br>vdB-Hagen 83              |
| 1521 <sup>20,*</sup> | 280.436     | -1.6247    | 14.8   | 0.8                | 4.00       | 9.45             | 0.30           | 0.00           | 1.67     | 4.0                     | 9.45             | 0.90            | —              | —             | OpC   | —   |

Continued on next page

Table A1 – continued from previous page

| FSR ID             | Coordinates |          | BIC    | $r_{core}$ [pc] | this paper |               |             |             |          | Literature <sup>1</sup> |               |              |             | SIMBAD |       | other Names                                   |
|--------------------|-------------|----------|--------|-----------------|------------|---------------|-------------|-------------|----------|-------------------------|---------------|--------------|-------------|--------|-------|---|
|                    | l [deg]     | b [deg]  |        |                 | d [kpc]    | log(age) [yr] | $A_K$ [mag] | [M/H] [dex] | $C_{HK}$ | d [kpc]                 | log(age) [yr] | E(B-V) [mag] | [M/H] [dex] | r ["]  | Class |   |
| 1523*              | 281.008     | -0.2456  | -2.1   | 1.2             | 7.50       | 8.10          | 0.82        | 0.00        | 1.63     | 4.5                     | 9.30          | 1.10         | —           | —      | OpC   |   |
| 1528*              | 282.172     | +2.2751  | 14.5   | 1.5             | 6.70       | 9.15          | 0.09        | 0.00        | 2.02     | —                       | —             | —            | —           | 36     | Cl*   | Schuster CL                                   |
| 1529*              | 282.195     | -11.2454 | -332.0 | 3.4             | 11.50      | 9.90          | 0.03        | -0.68       | 3.21     | —                       | —             | —            | —           | 61     | Cl*   | Teutsch 44                                    |
| 1534*              | 283.139     | -1.4575  | 14.6   | 0.2             | 1.00       | 9.10          | 0.01        | 0.00        | 7.62     | 8.9                     | —             | 0.23         | -1.37       | 29     | GIC   | NGC 2808                                      |
| 1544               | 285.342     | -8.8249  | 10.0   | 0.2             | 1.30       | 8.70          | 0.04        | 0.00        | 2.04     | 2.6                     | 7.94          | 0.53         | —           | 34     | Cl*   | Bochum 8,<br>vdB-Hagen 90                     |
| 1546*              | 286.090     | -2.6269  | 10.0   | 0.5             | 3.70       | 9.00          | 0.05        | 0.00        | 2.16     | 1.8                     | 8.56          | 0.10         | —           | 73     | OpC   | Ruprecht 84                                   |
| 1548               | 286.770     | +16.9063 | 98.0   | 0.2             | 1.00       | 9.20          | 0.00        | 0.00        | 1.67     | 1.5                     | 8.30          | 0.25         | —           | 30     | Cl*   | NGC 3255,<br>vdB-Hagen 96                     |
| 1550*              | 287.007     | -2.0929  | 8.2    | 0.8             | 6.30       | 9.00          | 0.16        | 0.00        | 1.67     | 0.9                     | 9.08          | 0.07         | -0.09       | 48     | OpC   | NGC 3680,<br>Melotte 106                      |
| 1555 <sup>21</sup> | 287.768     | +0.1677  | 9.3    | 0.8             | 3.50       | 9.40          | 0.33        | 0.00        | 1.77     | —                       | —             | —            | —           | 13     | Cl*   | Teutsch 105                                   |
| 1559*              | 289.160     | +0.3060  | 8.4    | 1.1             | 6.90       | 8.80          | 0.25        | 0.00        | 1.75     | 3.1                     | 9.18          | 1.19         | —           | —      | OpC   |   |
| 1565*              | 290.185     | +2.8847  | 11.5   | 0.7             | 3.10       | 9.10          | 0.08        | 0.00        | 1.67     | 4.8                     | 9.25          | 0.76         | —           | —      | OpC   |   |
| 1586*              | 292.841     | -1.1984  | 17.8   | 0.5             | 2.40       | 8.90          | 0.43        | 0.00        | 1.57     | —                       | —             | —            | —           | 34     | Cl*   | Teutsch 106                                   |
| 1587               | 292.916     | -2.4062  | 5.1    | 0.5             | 1.50       | 8.80          | 0.08        | 0.00        | 1.94     | —                       | —             | —            | —           | 80     | OpC   | Trumpler 19                                   |
| 1590               | 294.376     | +6.1789  | -8.4   | 0.5             | 2.10       | 8.90          | 0.07        | 0.00        | 1.67     | —                       | —             | —            | —           | —      | —     | —   |
| 1603 <sup>22</sup> | 298.222     | -0.5070  | 15.9   | 0.6             | 2.90       | 8.90          | 0.20        | 0.00        | 1.67     | 2.2                     | 8.30          | 0.48         | —           | 143    | OpC   | Melotte 105,<br>vdB-Hagen 117                 |
| 1611*              | 299.317     | +4.5611  | -8.6   | 0.4             | 2.50       | 9.10          | 0.10        | 0.00        | 1.91     | 2.3                     | 8.80          | 0.30         | -0.17       | 168    | OpC   | NGC 3960,<br>Melotte 108,<br>vdB-Hagen 123    |
| 1619               | 301.002     | -9.8778  | -129.9 | 1.5             | 4.60       | 10.20         | 0.15        | -2.28       | 1.67     | 2.7                     | 9.00          | 0.55         | —           | 33     | OpC   | Ruprecht 101                                  |
| 1624*              | 301.495     | +2.1968  | 19.6   | 0.5             | 3.70       | 9.20          | 0.10        | 0.00        | 1.67     | 0.5                     | 8.45          | 0.15         | —           | 14     | Cl*   | NGC 4337,<br>vdB-Hagen 129                    |
| 1627               | 301.706     | -5.5266  | 12.7   | 0.7             | 2.80       | 9.50          | 0.12        | 0.00        | 1.82     | 4.6                     | —             | 0.45         | -2.09       | 38     | GIC   | NGC 4372                                      |
| 1632*              | 303.183     | -4.2944  | 19.9   | 1.1             | 5.00       | 9.40          | 0.13        | 0.00        | 1.84     | 2.4                     | 8.20          | 0.26         | —           | 152    | OpC   | Trumpler 20,<br>vdB-Hagen 137                 |
| 1633               | 303.216     | +2.4710  | 16.9   | 0.4             | 2.00       | 7.20          | 0.10        | 0.00        | 1.67     | 2.2                     | 9.95          | 0.27         | -0.14       | 372    | OpC   | Collinder 261,<br>Harvard 6,<br>vdB-Hagen 136 |
| 1636               | 303.611     | -8.0112  | -219.2 | 1.8             | 5.70       | 10.20         | 0.15        | -1.68       | 1.92     | —                       | —             | —            | —           | 355    | Cl*   | vdB-Hagen 140                                 |
| 1637*              | 303.635     | -2.0850  | 15.1   | 0.4             | 2.00       | 9.00          | 0.18        | 0.00        | 1.67     | 2.0                     | 7.20          | 0.39         | —           | 119    | OpC   | NGC 4755,<br>Melotte 114,<br>vdB-Hagen 141    |
|                    |             |          |        |                 |            |               |             |             |          | 5.7                     | —             | 0.33         | -1.79       | 21     | GIC   | NGC 4833                                      |
|                    |             |          |        |                 |            |               |             |             |          | 3.1                     | 8.37          | 0.80         | —           | 30     | OpC   | NGC 4815,<br>vdB-Hagen 142                    |

Continued on next page

Table A1 – continued from previous page

| FSR ID               | Coordinates |          | BIC    | $r_{core}$ [pc] | d [kpc] | this paper    |             |             |         | $C_{HK}$          | Literature <sup>1</sup> |                      |             |             | SIMBAD                        |  | other Names |
|----------------------|-------------|----------|--------|-----------------|---------|---------------|-------------|-------------|---------|-------------------|-------------------------|----------------------|-------------|-------------|-------------------------------|--|-------------|
|                      | l [deg]     | b [deg]  |        |                 |         | log(age) [yr] | $A_K$ [mag] | [M/H] [dex] | d [kpc] |                   | log(age) [yr]           | E(B-V) [mag]         | [M/H] [dex] | r ["]       | Class                         |  |             |
| 1657*                | 307.931     | +3.7544  | -1.0   | 1.2             | 7.00    | 9.00          | 0.00        | -0.68       | 1.67    | —                 | —                       | —                    | —           | —           | —                             | —  |             |
| 1664                 | 309.104     | +14.9708 | 27.1   | 1.4             | 4.90    | 10.20         | 0.07        | -1.68       | 1.99    | 4.9               | —                       | 0.12                 | -1.57       | 19          | GIC                           | NGC 5139,<br>OmegaCen                        |             |
| 1670*                | 310.840     | +0.1621  | 14.2   | 0.5             | 2.50    | 8.40          | 0.69        | 0.00        | 1.60    | —                 | —                       | —                    | —           | 195         | Cl*                           | Loden 1101                                   |             |
| 1671                 | 311.620     | +10.5731 | -299.2 | 3.0             | 11.30   | 10.20         | 0.08        | -1.68       | 1.67    | 11.3              | —                       | 0.24                 | -1.79       | 27          | GIC                           | NGC 5286                                     |             |
| 1691                 | 317.753     | -15.8235 | -102.9 | 2.9             | 14.70   | 10.20         | 0.02        | -1.68       | 1.67    | 14.7              | —                       | 0.04                 | -1.82       | 21          | GIC                           | NGC 6101                                     |             |
| 1702                 | 325.559     | -17.5671 | -293.4 | 1.6             | 7.20    | 10.20         | 0.04        | -1.28       | 1.67    | 7.2               | —                       | 0.09                 | -1.06       | 16          | GIC                           | NGC 6362                                     |             |
| 1704                 | 325.802     | -2.9680  | 22.2   | 0.7             | 2.30    | 9.00          | 0.16        | 0.00        | 1.67    | 2.7               | 9.08                    | 0.45                 | —           | 175         | OpC                           | NGC 6005,<br>Melotte 138,<br>vdB-Hagen 179   |             |
| 1707                 | 326.609     | +4.8675  | -8.5   | 2.0             | 7.00    | 10.20         | 0.12        | -0.38       | 1.67    | 7.0               | —                       | 0.47                 | -0.37       | 32          | GIC                           | NGC 5927,<br>vdB-Hagen 173                   |             |
| 1708                 | 327.593     | +4.1951  | -41.8  | 2.8             | 11.90   | 10.20         | 0.19        | -1.68       | 1.67    | 11.9              | —                       | 0.55                 | -1.38       | 40          | GIC                           | NGC 5946,<br>vdB-Hagen 175                   |             |
| 1711                 | 328.786     | -2.7899  | 3.0    | 1.2             | 6.60    | 10.20         | 0.25        | -0.68       | 1.57    | 6.6               | —                       | 0.73                 | -0.62       | 58          | GIC                           | Lynga 7, vdB-Hagen 184                       |             |
| 1716 <sup>23,*</sup> | 329.792     | -1.5892  | 14.3   | 1.0             | 7.00    | 9.30          | 0.45        | 0.00        | 1.67    | 0.8<br>2.3<br>7.0 | 9.85<br>10.08<br>9.30   | 2.03<br>2.03<br>1.69 | —<br>—<br>— | —<br>—<br>— | OpC/GIC<br>OpC/GIC<br>OpC/GIC |  |             |
| 1724*                | 333.701     | -5.7745  | 15.9   | 0.6             | 3.20    | 8.80          | 0.24        | 0.00        | 1.54    | 0.9               | 9.07                    | 0.21                 | —           | 195         | OpC                           | NGC 6208,<br>Collinder 313,<br>vdB-Hagen 198 |             |
| 1726*                | 334.549     | +1.0916  | 14.5   | 0.4             | 2.50    | 8.80          | 0.31        | 0.00        | 1.63    | —                 | —                       | —                    | —           | 162         | OpC                           | Lynga 9, vdB-Hagen 189                       |             |
| 1730                 | 335.469     | -6.2363  | 20.9   | 0.4             | 1.60    | 9.50          | 0.10        | 0.00        | 1.67    | 1.5               | 9.70                    | 0.20                 | 0.36        | 93          | OpC                           | NGC 6253,<br>Melotte 156,<br>vdB-Hagen 207   |             |
| 1731                 | 337.027     | +13.2725 | -293.7 | 2.4             | 10.00   | 10.20         | 0.09        | -1.68       | 1.80    | 10.0              | —                       | 0.27                 | -1.67       | 21          | GIC                           | NGC 5986                                     |             |
| 1733                 | 338.165     | -11.9562 | -86.9  | 0.6             | 2.20    | 10.20         | 0.05        | -1.68       | 2.10    | 2.2               | —                       | 0.18                 | -1.91       | 6           | GIC                           | NGC 6397                                     |             |
| 1735 <sup>24</sup>   | 339.196     | -1.8505  | 9.9    | 1.1             | 8.00    | 10.00         | 0.63        | -0.68       | 1.60    | 8.5               | —                       | 2.08                 | -0.67       | 0           | GIC                           |  |             |
| 1741                 | 341.430     | -7.1574  | -35.2  | 1.3             | 5.30    | 10.20         | 0.07        | -0.68       | 1.67    | 5.3               | —                       | 0.21                 | -0.70       | 46          | GIC                           | NGC 6352,<br>vdB-Hagen 226                   |             |
| 1742                 | 342.146     | -16.4097 | -98.4  | 3.7             | 12.50   | 10.20         | 0.05        | -1.68       | 2.03    | 12.5              | —                       | 0.11                 | -1.49       | 16          | GIC                           | NGC 6584                                     |             |
| 1743                 | 342.366     | +6.9488  | -22.8  | 2.2             | 9.10    | 10.20         | 0.25        | -1.68       | 1.67    | 9.1               | —                       | 0.75                 | -1.65       | 36          | GIC                           | NGC 6139                                     |             |
| 1744 <sup>25</sup>   | 342.707     | +1.1774  | 11.8   | 0.6             | 3.50    | 9.00          | 0.75        | 0.00        | 1.59    | 3.1<br>3.5        | 8.85<br>9.00            | 2.58<br>2.56         | —<br>—      | —<br>—      | OpC<br>OpC                    |  |             |
| 1745                 | 345.084     | +9.1991  | -38.4  | 6.1             | 25.20   | 10.20         | 0.11        | -1.28       | 1.93    | 25.2              | —                       | 0.32                 | —           | 52          | GIC                           | Terzan 3                                     |             |

Continued on next page

**Table A1 – continued from previous page**

| FSR ID | Coordinates |          | BIC    | $r_{core}$ [pc] | this paper |               |             |             |          | Literature <sup>1</sup> |               |              |             | SIMBAD |         | other Names                                   |
|--------|-------------|----------|--------|-----------------|------------|---------------|-------------|-------------|----------|-------------------------|---------------|--------------|-------------|--------|---------|---|
|        | l [deg]     | b [deg]  |        |                 | d [kpc]    | log(age) [yr] | $A_K$ [mag] | [M/H] [dex] | $C_{HK}$ | d [kpc]                 | log(age) [yr] | E(B-V) [mag] | [M/H] [dex] | r ["]  | Class   |   |
| 1747   | 345.563     | -6.7361  | 23.1   | 2.9             | 10.90      | 10.20         | 0.13        | -0.68       | 1.67     | 10.9                    | —             | 0.38         | -0.60       | 23     | GIC     | NGC 6388,<br>vdB-Hagen 234                    |
| 1750*  | 346.724     | +1.8355  | 18.4   | 0.4             | 2.40       | 8.90          | 0.46        | 0.00        | 1.47     | —                       | —             | —            | —           | —      | —       |   |
| 1752   | 347.795     | +3.3098  | 16.9   | 1.1             | 8.90       | 10.20         | 0.28        | -0.68       | 1.76     | 8.9                     | —             | 0.84         | -0.70       | 17     | GIC     | NGC 6256,<br>vdB-Hagen 208                    |
| 1753   | 348.027     | -10.0118 | -62.9  | 2.6             | 10.90      | 10.20         | 0.08        | -0.68       | 1.88     | 10.9                    | —             | 0.13         | -0.64       | 12     | GIC     | NGC 6496                                      |
| 1759   | 349.289     | -11.1792 | -194.4 | 2.6             | 7.20       | 10.20         | 0.05        | -1.68       | 2.00     | 7.2                     | —             | 0.12         | -1.83       | 25     | GIC     | NGC 6541                                      |
| 1762   | 350.805     | -3.4136  | 17.0   | 1.3             | 8.20       | 9.00          | 0.40        | 0.00        | 1.67     | 8.2                     | —             | 0.91         | —           | 48     | Cl*/GIC | Pismis 26,<br>vdB-Hagen 71,<br>Tonantzintla 2 |
| 1764   | 350.980     | +15.9773 | -40.6  | 0.9             | 2.10       | 10.20         | 0.12        | -1.28       | 1.67     | 2.1                     | —             | 0.36         | -1.18       | 30     | GIC     | M 4, NGC 6121                                 |
| 1765   | 351.937     | +15.7058 | -176.5 | 2.1             | 9.80       | 10.20         | 0.15        | -1.68       | 1.67     | 9.8                     | —             | 0.32         | -1.73       | 38     | GIC     | NGC 6144                                      |
| 1768   | 352.679     | +19.4671 | -294.0 | 1.7             | 8.40       | 10.20         | 0.10        | -1.68       | 1.67     | 8.4                     | —             | 0.18         | -1.62       | 21     | GIC     | M 80,<br>NGC 6093                             |
| 1770   | 353.544     | -5.0150  | 3.6    | 0.9             | 9.20       | 10.20         | 0.15        | -0.68       | 1.67     | 9.2                     | —             | 0.45         | -0.53       | 55     | GIC     | NGC 6441,<br>vdB-Hagen 248                    |
| 1777   | 355.833     | +5.3698  | 18.9   | 0.8             | 5.60       | 10.20         | 0.18        | -0.68       | 1.67     | 5.6                     | —             | 0.52         | -0.59       | 30     | GIC     | NGC 6304,<br>vdB-Hagen 216                    |
| 1779   | 356.877     | +9.3862  | 13.6   | 2.2             | 8.30       | 10.20         | 0.14        | -1.68       | 1.67     | 8.3                     | —             | 0.37         | -1.68       | 32     | GIC     | M 19,<br>NGC 6273                             |
| 1781*  | 357.441     | +2.1168  | 17.1   | 1.4             | 8.10       | 10.00         | 0.25        | -0.38       | 1.78     | 8.1                     | —             | 1.50         | -0.43       | 57     | GIC     | vdB-<br>Hagen 229,<br>Dufay 1, HP 1           |
| 1783   | 357.628     | +7.8380  | -15.0  | 1.9             | 8.60       | 10.20         | 0.13        | -1.68       | 1.67     | 8.6                     | —             | 0.39         | -1.92       | 29     | GIC     | NGC 6293,<br>vdB-Hagen 215                    |
| 1784   | 358.346     | +9.9509  | -21.8  | 2.7             | 13.80      | 10.20         | 0.13        | -1.28       | 1.83     | 13.8                    | —             | 0.28         | -1.32       | 43     | GIC     | NGC 6284                                      |
| 1787   | 358.927     | +13.5279 | -78.3  | 2.0             | 9.40       | 10.20         | 0.17        | -1.68       | 1.75     | 9.4                     | —             | 0.36         | -1.40       | 48     | GIC     | NGC 6235                                      |
| 1788   | 359.592     | +5.4229  | 15.2   | 1.3             | 6.80       | 10.20         | 0.26        | -1.68       | 1.79     | 6.8                     | —             | 0.75         | -1.50       | 30     | GIC     | NGC 6355                                      |

Table notes:

<sup>1</sup> Data for the globular clusters has been taken from Harris (1996) and the data for the open clusters from the WEBDA database, except when indicated otherwise by a footnote.<sup>2</sup> Literature data taken from Ivanov et al. (2000).<sup>3</sup> Literature data taken from Camargo et al. (2009).<sup>4</sup> Classified as not a cluster by Bica et al. (2008).<sup>5</sup> Literature data taken from Bica et al. (2008) and Glushkova et al. (2010).<sup>6</sup> Literature data taken from Bica et al. (2003).<sup>7</sup> Literature data taken from Camargo et al. (2009).<sup>8</sup> Literature data taken from Froeblich et al. (2008a).<sup>9</sup> Literature data taken from Bonatto & Bica (2009).

- <sup>10</sup> Literature data taken from Froebrich et al. (2009).
- <sup>11</sup> Literature data taken from Ortolani et al. (2005).
- <sup>12</sup> Literature data taken from Bica et al. (2007).
- <sup>13</sup> Literature data taken from Kopusov et al. (2008).
- <sup>14</sup> Literature data taken from Kopusov et al. (2008).
- <sup>15</sup> Classified as uncertain cluster by Bonatto & Bica (2008).
- <sup>16</sup> Literature data taken from Glushkova et al. (2010) and Bonatto & Bica (2008).
- <sup>17</sup> Literature data taken from Ortolani et al. (2005).
- <sup>18</sup> Literature data taken from Lata et al. (2010).
- <sup>19</sup> Literature data taken from Momamy et al. (2008) and Glushkova et al. (2010).
- <sup>20</sup> Literature data taken from Glushkova et al. (2010) and Bonatto & Bica (2009).
- <sup>21</sup> Literature data taken from Glushkova et al. (2010) and Bonatto & Bica (2009).
- <sup>22</sup> Literature data taken from Bica & Bonatto (2008).
- <sup>23</sup> Literature data taken from Froebrich et al. (2008b) and Bonatto & Bica (2008).
- <sup>24</sup> Literature data taken from Froebrich et al. (2010).
- <sup>25</sup> Literature data taken from Glushkova et al. (2010) and Bonatto & Bica (2007b).

**APPENDIX B: NOTES ON INDIVIDUAL CLUSTERS**

In the following we will discuss details to some clusters. These are either the objects with parameters determined here for the first time, or clusters with literature values that do not fit the 2MASS data. If the clusters is known already, then its other common names are given beside the FSR number.

**FSR 0039:** This seems to be a newly discovered old open cluster just 4.6 kpc from the Galactic Centre. The sequence in the CMD and CCD suggest we see a number of red giants, including red clump stars. There is no detectable main sequence in the 2MASS data, hence the age of 1 Gyr is an upper limit. The cluster seems highly reddened with  $A_K = 1.22$  mag, but at a distance of 3.5 kpc and a Galactic Longitude of just  $10^\circ$  this is no surprise.

**FSR 0050:** The CMD and CCD sequence suggest that this is an about 5 Gyr old open cluster. There are not many red giant stars to determine the properties accurately, however the isochrone fit seems to fit the top of the main sequence the giants well. If confirmed, this object as well would be an inner Galaxy old open cluster with only 5.6 kpc distance to the Galactic Centre.

**FSR 0076:** The fit to the high probability cluster members seems very uncertain and it is not clear if this object really represents an old stellar cluster. In particular the group of stars with  $J-K = 1.2$  mag and  $K = 13.6$  mag seems not to belong to the cluster sequence. We hence consider this object still as a cluster candidate.

**FSR 0119:** This object was classified as not being a cluster by Bica et al. (2008). It is, however, possible to fit a 2.5 Gyr old isochrone to the CMD. In the CCD the high probability members which should represent the upper end of the main sequence seem not to fit the same isochrone. They are scattered towards much too large J-H values. But this could simply be due to the fact that these stars are at the detection limit in all three bands, and in particular in the H-band, as similar scattering is observed in some other objects. In any case we consider this object still as a cluster candidate.

**FSR 0123:** There seems to be a clear top of the main sequence visible in the CMD, but only a small number of scattered giant stars. Hence the fit of an 0.5 Gyr old isochrone is uncertain.

**FSR 0131:** Similar to FSR 0123, there are only a few high probability membership red giant and clump of stars probably coincident with the top of the main sequence. The scatter of the later in the CCD could be attributed to the faint fluxes. Hence the determined cluster parameters are uncertain.

**FSR 0134:** This is a very nice example of a newly discovered old (0.8 Gyr) cluster in the FSR sample. There is a clearly visible top of the main sequence and more than a dozen red giant in the cluster.

**FSR 0141 (NGC 6802, Collinder 400):** In this case the isochrone with the literature parameters does not seem to fit the cluster main sequence and red giants. Our fit with a distance of 2.7 kpc and 0.5 Gyrs seems to represent the cluster much better.

**FSR 0155 (Teutsch 7):** The isochrone with the literature parameters seems not to fit the data at all. Instead the cluster is 3.8 kpc away and has an age of about 0.6 Gyrs.

**FSR 0156 (BDS 2003 158):** The cluster has been identified by Bica et al. (2003) but no parameters are determined. We find that this object can be well fit by an isochrone with 0.4 Gyrs age and a distance of 7.5 kpc, rendering this one of the most distant open clusters in our sample.

**FSR 0167:** There are only very few red giant stars that might be part of the cluster. Hence the parameters are uncertain.

**FSR 0170:** There are no main sequence stars visible in the 2MASS data. However, a clump of red giant stars as well as a RGB

are visible. The age of 1 Gyr is hence a lower limit and the distance uncertain.

**FSR 0177 (Kronberger 52):** There are a number of main sequence and giant stars visible in the CMD and CCD to properly determine the cluster parameter of this object. It is best fit by a 0.8 Gyr old cluster at a distance of 3.6 kpc.

**FSR 0184:** There seems to be a red clump of stars, as well as some sub-giants in the CMD. No main sequence stars are detected. Hence, the determined cluster parameters are uncertain. The strange value required for  $C_{HK}$  hints that this object might not be a real cluster.

**FSR 0191 (Berkeley 49):** This is another example where the literature parameters do not fit the 2MASS data at all. Using the small number of red giants we find that 0.2 Gyr old and 3.4 kpc distant cluster fits the data best.

**FSR 0202 (NGC 6819, Melotte 223):** Despite the nice fit, a rather large value for  $C_{HK}$  is required to fit the CCD.

**FSR 0203 (Kronberger 73):** There is only a small number of red giants that can be used to constrain the cluster parameters. We find that a 125 Myr old and distant (10.8 kpc) cluster fits the data best.

**FSR 0208 (Berkeley 85):** Using the six stars which are likely to be red giants we can obtain a better fit than with the literature parameters. We find an age of 125 Myrs and a distance of 4.4 kpc.

**FSR 0214 (IC 1311):** There only seem to be a handful of main sequence stars and in general the isochrone with the literature parameters does not fit the 2MASS data. We find a better fit with an age of 0.5 Gyr and a distance of 8.7 kpc.

**FSR 0222:** This newly identified cluster only stands out through a handful of red clump stars and about the same number of stars at the top of the main sequence. The remaining stars all have lower membership probabilities, rendering the parameters of the cluster uncertain.

**FSR 0256 (Berkeley 54):** What the literature parameter imply as the top of the main sequence, actually seems to be a red clump of stars. There are no main sequence stars visible in the 2MASS data. Using 4 Gyrs as the age, we find a distance of almost 7 kpc.

**FSR 0275:** This newly identified cluster shows a dozen or so high probability members which are red giants and the top of them main sequence. We determine an age of 1 Gyr and a distance of 3.6 kpc.

**FSR 0280 (Teutsch 156):** We can identify a number of cluster red giants as well as the top of the main sequence and fit an isochrone with an age of 0.8 Gyrs and a distance of 4.4 kpc.

**FSR 0282:** There are no or very few giants in the clusters. Hence the age and distance determination is very uncertain.

**FSR 0287 (Berkeley 91):** The isochrone with the literature parameters fails to fit the data. We clearly can identify a clump of red giant stars, but there is no main sequence. Hence the age of 0.4 Gyrs is a lower limit and consequently the distance is uncertain as well.

**FSR 0294 (NGC 7031):** There seem to be two possibilities to fit the CMD of this cluster. Either using the literature parameters (140 Myrs, 900 pc) or a much older distant cluster (0.5 Gyrs, 7.1 kpc). The latter fitting the high probability members at  $J-K = 1.5$  mag as red clump stars. Non of the two fits provides a satisfying result for all stars.

**FSR 0304:** This cluster contains a handful of red giant stars and one can identify the top of the main sequence. Those stars, however, show a large scatter in the CCD. The best fit can be obtained with an age of 0.4 Gyrs and a distance of 6.8 kpc.

**FSR 0313 (Kronberger 81):** This so far un-investigated clusters shows a very nice red giant branch with at least 30 or 40 stars.

There is no main sequence detected, hence the age of 1.6 Gyrs is an upper limit and the distance of 6 kpc is uncertain. Given the large number of giant stars, this object might well be a massive old and distant (10 kpc to the Galactic Centre) cluster.

**FSR 0327 (NGC 7128):** This is a very young cluster in our sample of old clusters. This is caused by the fact that there are three high probability members which could be red giants. However, no fit with an isochrone can be obtained that includes these three stars.

**FSR 0329 (Berkeley 92):** There is no main sequence, but a number of red giant stars detected for this cluster. It is best fit by a 1 Gyr old isochrone at a distance of 5.5 kpc, where the age is a lower limit.

**FSR 0333:** The main sequence stars in this cluster only have a low membership probability. But there are a sufficient number of high probability member red giants to determine an age of 1.2 Gyrs and a distance of 5 kpc.

**FSR 0338:** The high probability members of this newly identified cluster seem to indicate an object with an age of 0.4 Gyrs at a distance of 6 kpc. The scatter in the data points suggests larger than normal uncertainties for the parameters.

**FSR 0342:** This is a well populated newly identified old cluster. A large part of the main sequence as well as at least 10 red giant stars can be identified. The cluster has an age of 1.2 Gyrs and is at a distance of 2.6 kpc.

**FSR 0385:** There is only a small number (three) of high probability members in this cluster. Hence the parameters (age of 0.8 Gyrs, distance of 1.7 kpc) are uncertain.

**FSR 0386:** The very small number of high probability members make the determination of the cluster parameter very uncertain. We hence consider this object only a cluster candidate.

**FSR 0394:** There is only a small number of probable main sequence stars at the detection limit. The number of red giants allows us, however, to determine an age of 1.2 Gyrs and a distance of 4.1 kpc.

**FSR 0412 (Pfeiderer 3):** This so far uninvestigated cluster shows a large number of red giants and the top of the main sequence is visible as well. The cluster has an age of 1.2 Gyrs and is at a distance of 6.1 kpc.

**FSR 0460:** There are a number of red giant stars as well as the top of the main sequence just above the detection limit. Hence, the uncertainties for the parameters (1.2 Gyrs, 6.1 kpc) are larger than normal.

**FSR 0478 (Juchert-Saloranta 1):** This so far no investigated cluster shows about ten red giants and main sequence stars. It can be fit with an isochrone age of 0.8 Gyrs and a distance of 5.1 kpc.

**FSR 0480:** This is a newly identified cluster with a large number of red giants and just a hint of main sequence stars at the detection limit. It represents a 1.2 Gyr old cluster at a distance of 5.8 kpc.

**FSR 0514 (Berkeley 61):** This is another case where the literature parameters do not fit the 2MASS data. We find that the CMD can be best fit with an 125 Myr old isochrone at a distance of 8 kpc.

**FSR 0548 (NGC 609):** In this case the literature parameters do not fit the 2MASS data. We obtain a better fit using an age of 250 Myrs and a distance of 4.2 kpc.

**FSR 0563 (IC 166, Tombaugh 1):** Here as well, we cannot bring the literature parameters in agreement with the 2MASS data. Instead a good fit can be obtained using an age of 1.4 Gyrs and a distance of 5 kpc.

**FSR 0584:** It has been suggested by Bica et al. (2007) that this object is a nearby, highly reddened globular cluster without, or with only a very small number of giant stars. The parameters for this object listed in Table A1 are not a best fit, but rather the

parameters for the solid isochrone in Fig. C98. Given the fact that the four potentially reddened giant stars are the least likely of the cluster members, the object could well be an embedded younger cluster. Further investigation is certainly needed to determine its nature reliably.

**FSR 0648 (NGC 1245, Melotte 18):** To fit this cluster we require a rather large value for  $C_{HK}$ .

**FSR 0652 (IC 361):** The literature parameters do not fit the 2MASS data. We obtain an age of 1 Gyr and a distance of 3.9 kpc.

**FSR 0667:** This object contains only a small number of high probability members, which are, however, nicely represent an 0.8 Gyr old cluster at a distance of 750 pc.

**FSR 0731 (Berkeley 18, King 22):** Our decontamination suggests in this case that the age of the cluster is smaller than the literature value, since there seems to be a number of sub-dwarfs visible in the CMD. Our fit uses an age of 1.4 Gyrs and a distance of 4.7 kpc.

**FSR 0790:** This newly identified cluster lacks a clear detection of main sequence stars, which are all near the detection limit. This introduces a larger uncertainty into the determined parameters (2 Gyrs, 6 kpc).

**FSR 0828:** The literature values do not seem to fit the 2MASS data. We find an age of 1.6 Gyrs and a distance of 5.7 kpc.

**FSR 0877 (Basel 11b):** The literature parameters seem to fit the main sequence of the clusters. If we consider the three bright stars as cluster members than we can obtain a fit using an age of 0.6 Gyrs and a distance of 1.1 kpc.

**FSR 0879 (NGC 2266, Melotte 50):** To fit this cluster we require a rather large value for  $C_{HK}$ .

**FSR 0884:** This object was classified as uncertain cluster by Bonatto & Bica (2008). Given that we cannot fit the CMD and CCD simultaneously with the same isochrone (the fit to the CMD requires no extinction, while the fit to the CCD need an extinction), we conclude that this object indeed might not be a real cluster.

**FSR 0926 (Deutsch 58):** This so far uninvestigated cluster shows a number of red giant stars as well as the top of the main sequence. We find it to be a 1.2 Gyr old cluster at a distance of 6 kpc.

**FSR 0963:** The cluster shows only a small number of red giants, as a clear main sequence. It can be fit by an isochrone with an age of 0.5 Gyrs and a distance of 2.5 kpc.

**FSR 0972 (NGC 2429, Melotte 69, Collinder 154, Raab 56):** Despite its large number of member stars no literature values for this cluster could be found. From our isochrone fit we obtain an age of 2 Gyrs and a distance of 2.3 kpc. The CCD cannot be fit properly by the same, extinction free isochrone as the CMD.

**FSR 0995 (NGC 2355, Melotte 63):** To fit this cluster we require a rather large value for  $C_{HK}$ .

**FSR 1113:** There are only a handful of high probability members, which are difficult to fit consistently with an isochrone in both, the CMD and the CCD. Hence, we consider this object just as a cluster candidate.

**FSR 1119 (Czernik 28):** Here the literature data does not seem to fit the 2MASS data as good as it could. We find that a proper fit can only be obtained using a sub-solar metallicity. Then we find an age of 1.4 Gyrs and a distance of 5.5 kpc. this puts the cluster at a distance of almost 13 kpc from the Galactic Centre.

**FSR 1121 (King 23):** To fit this cluster we require a rather large value for  $C_{HK}$ .

**FSR 1138 (Berkeley 77):** Both sets of parameters (ours and the literature) are unable to fit the CCD simultaneously with the CMD.

**FSR 1201 (NGC 2204, Melotte 44):** The isochrone fit requires different parameters than the literature values. Furthermore, it only works with sub-solar metallicities. We find an age of 2 Gyrs and a distance of 4 kpc, placing the cluster 11 kpc from the Galactic Centre.

**FSR 1214 (Berkeley 36):** No main sequence visible, hence the age is an upper limit.

**FSR 1222 (Melotte 71, Collinder 155):** We find different cluster parameters than listed in literature. The best fit is obtained with an age of 1.2 Gyrs and a distance of 2.3 kpc.

**FSR 1225 (NGC 2360, Melotte 64):** To fit this cluster we require a rather large value for  $C_{HK}$ . Furthermore, the parameters differ from the literature values. We find an age of 1.2 Gyrs and a distance of 900 pc.

**FSR 1238 (NGC 2425):** The isochrone fit works better with a sub-solar metallicity. The cluster is 11.5 kpc from the Galactic Centre, has an age of 1.4 Gyrs and a distance of 4.7 kpc.

**FSR 1241 (M 46, NGC 2437):** To fit this cluster we require a rather large value for  $C_{HK}$ .

**FSR 1244 (Ruprecht 26):** The cluster parameters are highly uncertain as no reliable fit to all high probability members can be made.

**FSR 1250 (Haffner 2, Tombaugh 2):** There is no main sequence detected, hence the age of 1 Gyr is a lower limit, and the distance of 8 kpc is uncertain.

**FSR 1256 (NGC 2539, Melotte 83):** The isochrone fit works better with a sub-solar metallicity. The cluster is 1 Gyr old and has a distance of 1 kpc.

**FSR 1266 (Deutsch 61):** To fit this cluster we require a rather large value for  $C_{HK}$ .

**FSR 1267 (NGC 2432):** The isochrone using the literature parameters does not fit the 2MASS data. We find that the cluster has an age of 0.5 Gyrs and a distance of 2.1 kpc.

**FSR 1274 (NGC 2421):** To fit this cluster we require a rather large value for  $C_{HK}$ . The literature parameters do not fit the possible red giants in the cluster. This can be done using an age of 0.6 Gyrs and a distance of 1.8 kpc.

**FSR 1282 (NGC 2509, Melotte 81):** To fit this cluster we require a rather large value for  $C_{HK}$ . We also obtain a much better fit than the literature parameters. We find an age of 1.2 Gyrs and a distance of 2.5 kpc.

**FSR 1296 (NGC 2243, Melotte 46):** There is no main sequence detected, hence the age of 4 Gyrs is an upper limit and the distance of 4.5 kpc uncertain.

**FSR 1298:** There is only a small number of high probability members (giants and main sequence stars). Hence, the age of 1.4 Gyrs and the distance of 3.2 kpc are uncertain.

**FSR 1299 (Ruprecht 18):** We find that there are a few probable cluster red giants which are not fit by the literature parameters. We can include them into the fit by using an age of 110 Myrs and a distance of 2.3 kpc.

**FSR 1301 (M 93, NGC 2447, Collinder 160):** We obtain a better fit when using a sub-solar metallicity.

**FSR 1313 (Trumpler 9):** There is one possible giant star, but it cannot be fit by any isochrone.

**FSR 1330 (NGC 2489, vdB-Hagen 15):** There are six possible cluster red giants which are not fit at all when using the literature parameters. We find an age of 0.6 Gyrs and a distance of 1.3 kpc.

**FSR 1337 (Haffner 17, vdB-Hagen 12):** The two probable cluster red giants are not fit by the literature parameters. They are included if one uses an age of 120 Myrs and a distance of 3 kpc.

**FSR 1354 (NGC 2567, vdB-Hagen 26):** To fit this cluster we require a rather large value for  $C_{HK}$ .

**FSR 1361:** There are a handful of cluster red giants and a large number of main sequence stars. The best fit can be obtained using an age of 1 Gyr and a distance of 1.5 kpc.

**FSR 1362 (NGC 2627, Collinder 188, Melotte 87, vdB-Hagen 38):** To fit this cluster we require a rather large value for  $C_{HK}$ . Using an age of 1.4 Gyrs and a distance of 1.8 kpc fits the data much better than the literature parameters.

**FSR 1385 (Pismis 3, vdB-Hagen 33):** The literature parameters do not lead to a satisfactory fit of the 2MASS data. Instead we use an age of 3 Gyrs and a distance of 2.1 kpc.

**FSR 1386 (Saurer 2):** There is no detectable main sequence, hence the age of 1.4 Gyrs is an upper limit and the distance of 5 kpc is uncertain.

**FSR 1388 (Ruprecht 66, vdB-Hagen 41):** This so far uninvestigated cluster shows a number of red clump stars as well as many main sequence stars. We find an age of 1.2 Gyrs and a distance of 3.9 kpc.

**FSR 1396 (Collinder 147, Melotte 66):** There is no main sequence detected, hence the age of 3 Gyrs is an upper limit and the distance of 5 kpc uncertain.

**FSR 1399:** This cluster contains a handful of giant stars as well as a clear detection of the top of the main sequence. We find an age of 250 Myrs and a distance of 6.8 kpc.

**FSR 1404 (vdB-Hagen 55):** This so far uninvestigated cluster has a number of red giants and the top of the main sequence is detected as well. This enables us to fit an isochrone with an age of 1 Gyr and a distance of 3.7 kpc.

**FSR 1408 (NGC 2818A, Melotte 96, vdB-Hagen 59):** The isochrone using the the literature parameter does not seem to fit the data. Instead we find an age of 1.2 Gyrs and a distance of 3.2 kpc.

**FSR 1409 (NGC 2671, vdB-Hagen 51):** If we include the potential red giant into the isochrone fit we find an age of 250 Myrs and a distance of 1.5 kpc, slightly different to the literature values.

**FSR 1415:** There is no main sequence, hence the determined age of 2.5 Gyrs has to be considered an upper limit, while the distance of 10 kpc is uncertain. If correct, this places the cluster 13.5 kpc from the Galactic Centre.

**FSR 1420 (Ruprecht 60, vdB-Hagen 31):** This so far uninvestigated cluster shows a few likely giant members as well as the top of the main sequence. We find an age of 1 Gyr and a distance of 3.9 kpc.

**FSR 1439 (NGC 2849, vdB-Hagen 61):** To fit this cluster we require a rather large value for  $C_{HK}$ .

**FSR 1458 (Pismis 12, vdB-Hagen 62):** This cluster has no literature parameters but shows a handful of red giants as well as the main sequence. We determine an age of 1.2 Gyrs and a distance of 2.1 kpc.

**FSR 1463:** This newly identified cluster shows a number of red giants as well as the top of the main sequence. We find an age of 1 Gyr and a distance of 4.5 kpc.

**FSR 1480 (Pismis 15):** The isochrone using the literature parameters does not seem to fit the data properly. We find that an age of 1.2 Gyrs and a distance of 2.3 kpc leads to a better fit.

**FSR 1483 (vdB-Hagen 73):** This cluster has no literature data but shows a number of red clump stars as well as the top of the main sequence. We find an age of 1 Gyr and a distance of 5 kpc.

**FSR 1486 (vdB-Hagen 67):** There seems to be only a few top of the main sequence stars with reasonably high membership probabilities. Hence the determined age of 0.4 Gyrs and the distance of 7.6 kpc are uncertain.

**FSR 1494 (vdB-Hagen 72):** This cluster without literature data can be fit using an age of 1 Gyr and a distance of 3.2 kpc.

**FSR 1520 (Ruprecht 85, vdB-Hagen 83):** The isochrone with the literature data clearly fails to fit the data. The potential cluster red giants have only a low membership probability, hence the age of 0.4 Gyrs and the distance of 4 kpc are uncertain.

**FSR 1521:** There are no main sequence stars detected, hence the age of 3 Gyrs is an upper limit and the distance of 4 kpc is uncertain.

**FSR 1523 (Schuster CL):** This cluster without literature parameters shows a number of high probability members (giants and main sequence stars). We find that an age of 125 Myrs and a distance of 7.5 kpc fits the 2MASS data.

**FSR 1528 (Teutsch 44):** This so far uninvestigated cluster can be fit using an age of 1.4 Gyrs and a distance of 6.7 kpc.

**FSR 1529 (NGC 2808):** To fit this cluster we require a rather large value for  $C_{HK}$ .

**FSR 1534 (Bochum 8, vdB-Hagen 90):** To fit this cluster we require a rather large value for  $C_{HK}$ . If we include the two potential giants into the fit we obtain an age of 1.2 Gyrs and a distance of 1 kpc, very different from the literature values.

**FSR 1546 (NGC 3255, vdB-Hagen 96):** There seem to be a number of cluster red giants which are not at all fit by an isochrone using the literature parameters. We find an age of 1 Gyr and a distance of 3.7 kpc instead.

**FSR 1550 (Teutsch 105):** This cluster without literature parameters can be fit using an age of 1 Gyr and a distance of 6.3 kpc.

**FSR 1559 (Teutsch 106):** So far uninvestigated, this cluster shows a clear red clump as well as the top of the main sequence. We find an age of 0.6 Gyrs and a distance of 6.9 kpc.

**FSR 1565 (Trumpler 19):** We find a clear main sequence and a dozen giant stars in this so far uninvestigated cluster. We fit an isochrone with an age of 1.2 Gyrs and a distance of 3.1 kpc.

**FSR 1586:** There are only a few possible cluster red giants, hence the parameters are uncertain. We find an age of 0.8 Gyrs and a distance of 2.4 kpc.

**FSR 1611 (NGC 4337, vdB-Hagen 129):** The isochrone with the literature parameters fails to fit the 2MASS data. We find that the clusters has an age of 1.2 Gyrs and a distance of 2.5 kpc.

**FSR 1624 (Trumpler 20, vdB-Hagen 137):** Our fit using an age of 1.4 Gyrs and a distance of 3.7 kpc fits the data much better than using the literature parameters.

**FSR 1632 (vdB-Hagen 140):** This cluster without literature parameters shows a number of red giants, but the top of the main sequence seems to be just below the detection limit. Thus, the age of 2.5 Gyrs is a lower limit and the distance of 5 kpc is uncertain.

**FSR 1637 (NGC 4815, vdB-Hagen 142):** There are two potential cluster red giants which could either be fit using the literature parameters or the values obtained by us: an age of 1 Gyr and a distance of 2 kpc.

**FSR 1657:** There seems to be a clump of red giant stars and a few brighter giants, but no indication of a main sequence, which could tentatively be fit using an age of 1 Gyr and a distance of 7 kpc. However, the slope of the RGB cannot be reproduced by any sensible value for the metallicity. We hence consider this object only as a cluster candidate.

**FSR 1670 (Loden 1101):** This so far uninvestigated cluster shows a number of giant stars as well as a main sequence. We fit an isochrone using an age of 250 Myrs and a distance of 2.5 kpc.

**FSR 1716:** This potential globular cluster shows no main sequence, hence the age of 2 Gyrs is an upper limit and the distance of 7 kpc uncertain.

**FSR 1724 (NGC 6208, Collinder 313, vdB-Hagen 198):** The potential cluster red giants detected in the 2MASS data can only be fit if we use an age of 0.6 Gyrs and a distance of 3.2 kpc.

**FSR 1726 (Lynga 9, vdB-Hagen 189):** WEBDA states that this object actually may not be a real cluster. However, one can obtain a very well fitting isochrone using an age of 0.6 Gyrs and a distance of 2.5 kpc.

**FSR 1750:** This newly identified cluster shows a clear main sequence but only a handful of probable giants, rendering the determined parameters uncertain. We find that the age is 0.8 Gyrs and the distance 2.4 kpc.

**FSR 1781 (vdB-Hagen 229, Dufay 1, HP 1):** The reddening for this cluster seems to be much smaller than what is given in the literature.

**APPENDIX C: COLOUR-MAGNITUDE AND  
COLOUR-COLOUR DIAGRAMS**

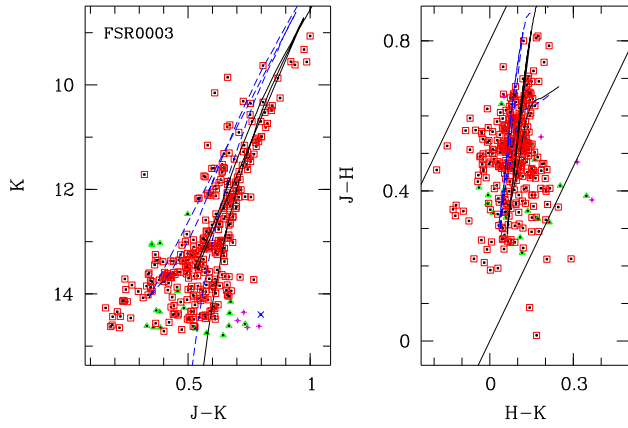


**Figure C1.** Example of our colour-magnitude (left) and colour-colour diagrams for the cluster FSR0003 (NGC 6723). Red squares are stars with  $P > 80\%$ , green triangles are stars with  $60\% < P < 80\%$ , pink + signs are stars with  $40\% < P < 60\%$ , blue crosses are stars with  $20\% < P < 40\%$  and black dots are stars with  $P < 20\%$ . Overplotted in black is the best fitting isochrone (see Table A1 for the parameters). The two vertical lines enclose the reddening band for stellar atmospheres.

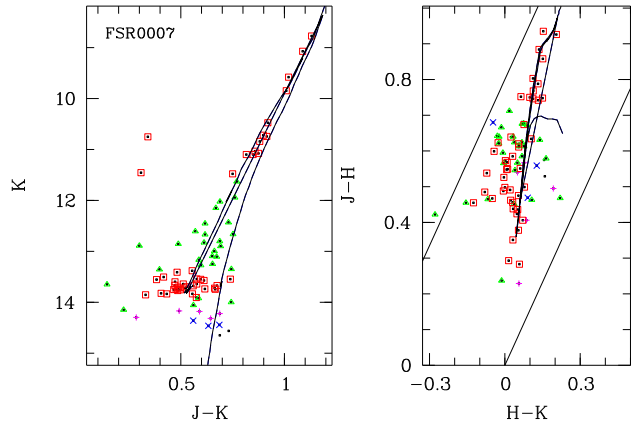


**Figure C4.** As Fig. C1 but for FSR 0007

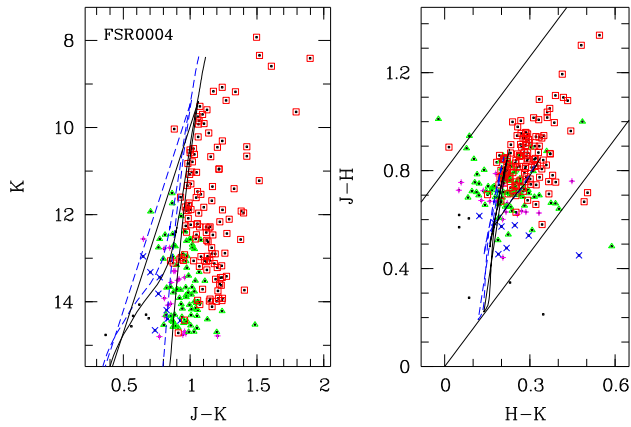


**Figure C2.** As Fig. C1 but for FSR 0004

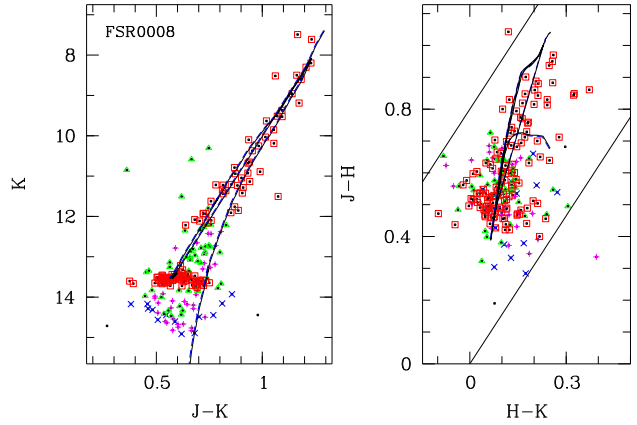


**Figure C5.** As Fig. C1 but for FSR 0008

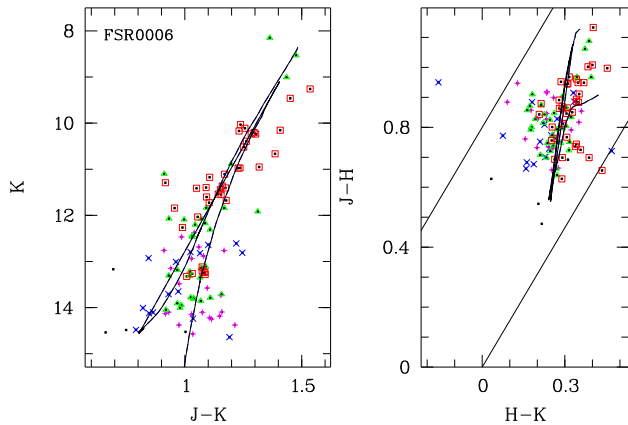


**Figure C3.** As Fig. C1 but for FSR 0006

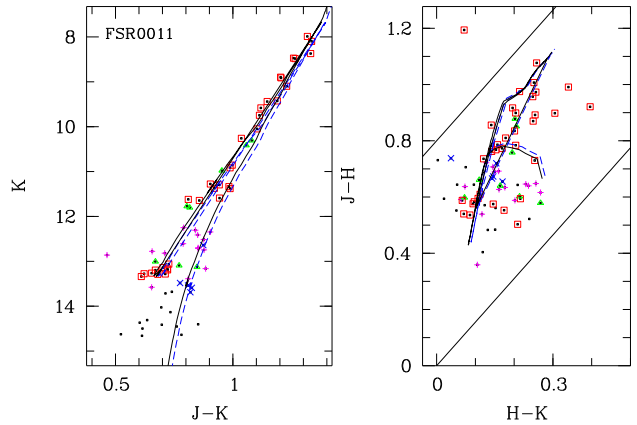


**Figure C6.** As Fig. C1 but for FSR 0011

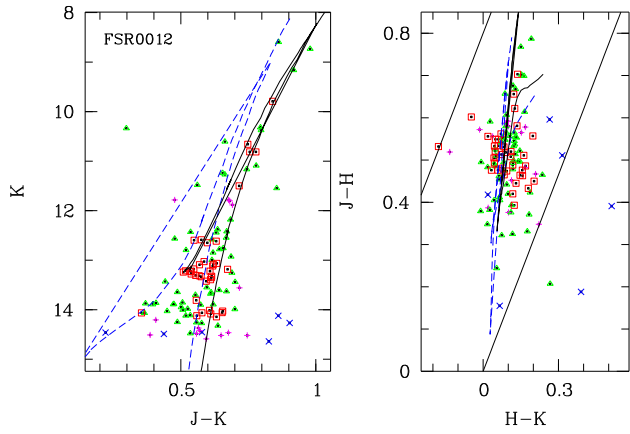


**Figure C7.** As Fig. C1 but for FSR 0012

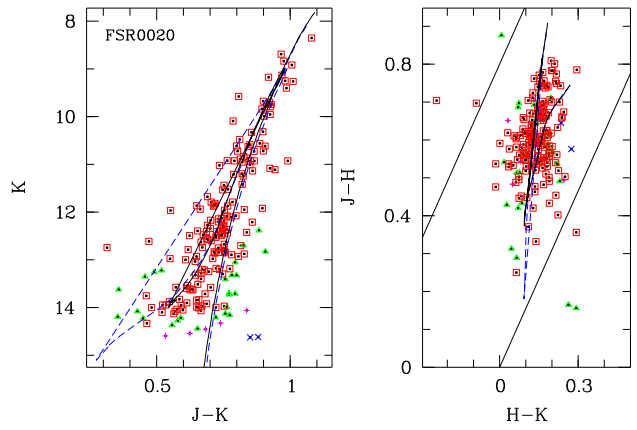


**Figure C10.** As Fig. C1 but for FSR 0020

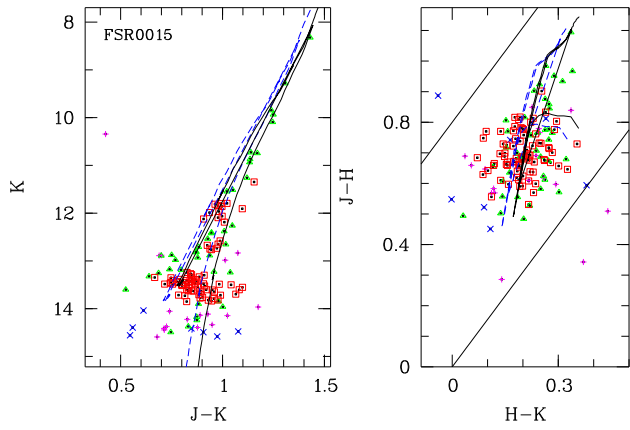


**Figure C8.** As Fig. C1 but for FSR 0015

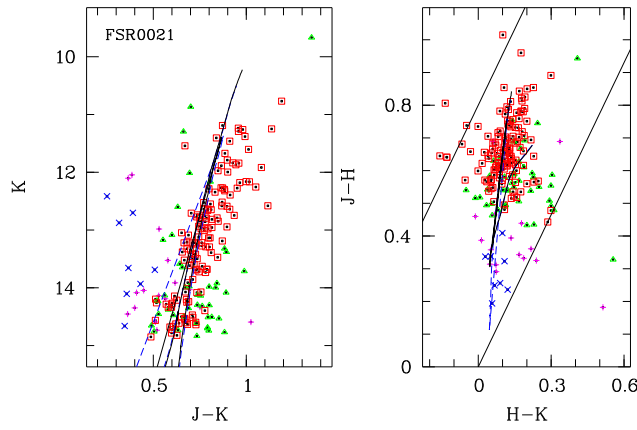


**Figure C11.** As Fig. C1 but for FSR 0021

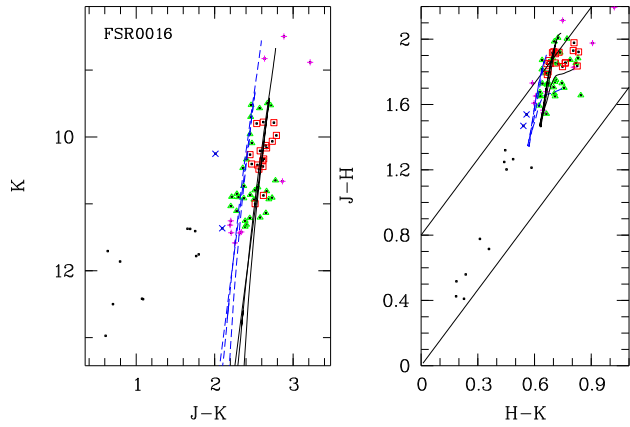


**Figure C9.** As Fig. C1 but for FSR 0016

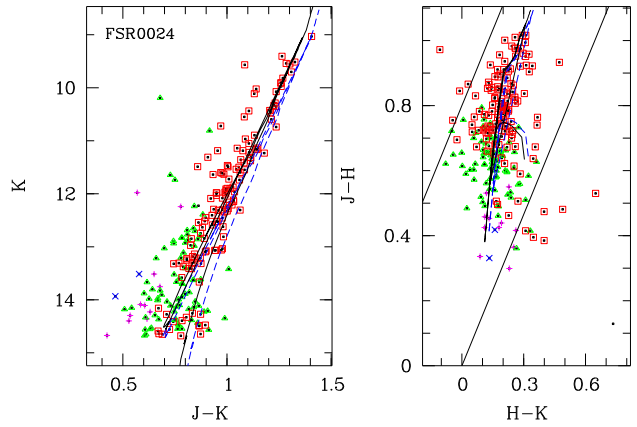


**Figure C12.** As Fig. C1 but for FSR 0024

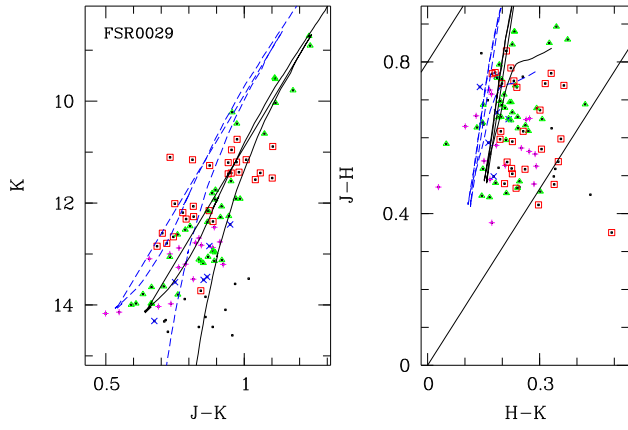


Figure C13. As Fig. C1 but for FSR0029

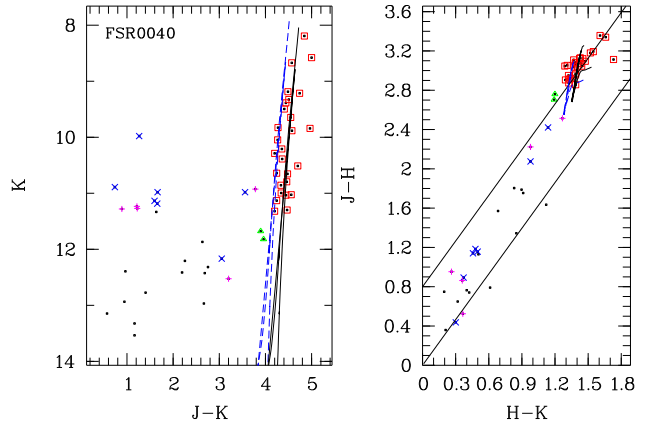


Figure C16. As Fig. C1 but for FSR0040

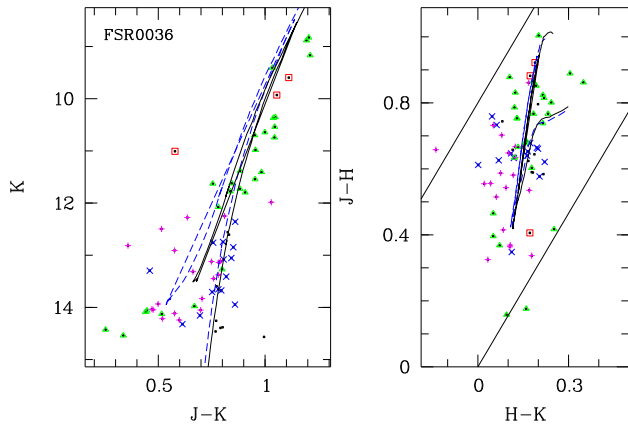


Figure C14. As Fig. C1 but for FSR0036

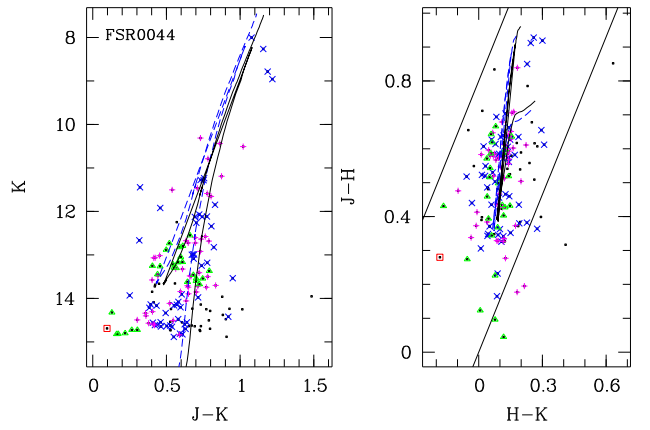


Figure C17. As Fig. C1 but for FSR0044

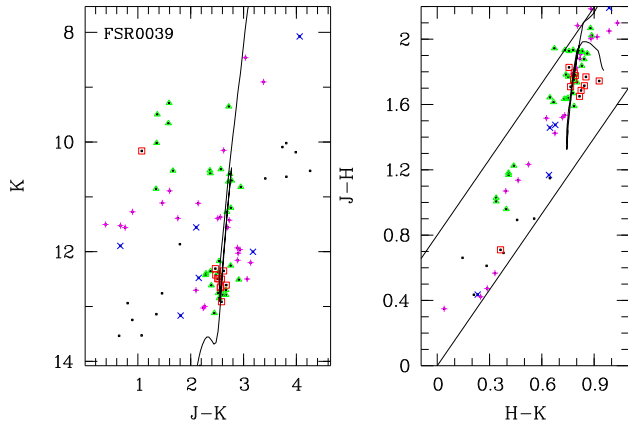


Figure C15. As Fig. C1 but for FSR0039

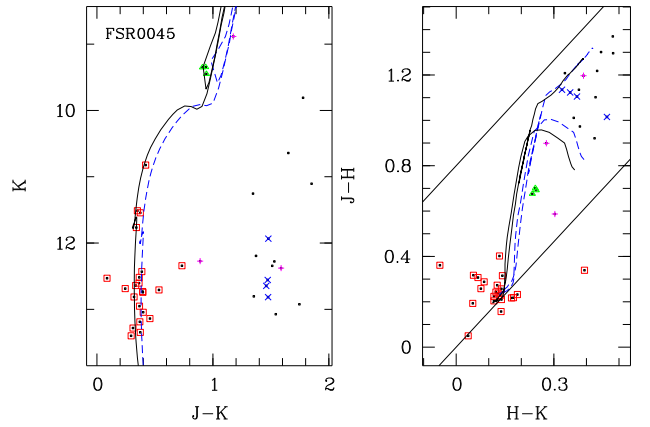
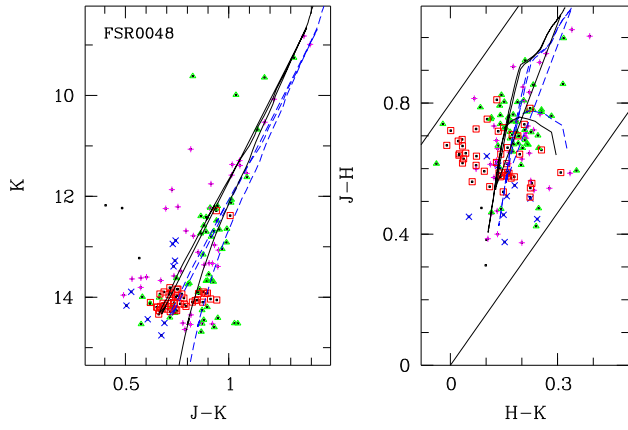
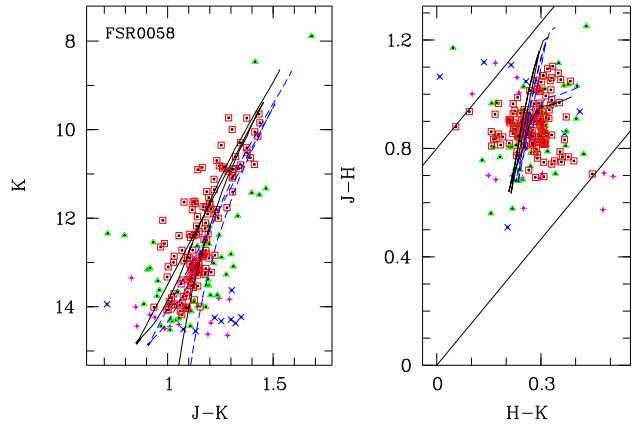


Figure C18. As Fig. C1 but for FSR0045



**Figure C19.** As Fig. C1 but for FSR0048



**Figure C22.** As Fig. C1 but for FSR0058

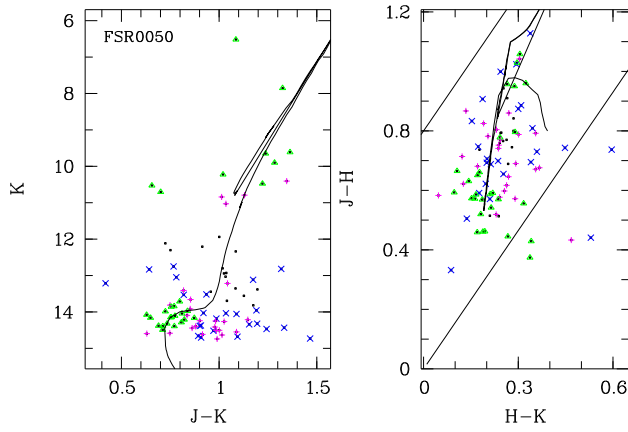


**Figure C20.** As Fig. C1 but for FSR0050

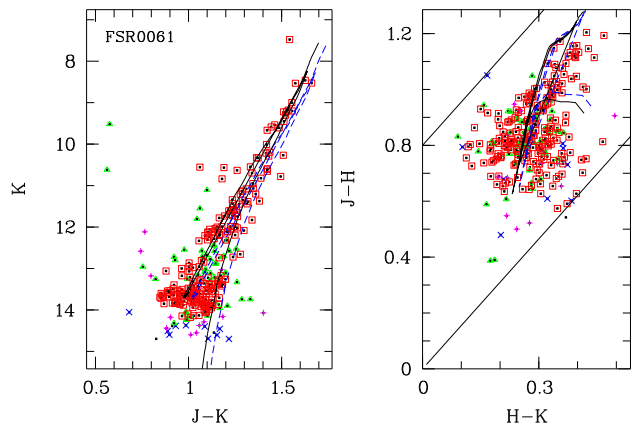


**Figure C23.** As Fig. C1 but for FSR0061

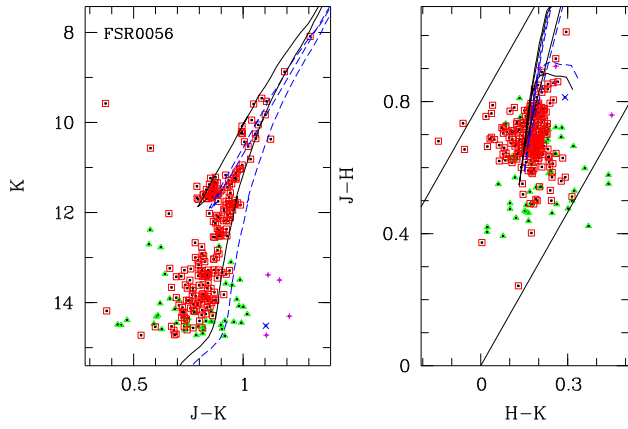


**Figure C21.** As Fig. C1 but for FSR0056

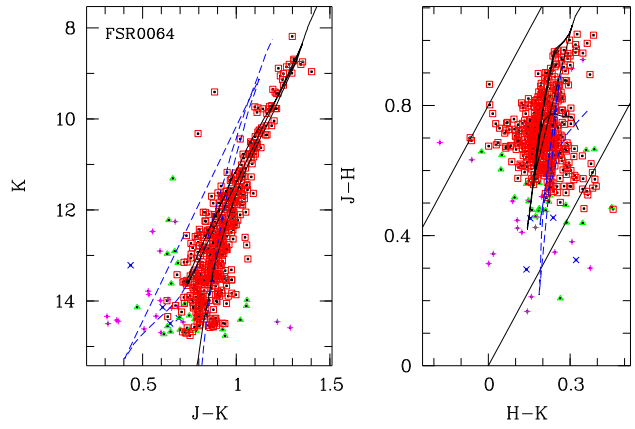


**Figure C24.** As Fig. C1 but for FSR0064

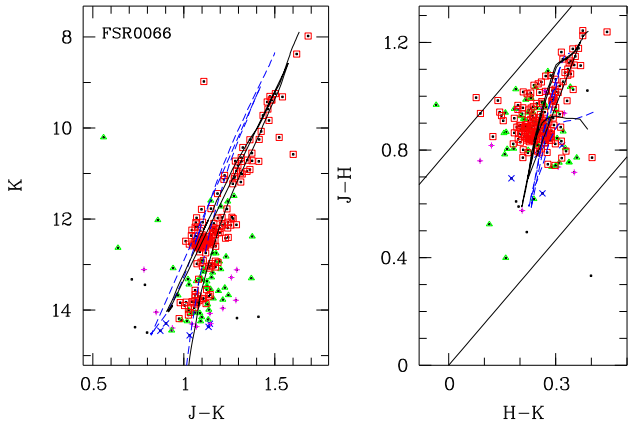


Figure C25. As Fig. C1 but for FSR0066

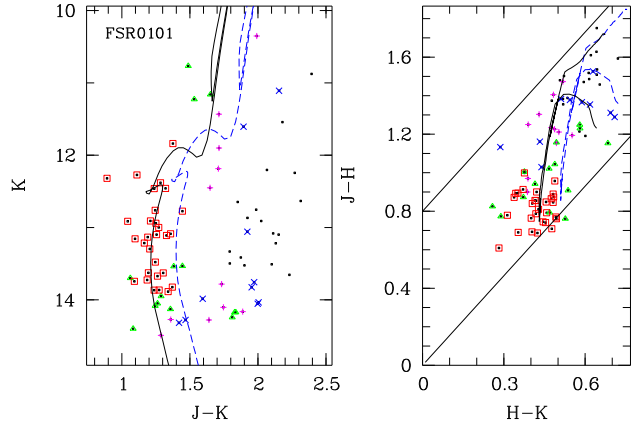


Figure C28. As Fig. C1 but for FSR0101

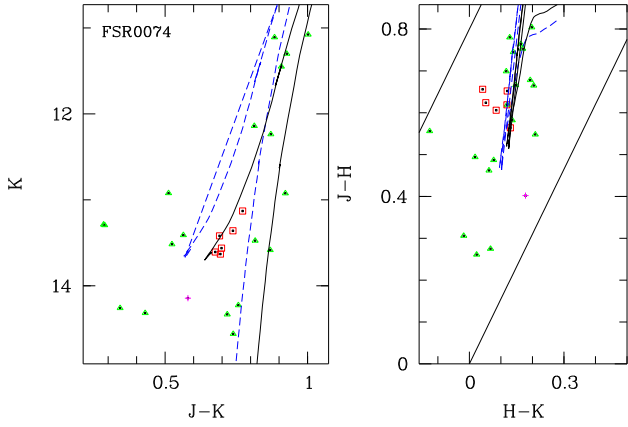


Figure C26. As Fig. C1 but for FSR0074

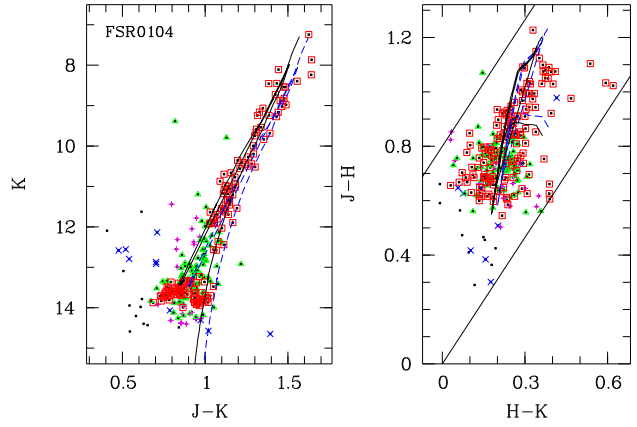


Figure C29. As Fig. C1 but for FSR0104

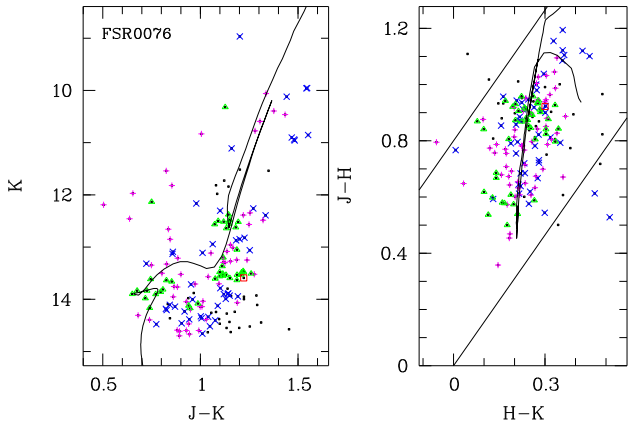


Figure C27. As Fig. C1 but for FSR0076

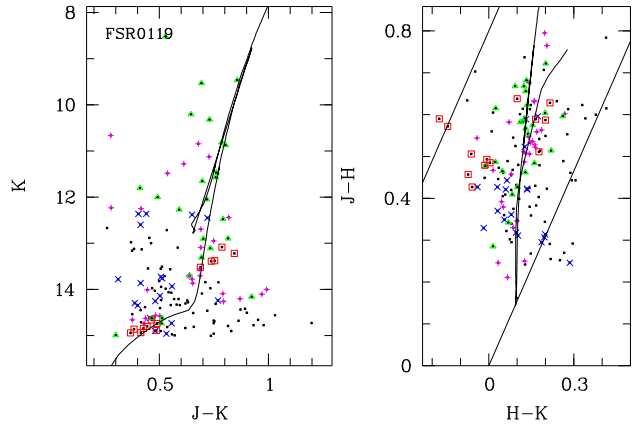
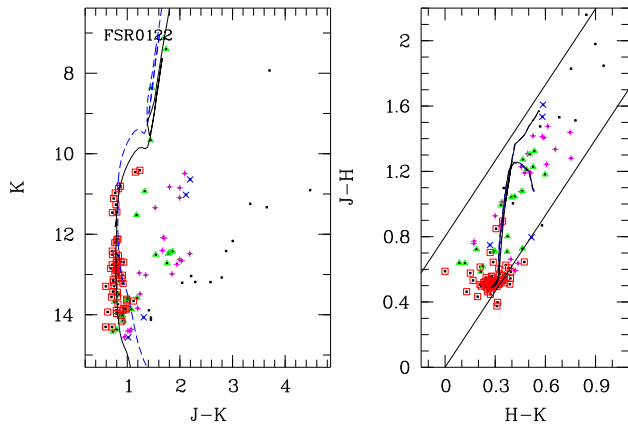
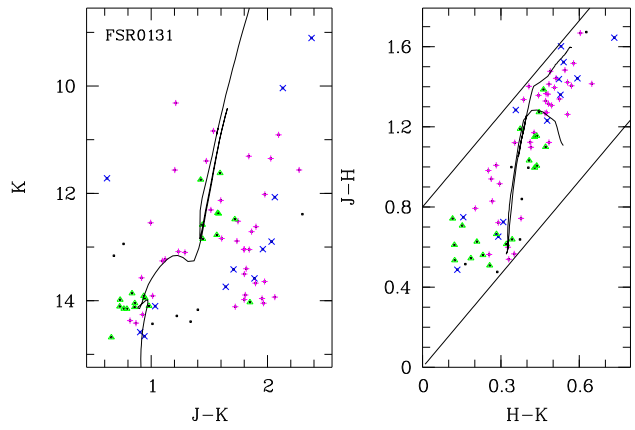


Figure C30. As Fig. C1 but for FSR0119



**Figure C31.** As Fig. C1 but for FSR0122



**Figure C34.** As Fig. C1 but for FSR0131

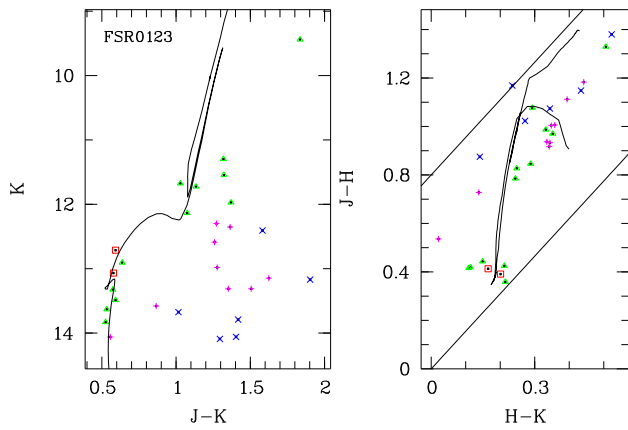


**Figure C32.** As Fig. C1 but for FSR0123

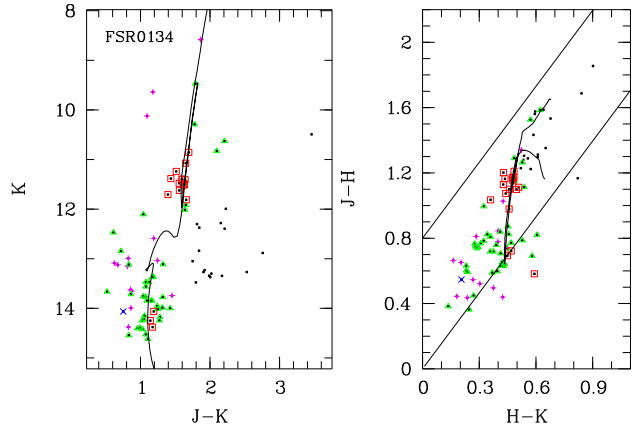


**Figure C35.** As Fig. C1 but for FSR0134

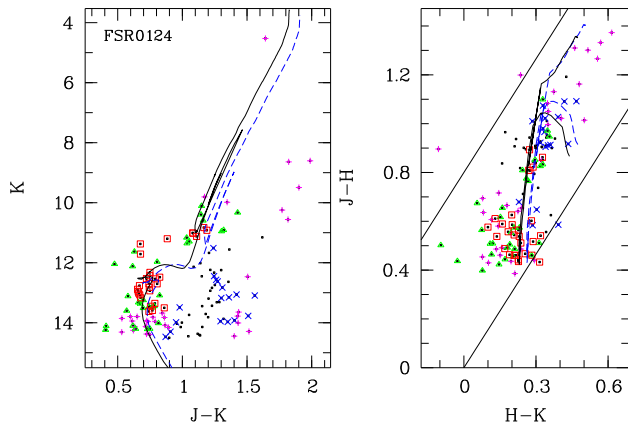


**Figure C33.** As Fig. C1 but for FSR0124

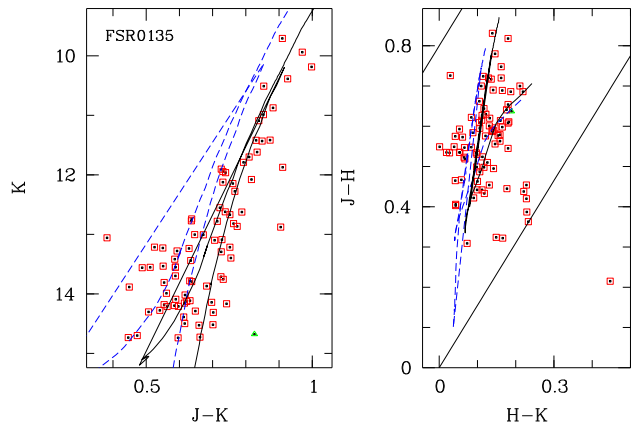


**Figure C36.** As Fig. C1 but for FSR0135

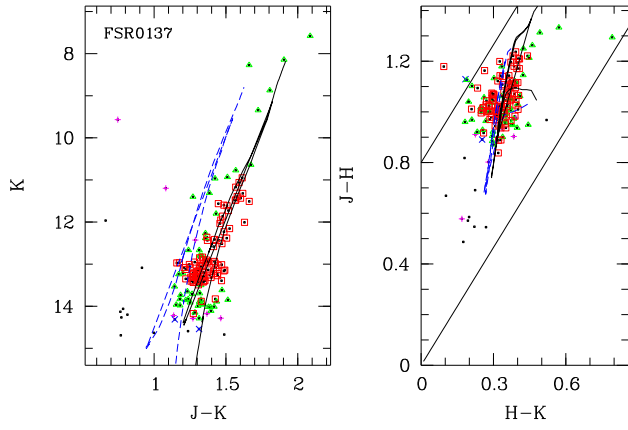


Figure C37. As Fig. C1 but for FSR0137

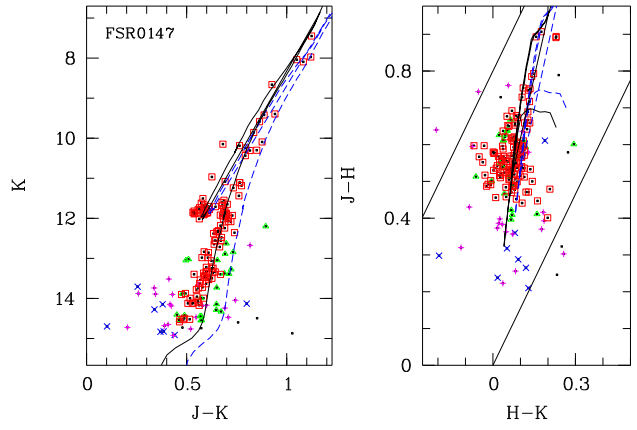


Figure C40. As Fig. C1 but for FSR0147

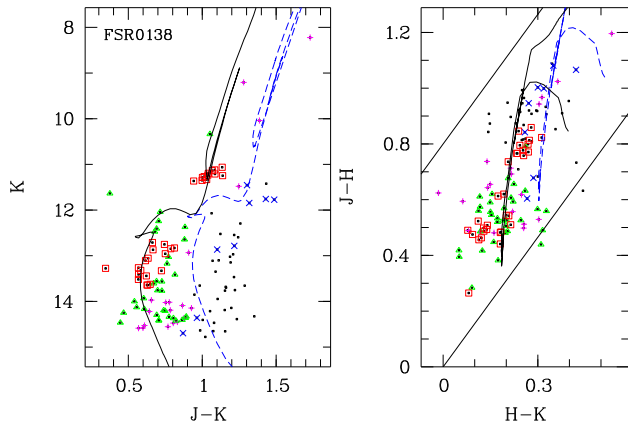


Figure C38. As Fig. C1 but for FSR0138

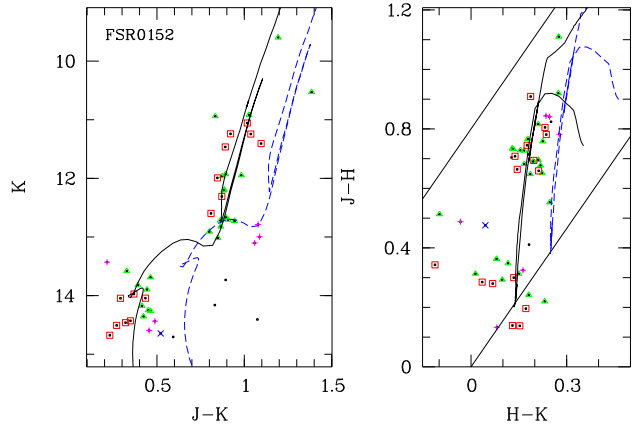


Figure C41. As Fig. C1 but for FSR0152

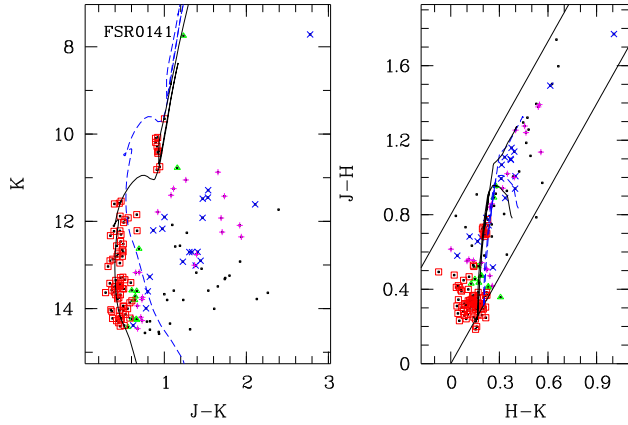


Figure C39. As Fig. C1 but for FSR0141

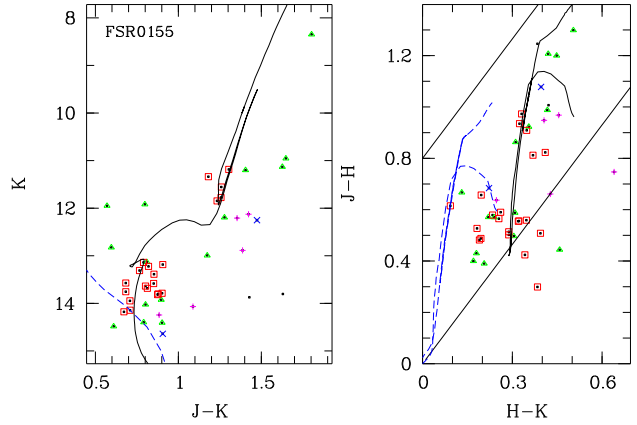


Figure C42. As Fig. C1 but for FSR0155

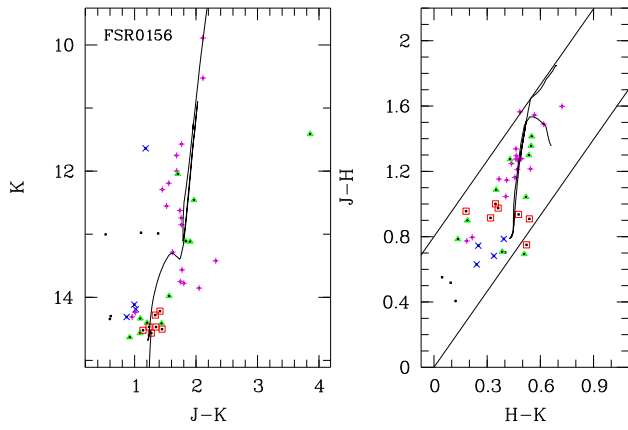


Figure C43. As Fig. C1 but for FSR0156

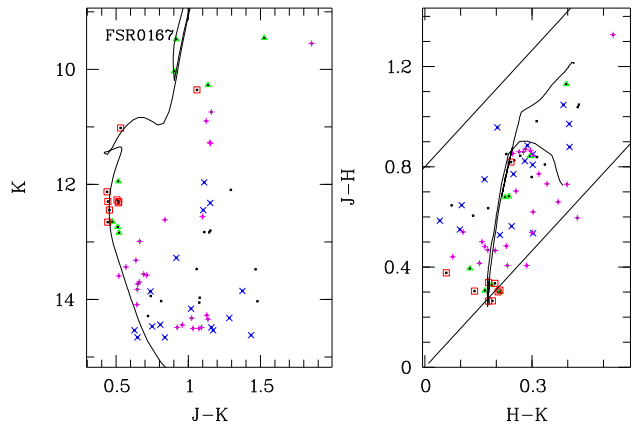


Figure C46. As Fig. C1 but for FSR0167

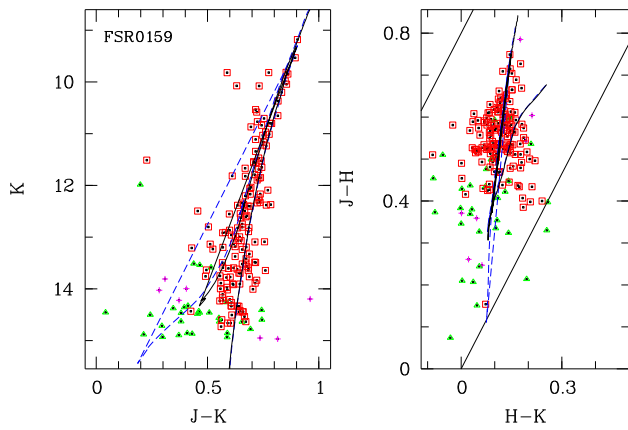


Figure C44. As Fig. C1 but for FSR0159

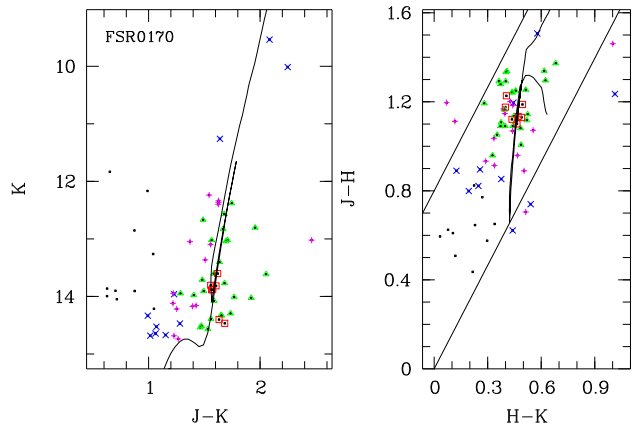


Figure C47. As Fig. C1 but for FSR0170

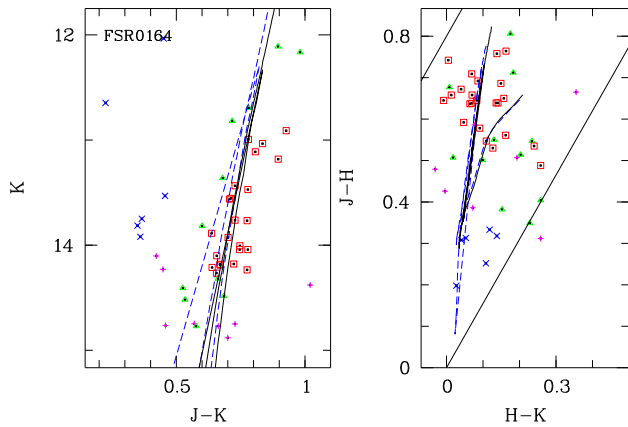


Figure C45. As Fig. C1 but for FSR0164

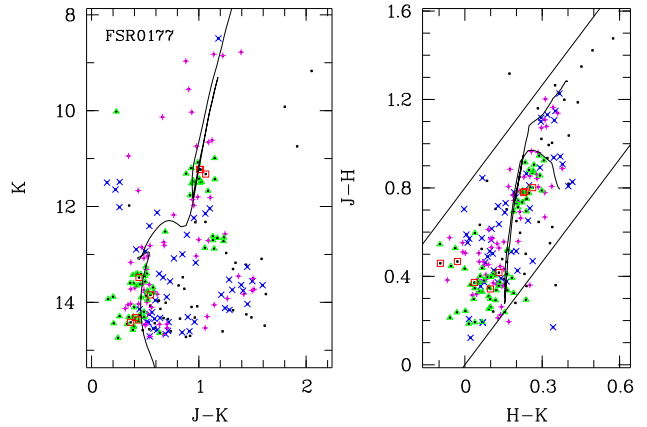


Figure C48. As Fig. C1 but for FSR0177

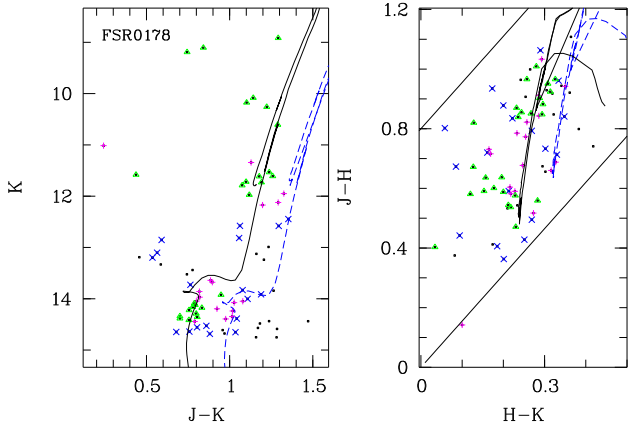


Figure C49. As Fig. C1 but for FSR0178

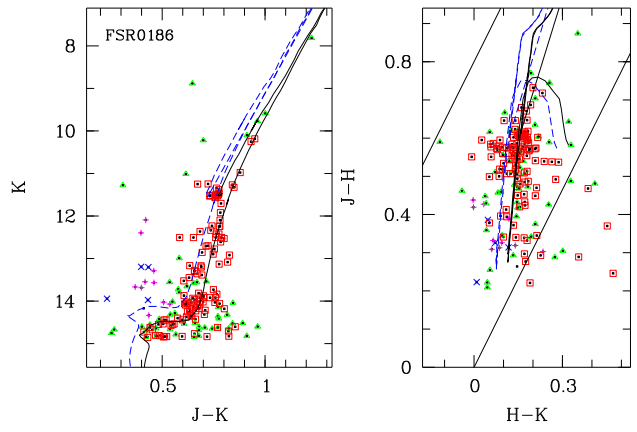


Figure C52. As Fig. C1 but for FSR0186

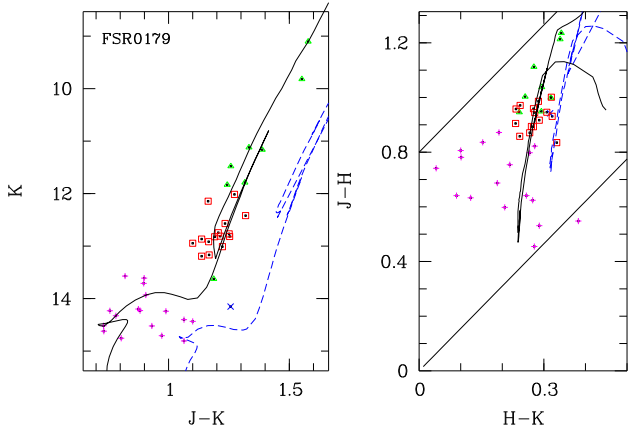


Figure C50. As Fig. C1 but for FSR0179

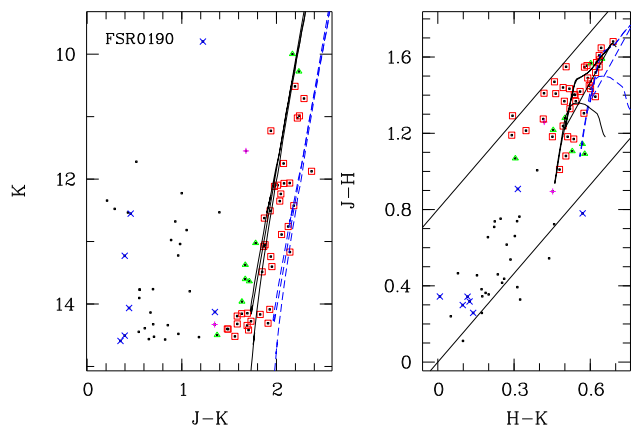


Figure C53. As Fig. C1 but for FSR0190

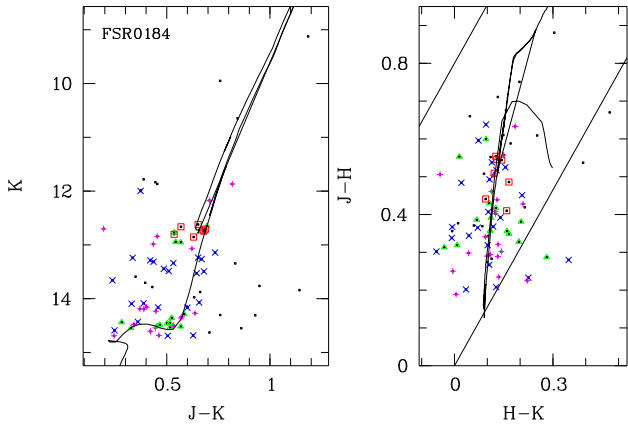


Figure C51. As Fig. C1 but for FSR0184

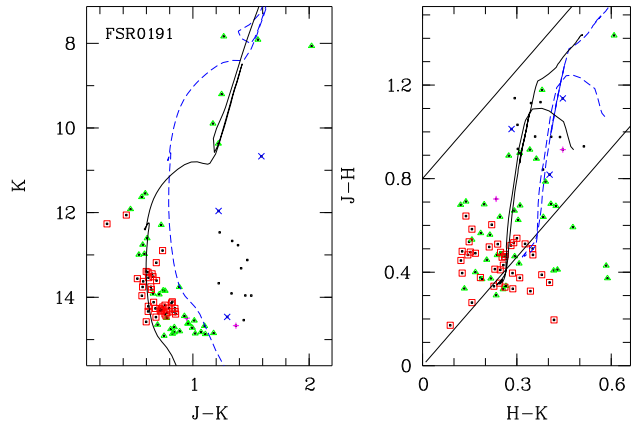
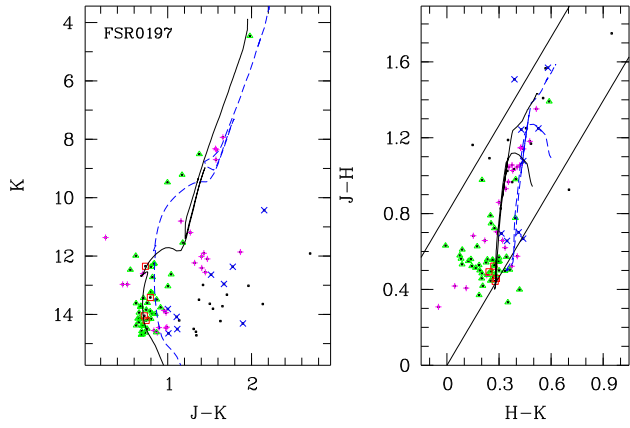
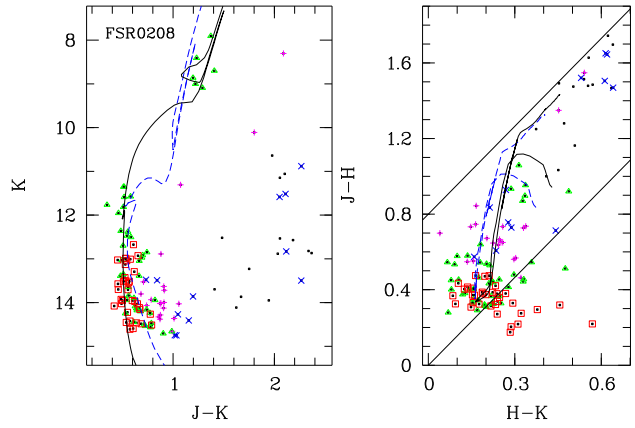


Figure C54. As Fig. C1 but for FSR0191



**Figure C55.** As Fig. C1 but for FSR0197



**Figure C58.** As Fig. C1 but for FSR0208

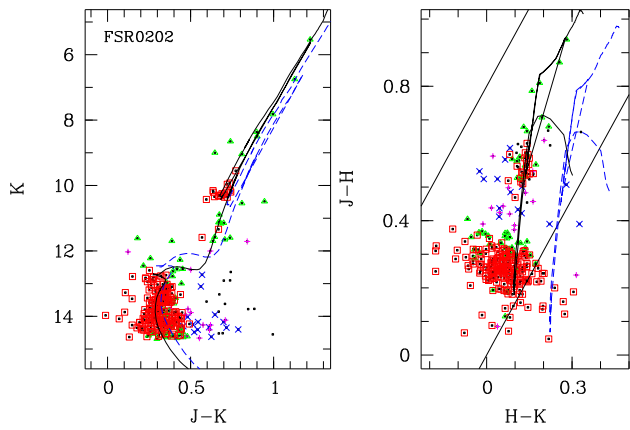


**Figure C56.** As Fig. C1 but for FSR0202

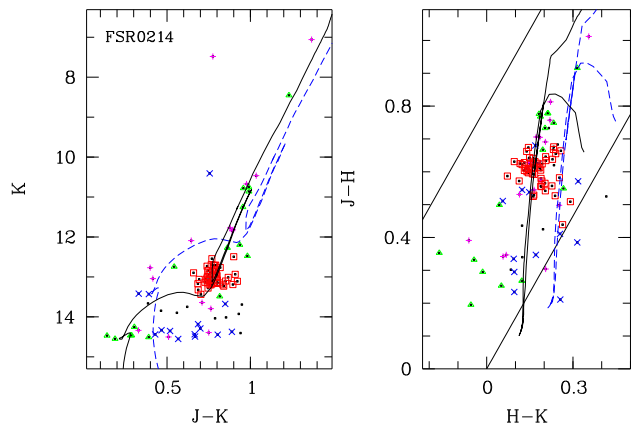


**Figure C59.** As Fig. C1 but for FSR0214

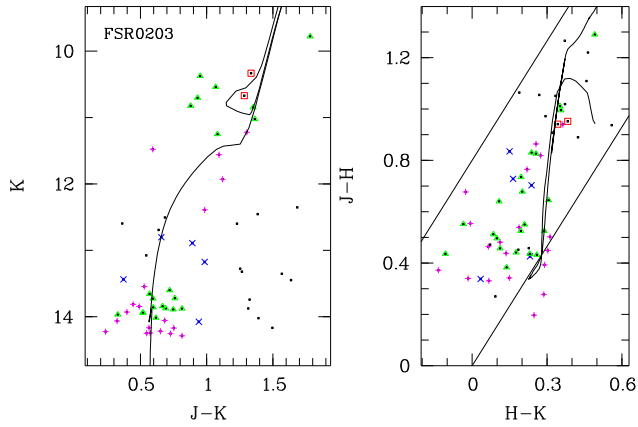


**Figure C57.** As Fig. C1 but for FSR0203

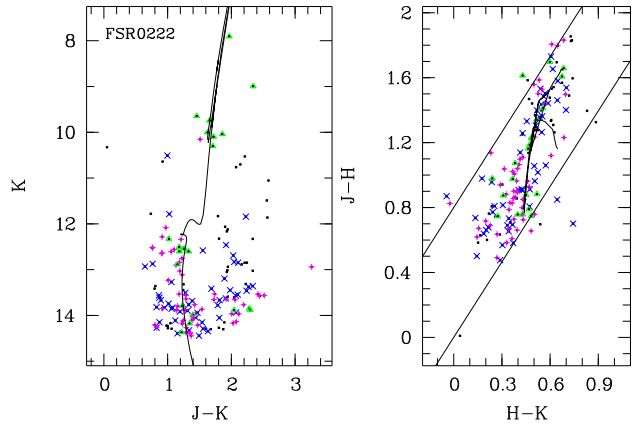


**Figure C60.** As Fig. C1 but for FSR0222

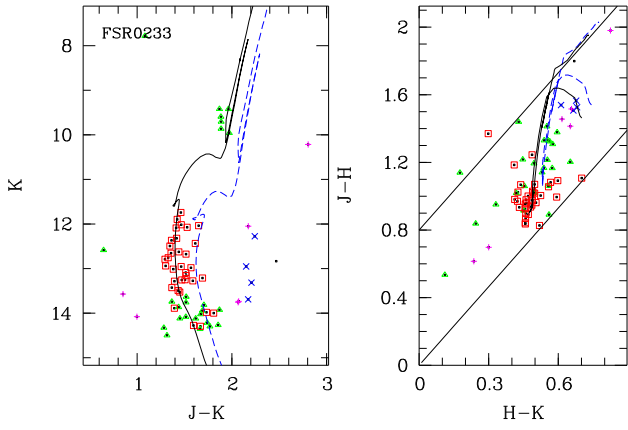


Figure C61. As Fig. C1 but for FSR 0233

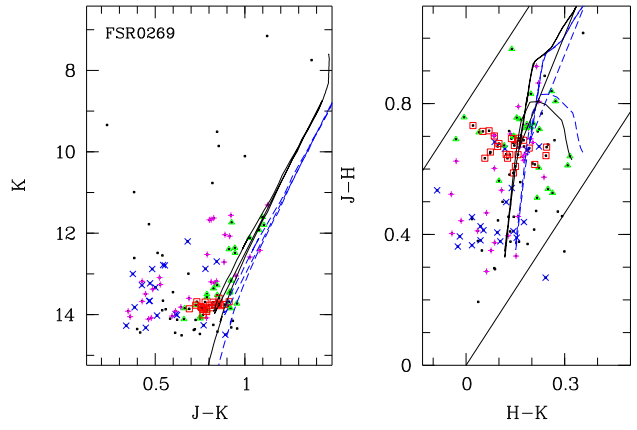


Figure C64. As Fig. C1 but for FSR 0269

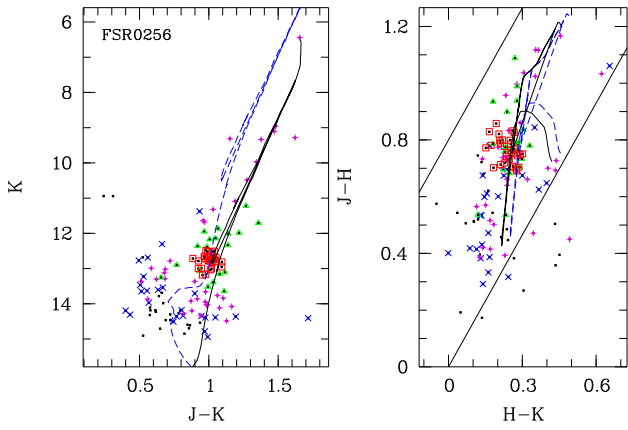


Figure C62. As Fig. C1 but for FSR 0256

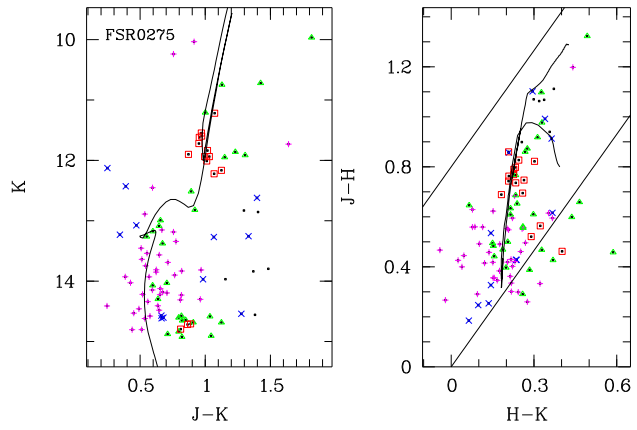


Figure C65. As Fig. C1 but for FSR 0275

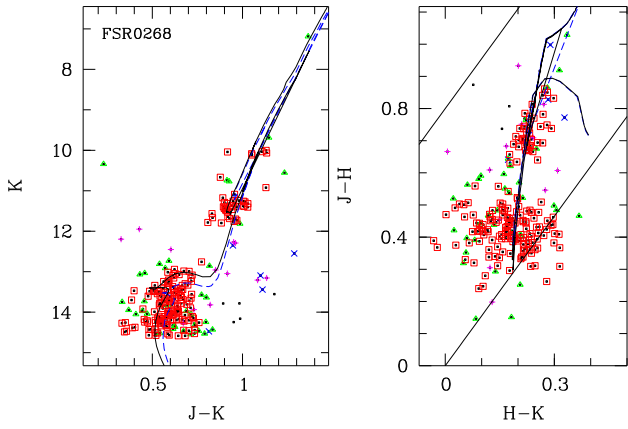


Figure C63. As Fig. C1 but for FSR 0268

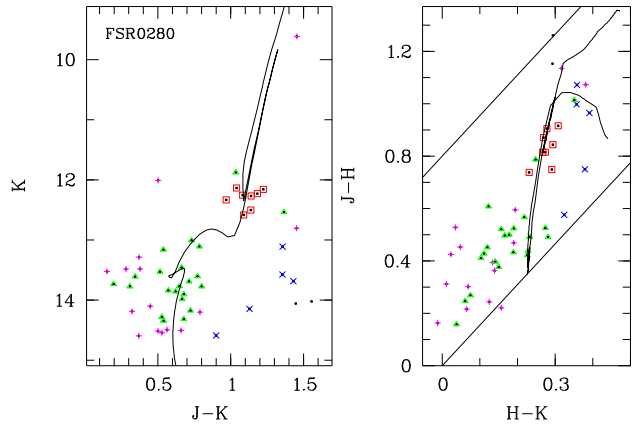
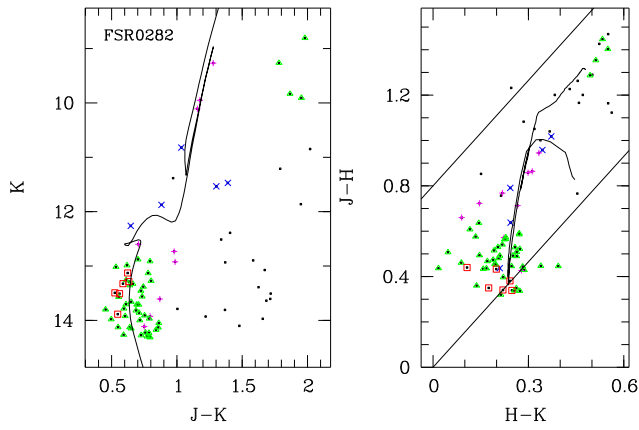
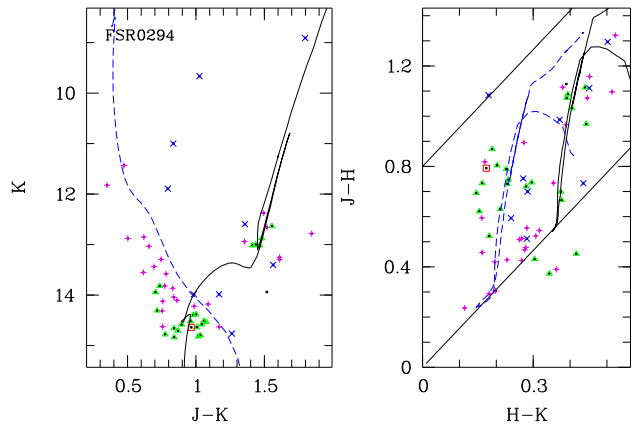


Figure C66. As Fig. C1 but for FSR 0280



**Figure C67.** As Fig. C1 but for FSR0282



**Figure C70.** As Fig. C1 but for FSR0294

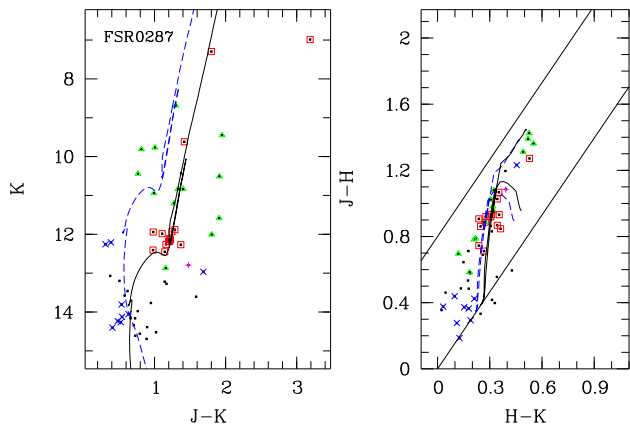


**Figure C68.** As Fig. C1 but for FSR0287

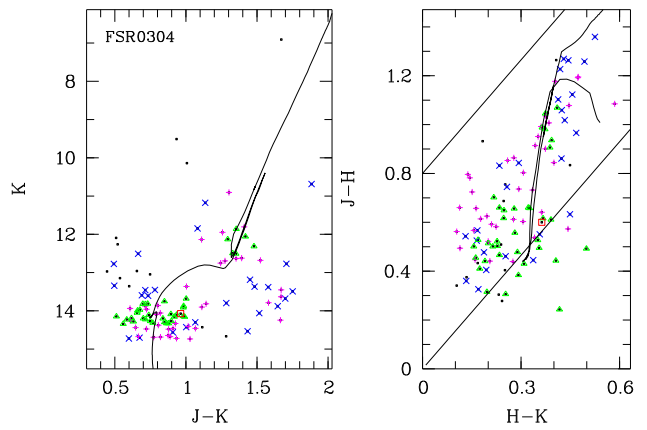


**Figure C71.** As Fig. C1 but for FSR0304

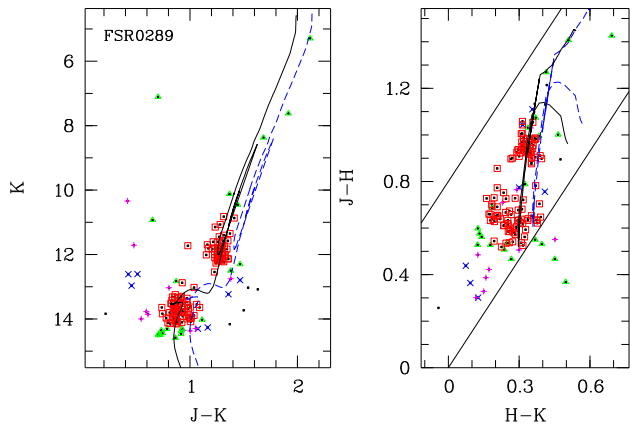


**Figure C69.** As Fig. C1 but for FSR0289

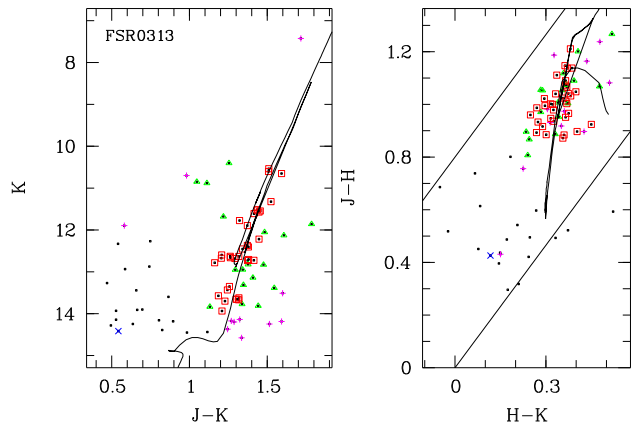


**Figure C72.** As Fig. C1 but for FSR0313

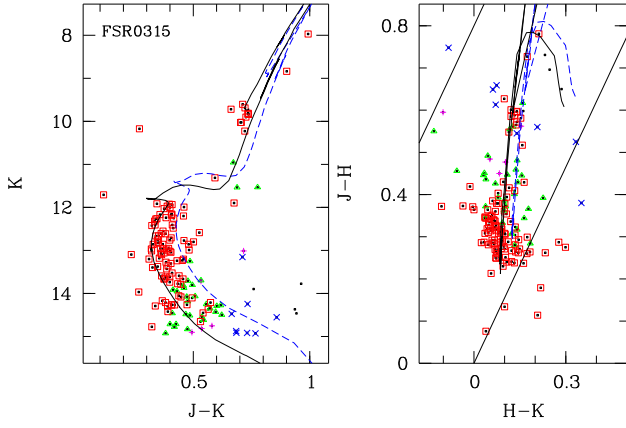


Figure C73. As Fig. C1 but for FSR0315

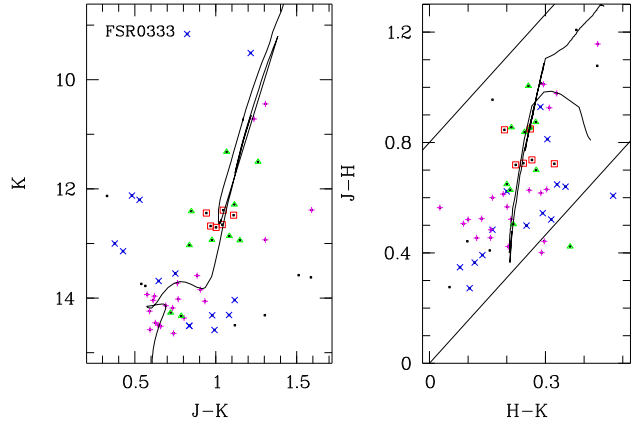


Figure C76. As Fig. C1 but for FSR0333

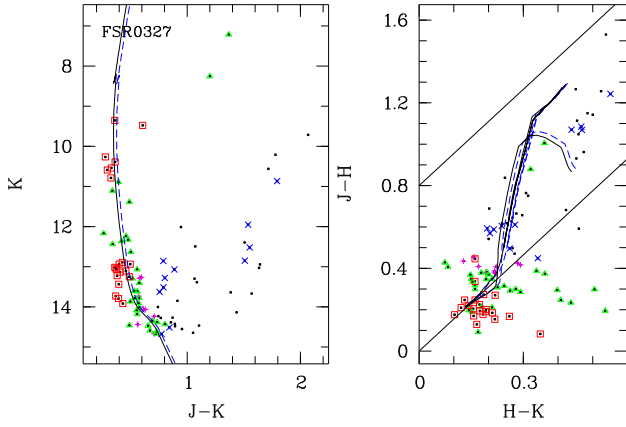


Figure C74. As Fig. C1 but for FSR0327

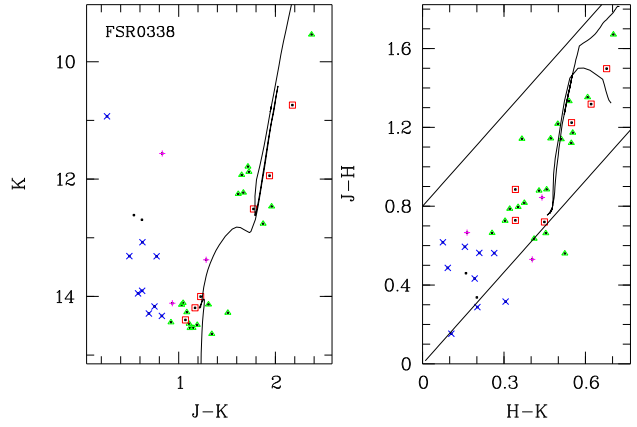


Figure C77. As Fig. C1 but for FSR0338

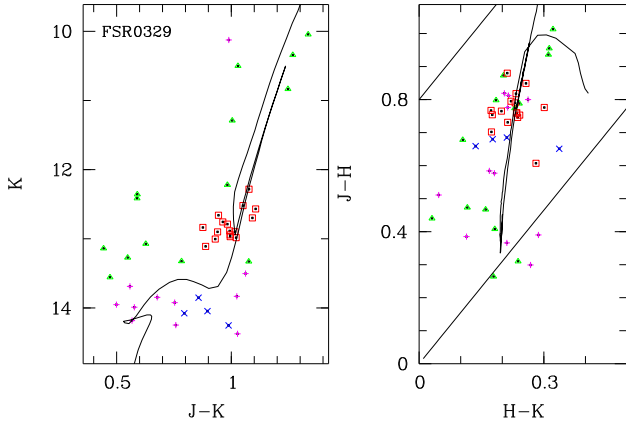


Figure C75. As Fig. C1 but for FSR0329

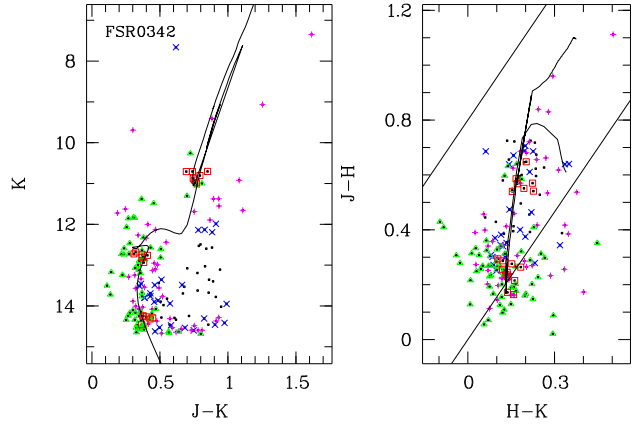
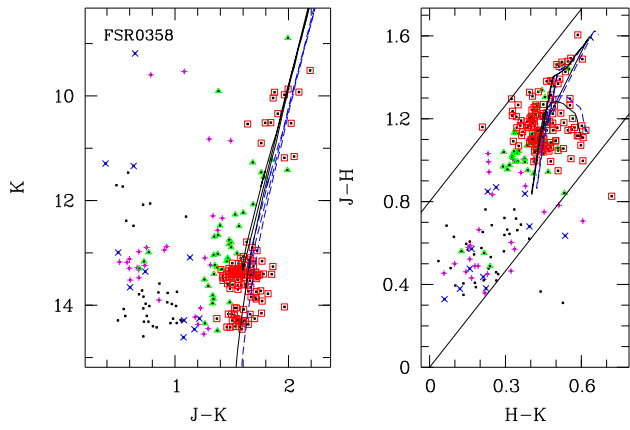
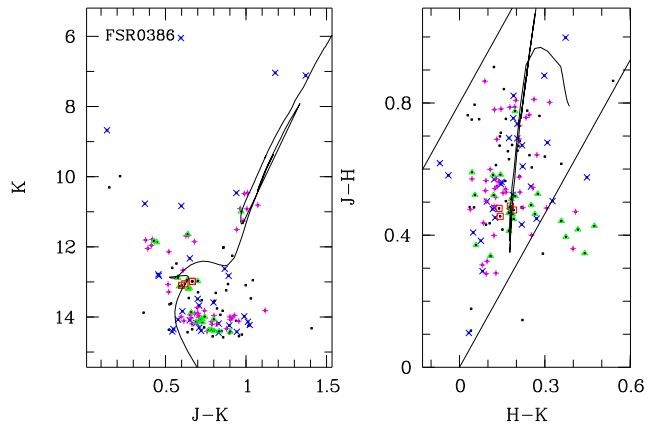


Figure C78. As Fig. C1 but for FSR0342



**Figure C79.** As Fig. C1 but for FSR0358



**Figure C82.** As Fig. C1 but for FSR0386

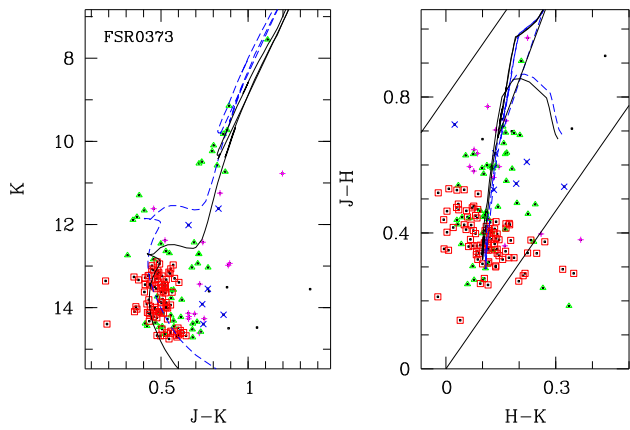


**Figure C80.** As Fig. C1 but for FSR0373

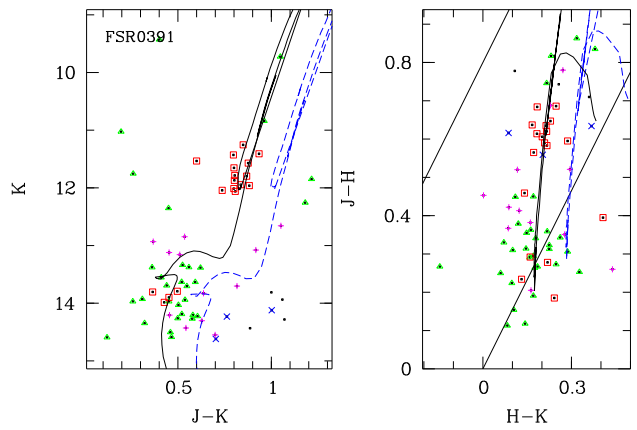


**Figure C83.** As Fig. C1 but for FSR0391

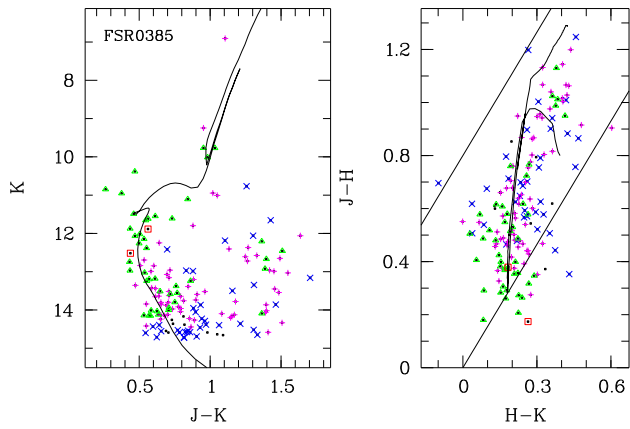


**Figure C81.** As Fig. C1 but for FSR0385

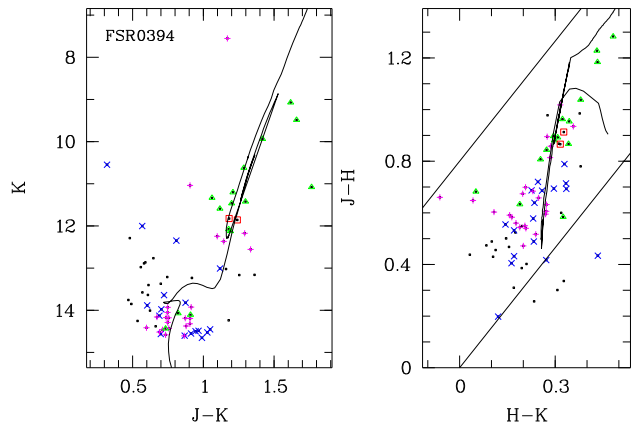


**Figure C84.** As Fig. C1 but for FSR0394

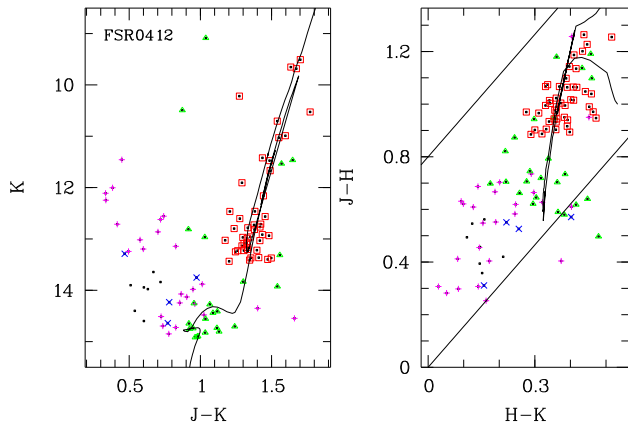


Figure C85. As Fig. C1 but for FSR 0412

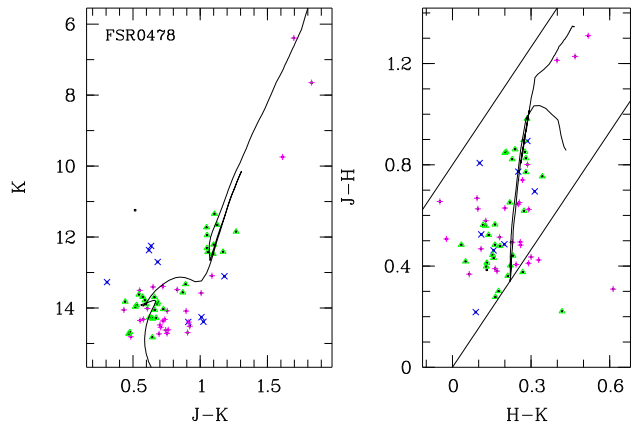


Figure C88. As Fig. C1 but for FSR 0478

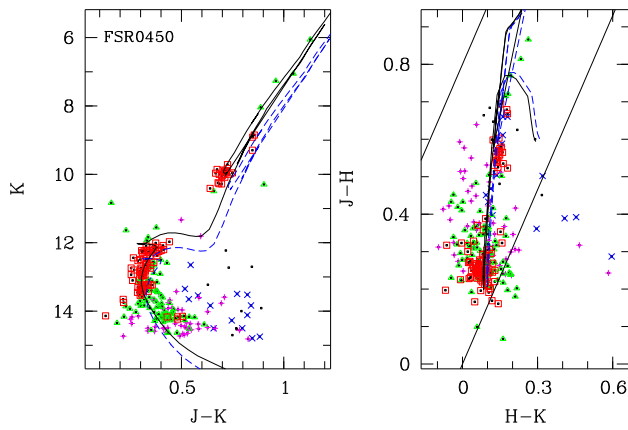


Figure C86. As Fig. C1 but for FSR 0450

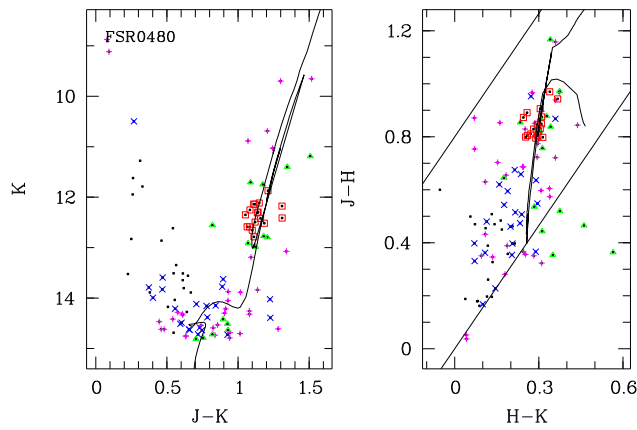


Figure C89. As Fig. C1 but for FSR 0480

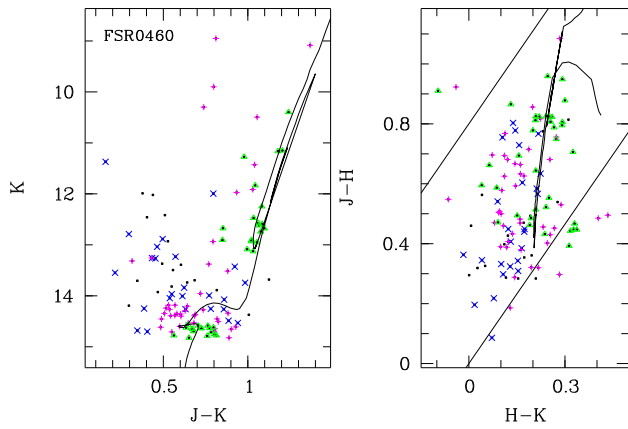


Figure C87. As Fig. C1 but for FSR 0460

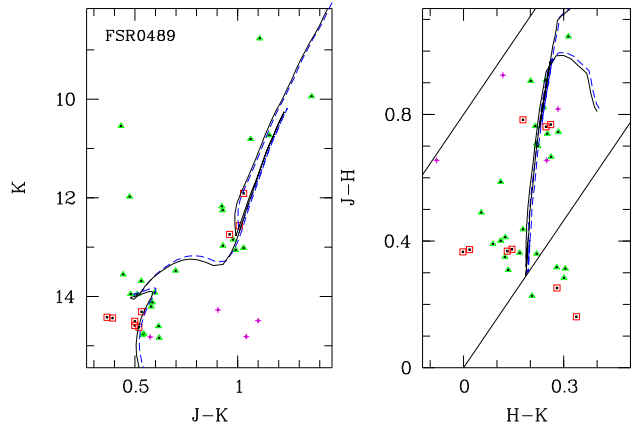
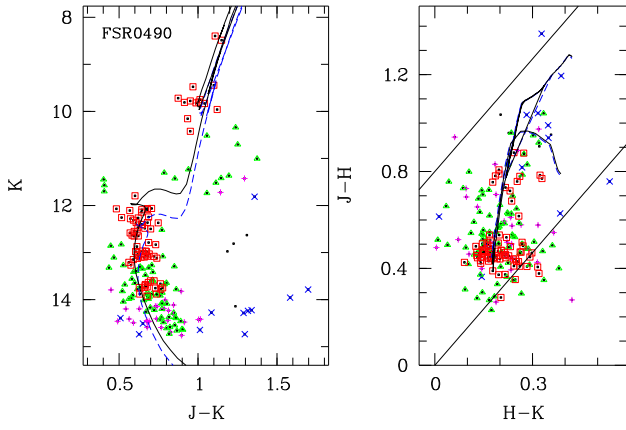
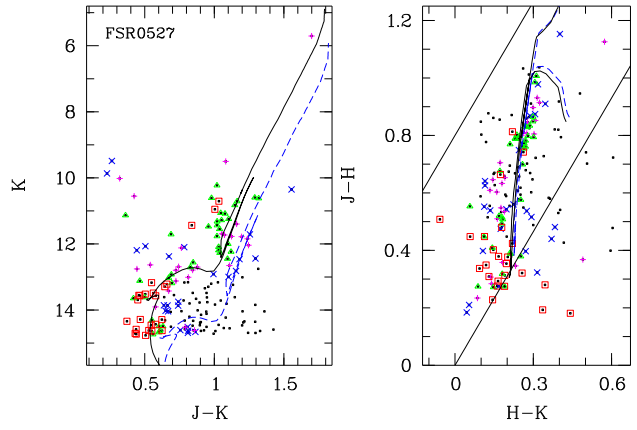


Figure C90. As Fig. C1 but for FSR 0489



**Figure C91.** As Fig. C1 but for FSR 0490



**Figure C94.** As Fig. C1 but for FSR 0527

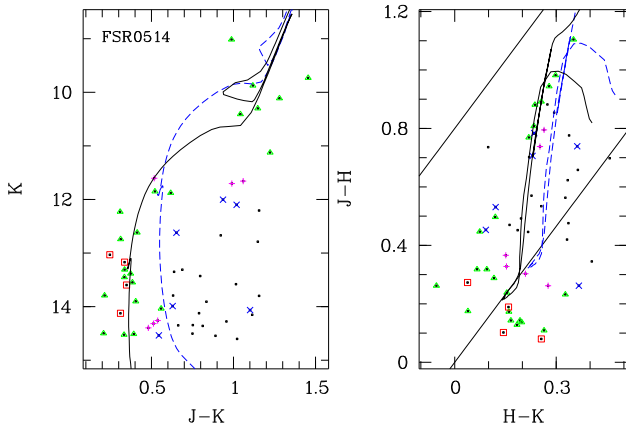


**Figure C92.** As Fig. C1 but for FSR 0514

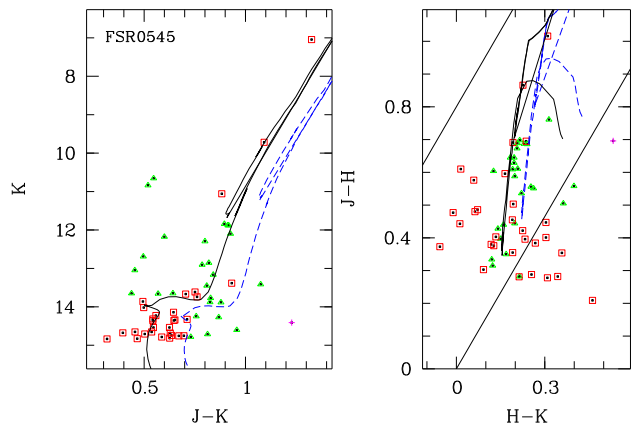


**Figure C95.** As Fig. C1 but for FSR 0545

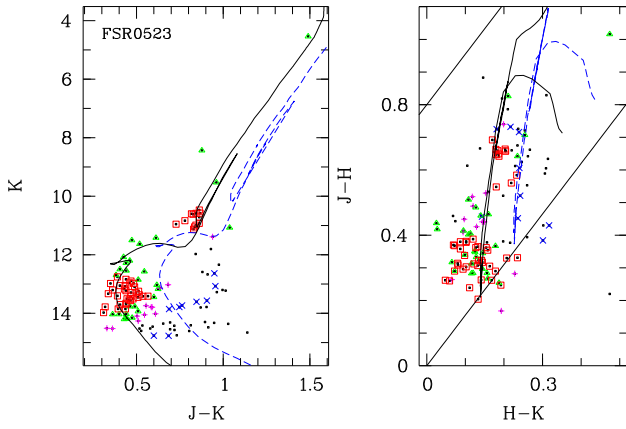


**Figure C93.** As Fig. C1 but for FSR 0523

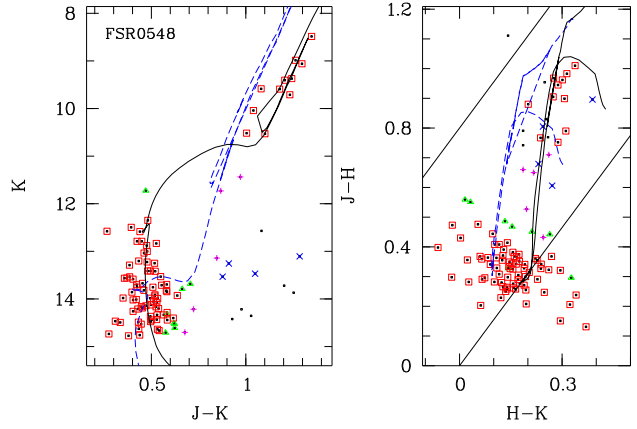


**Figure C96.** As Fig. C1 but for FSR 0548

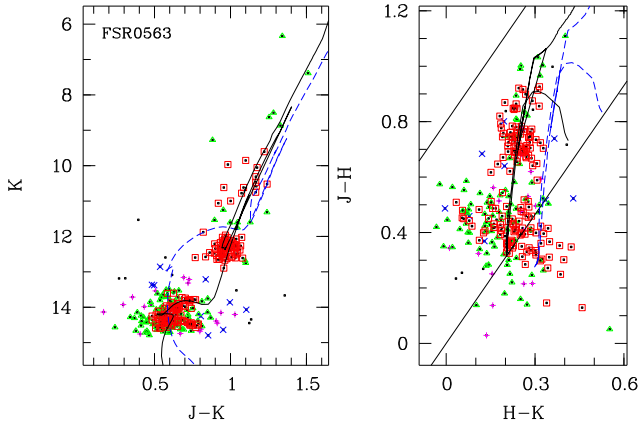


Figure C97. As Fig. C1 but for FSR 0563

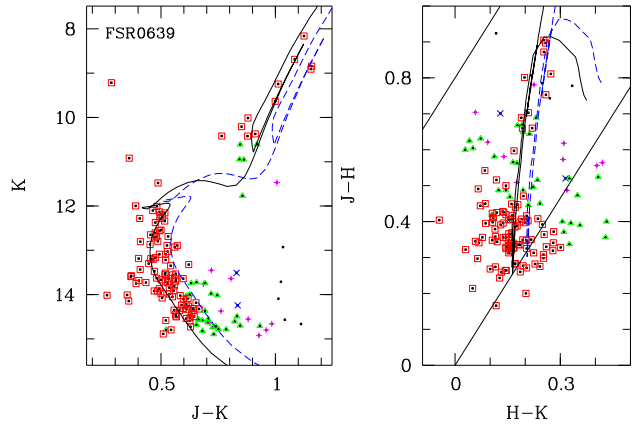


Figure C100. As Fig. C1 but for FSR 0639

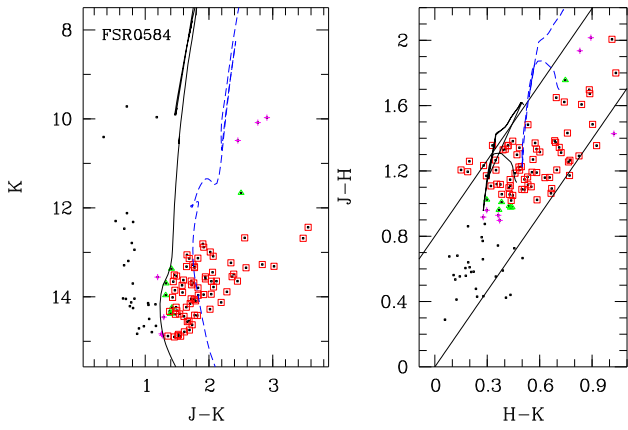


Figure C98. As Fig. C1 but for FSR 0584

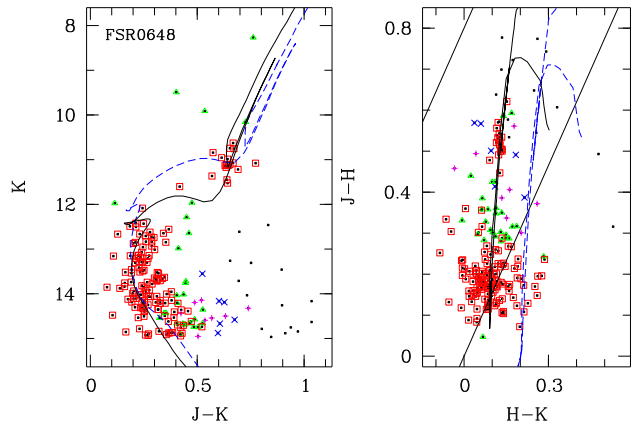


Figure C101. As Fig. C1 but for FSR 0648

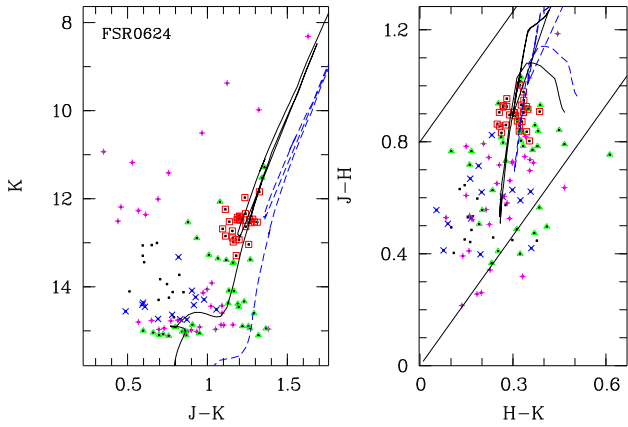


Figure C99. As Fig. C1 but for FSR 0624

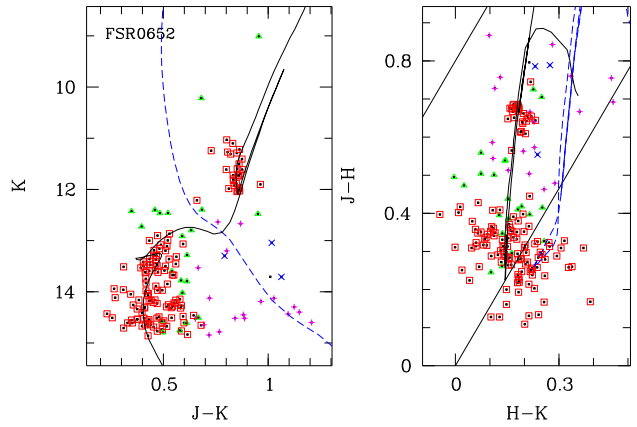
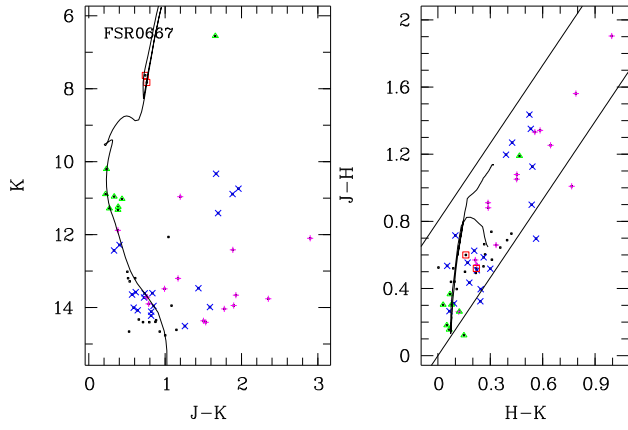
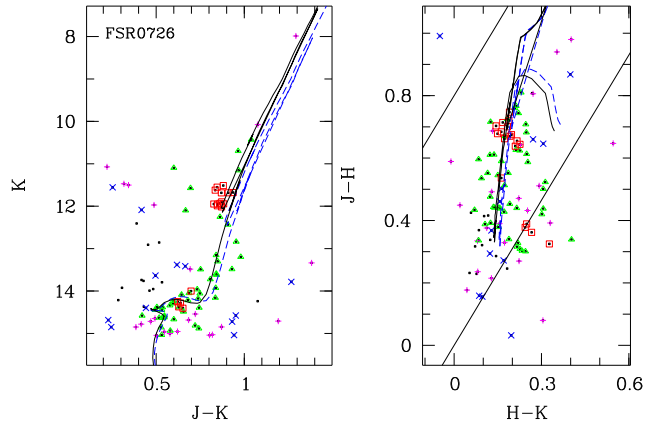


Figure C102. As Fig. C1 but for FSR 0652



**Figure C103.** As Fig. C1 but for FSR 0667



**Figure C106.** As Fig. C1 but for FSR 0726

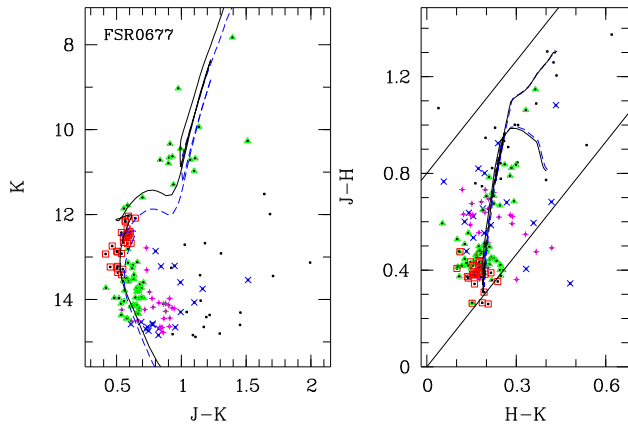


**Figure C104.** As Fig. C1 but for FSR 0677

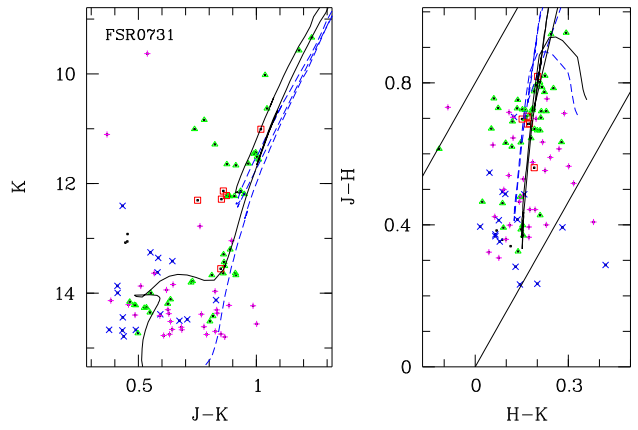


**Figure C107.** As Fig. C1 but for FSR 0731

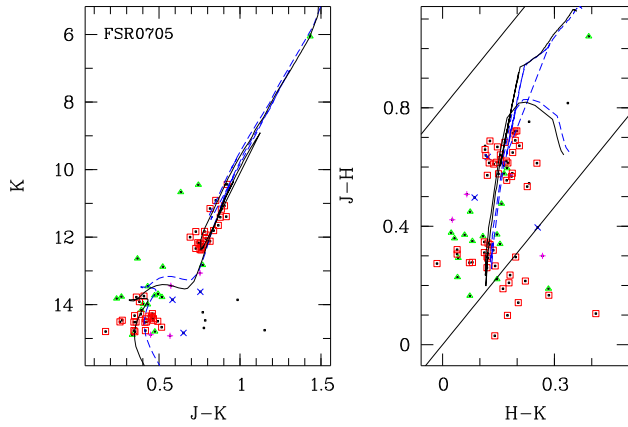


**Figure C105.** As Fig. C1 but for FSR 0705

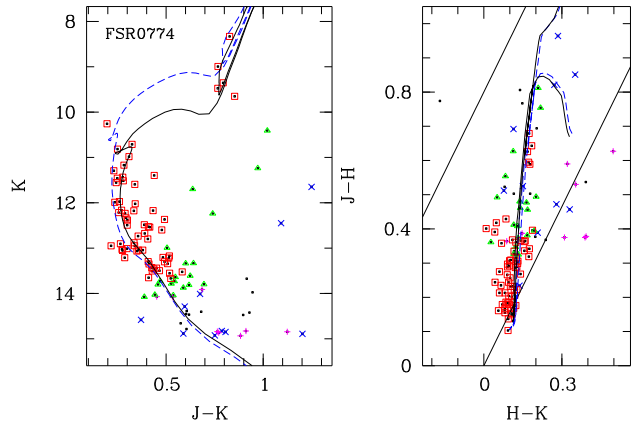


**Figure C108.** As Fig. C1 but for FSR 0774

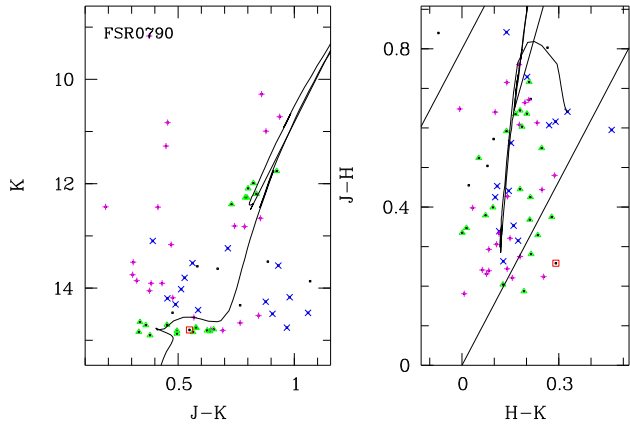


Figure C109. As Fig. C1 but for FSR 0790

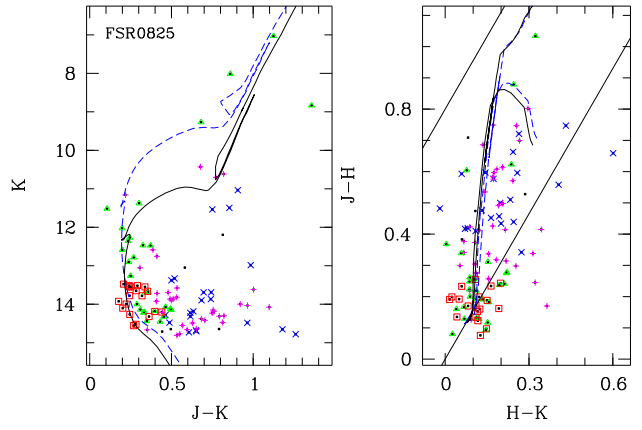


Figure C112. As Fig. C1 but for FSR 0825

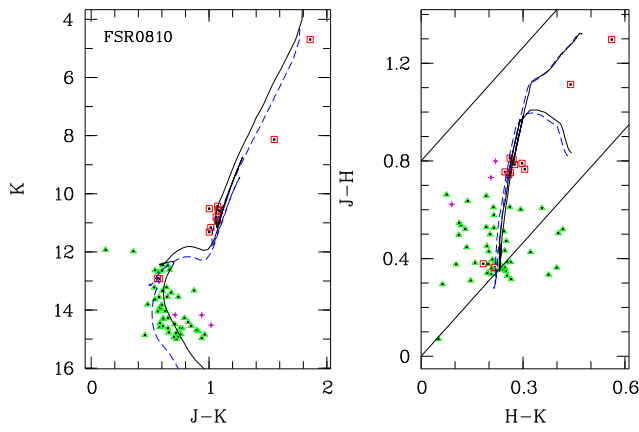


Figure C110. As Fig. C1 but for FSR 0810

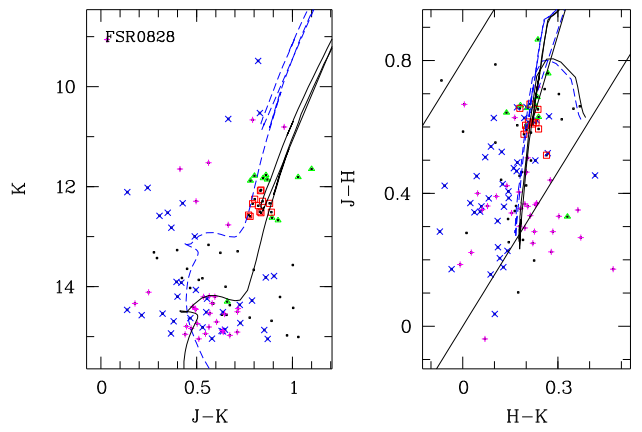


Figure C113. As Fig. C1 but for FSR 0828

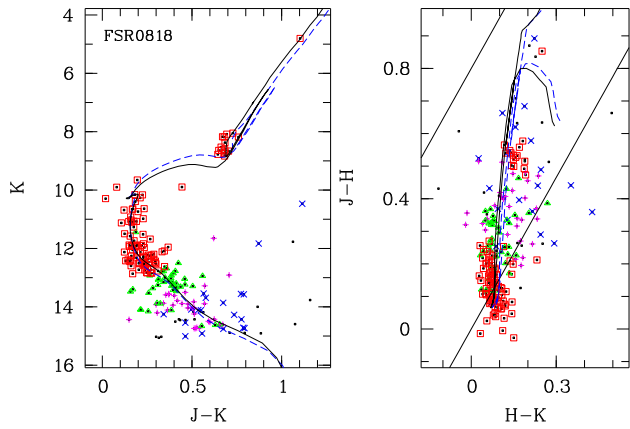


Figure C111. As Fig. C1 but for FSR 0818

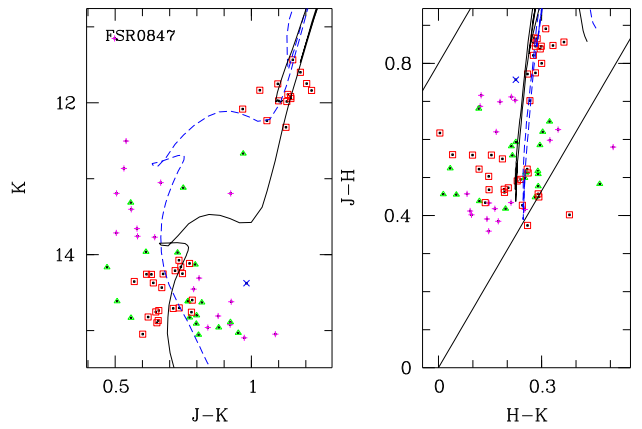
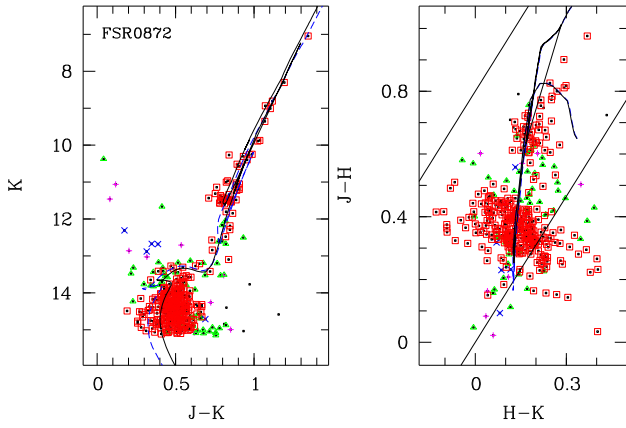
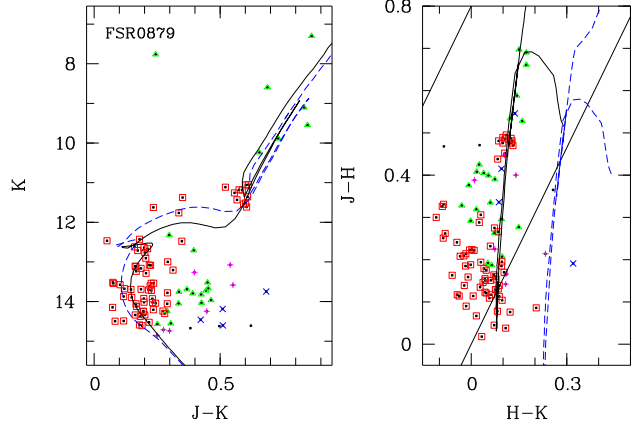


Figure C114. As Fig. C1 but for FSR 0847



**Figure C115.** As Fig. C1 but for FSR 0872



**Figure C118.** As Fig. C1 but for FSR 0879

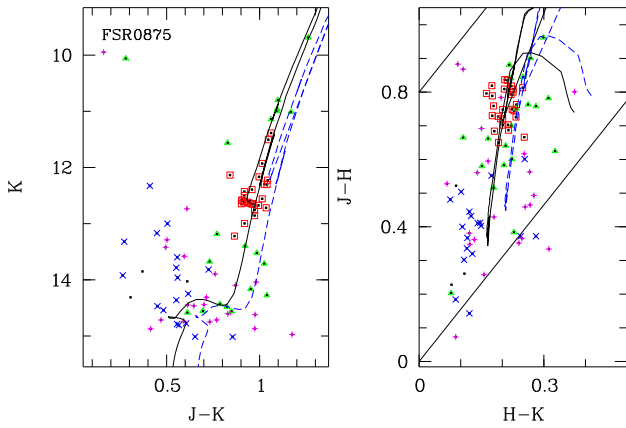


**Figure C116.** As Fig. C1 but for FSR 0875

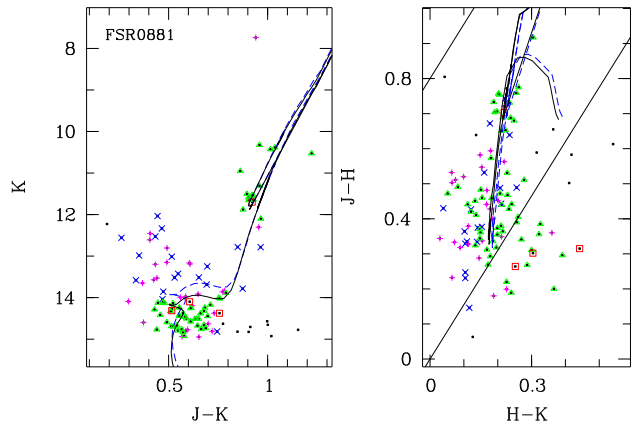


**Figure C119.** As Fig. C1 but for FSR 0881

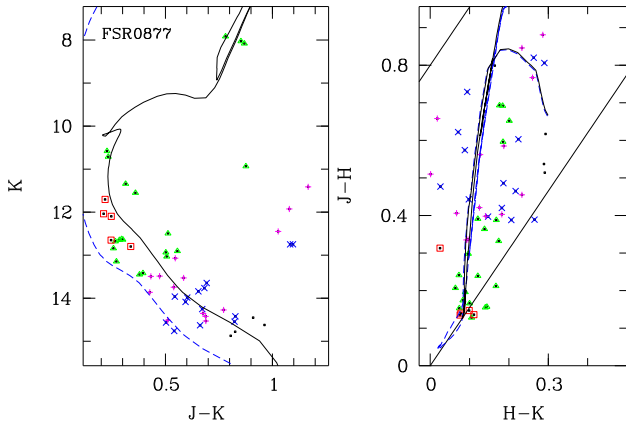


**Figure C117.** As Fig. C1 but for FSR 0877

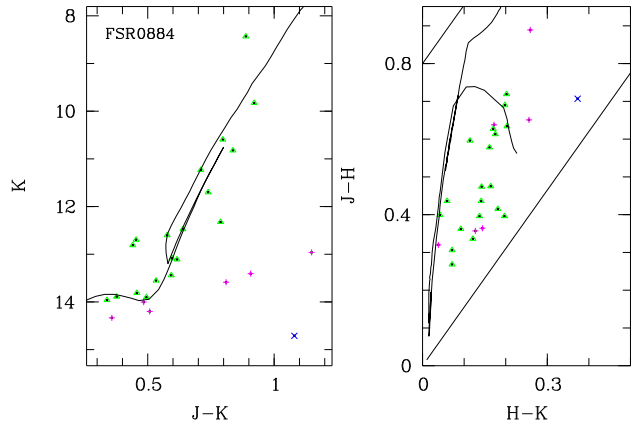


**Figure C120.** As Fig. C1 but for FSR 0884

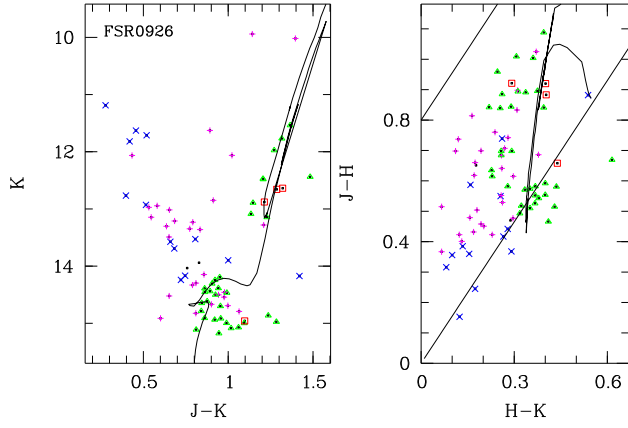


Figure C121. As Fig. C1 but for FSR 0926

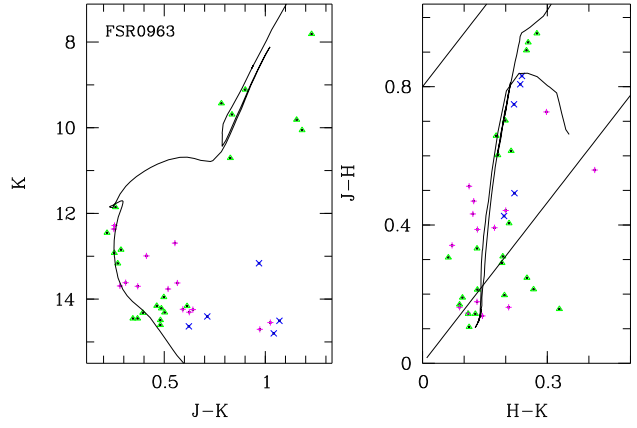


Figure C124. As Fig. C1 but for FSR 0963

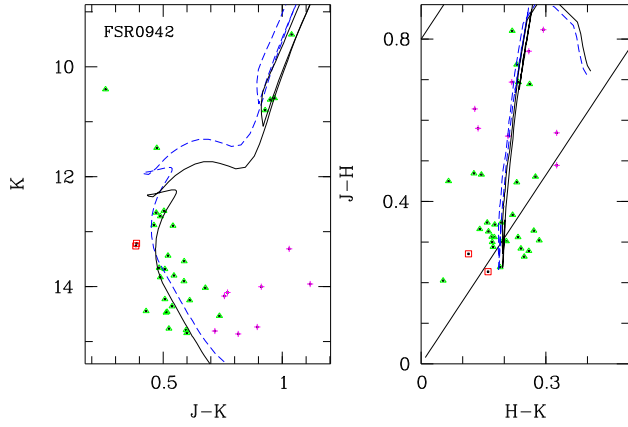


Figure C122. As Fig. C1 but for FSR 0942

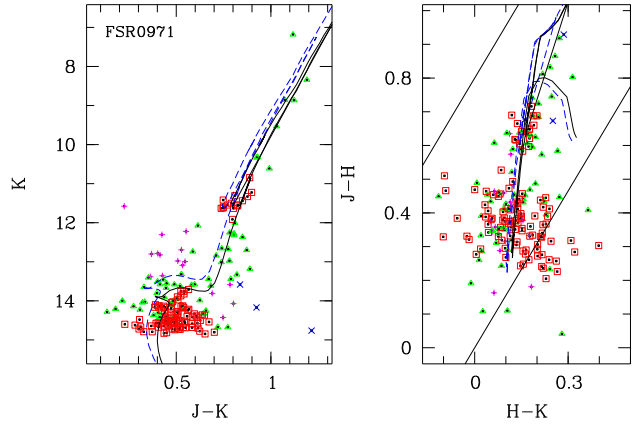


Figure C125. As Fig. C1 but for FSR 0971

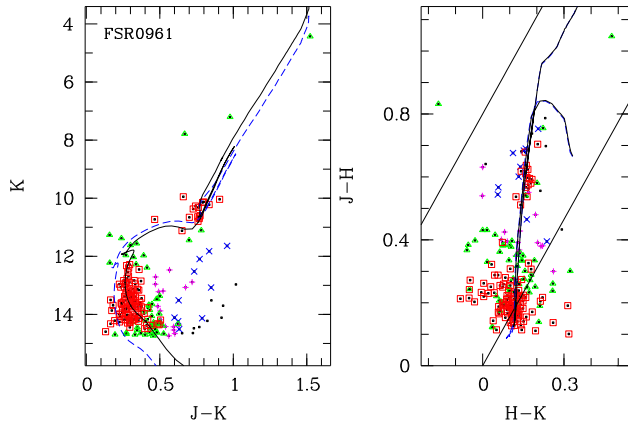


Figure C123. As Fig. C1 but for FSR 0961

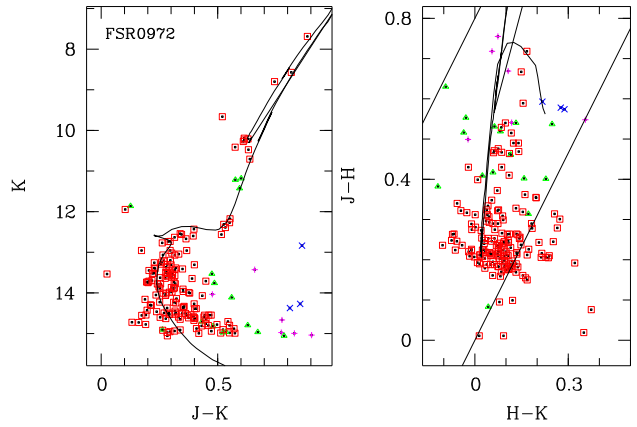
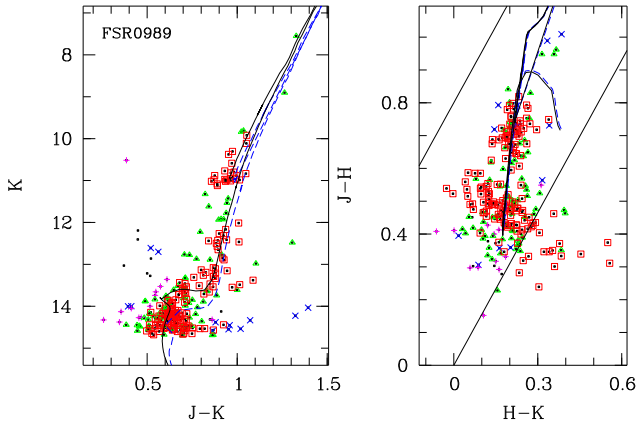
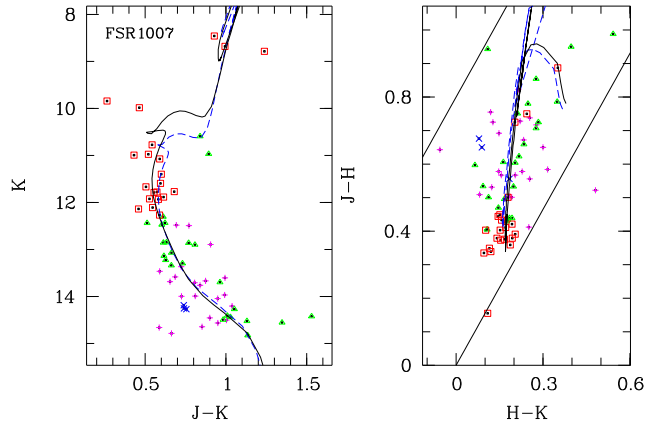


Figure C126. As Fig. C1 but for FSR 0972



**Figure C127.** As Fig. C1 but for FSR 0989



**Figure C130.** As Fig. C1 but for FSR 1007

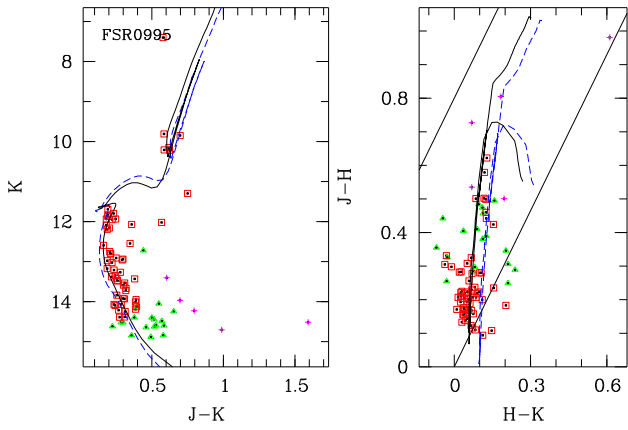


**Figure C128.** As Fig. C1 but for FSR 0995

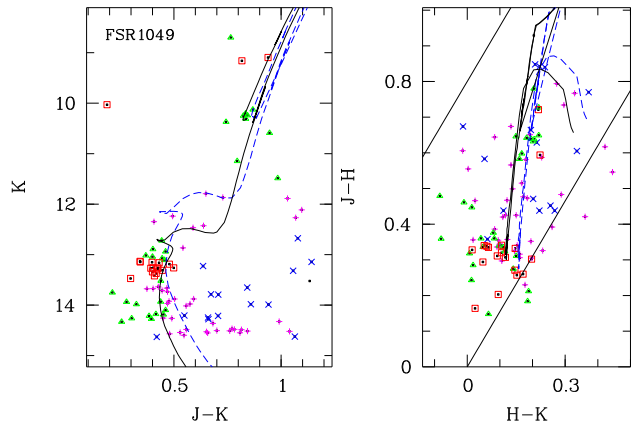


**Figure C131.** As Fig. C1 but for FSR 1049

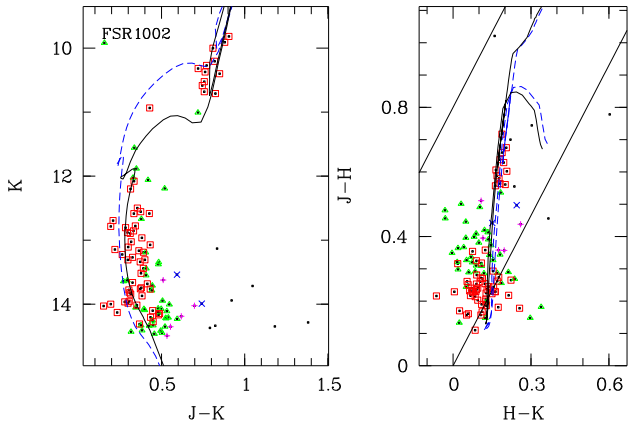


**Figure C129.** As Fig. C1 but for FSR 1002

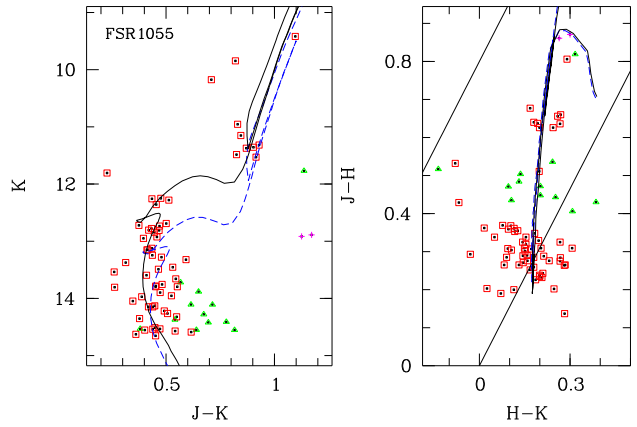


**Figure C132.** As Fig. C1 but for FSR 1055

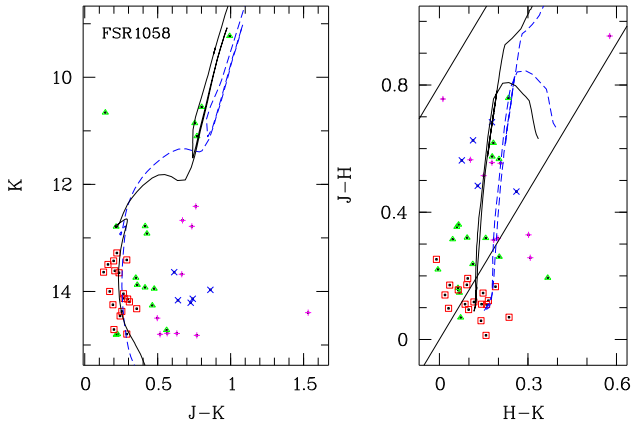


Figure C133. As Fig. C1 but for FSR 1058

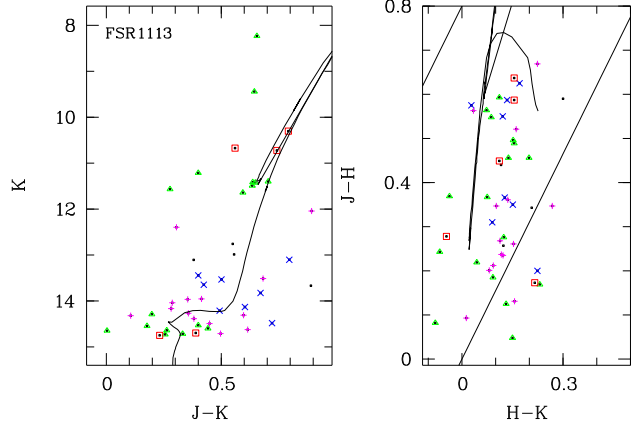


Figure C136. As Fig. C1 but for FSR 1113

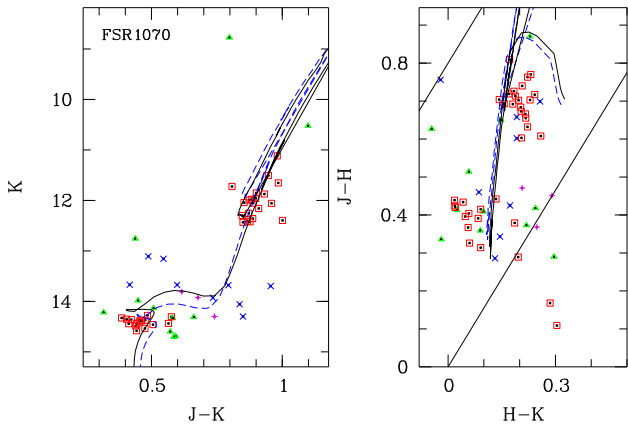


Figure C134. As Fig. C1 but for FSR 1070

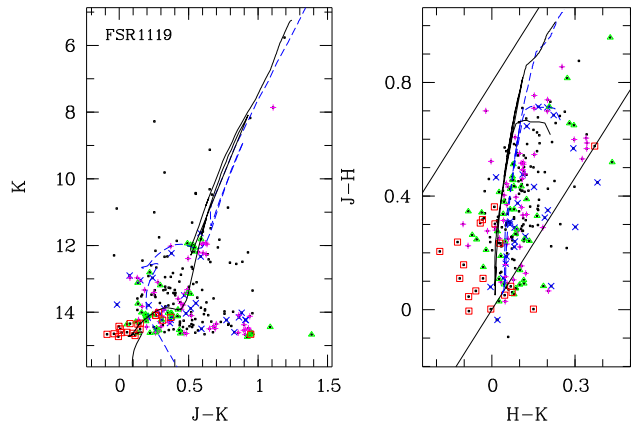


Figure C137. As Fig. C1 but for FSR 1119

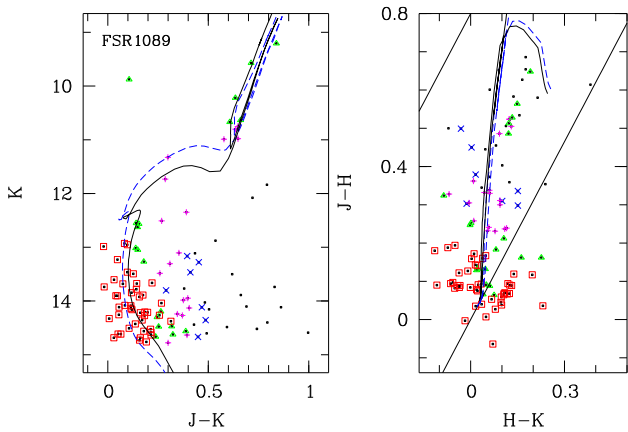


Figure C135. As Fig. C1 but for FSR 1089

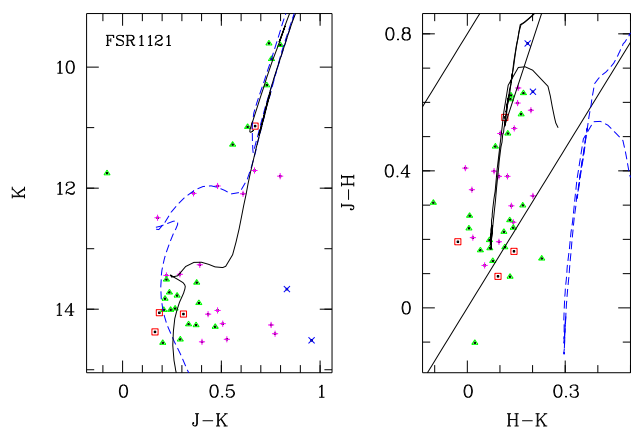
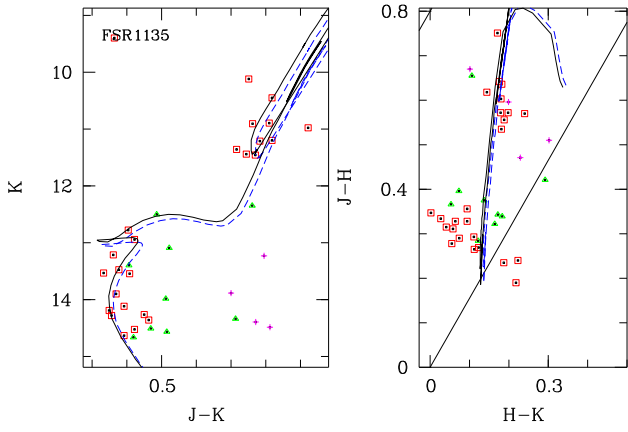
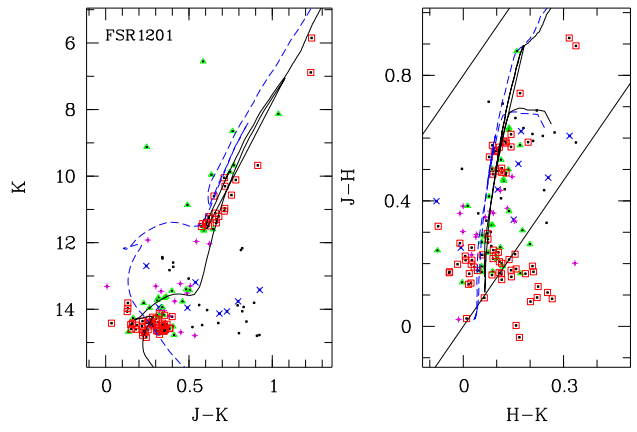


Figure C138. As Fig. C1 but for FSR 1121



**Figure C139.** As Fig. C1 but for FSR 1135



**Figure C142.** As Fig. C1 but for FSR 1201

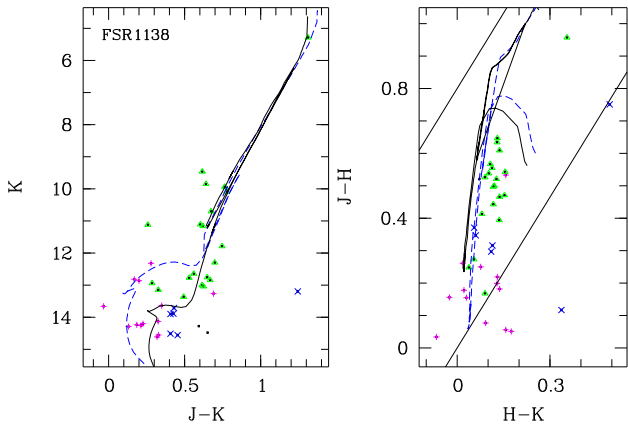


**Figure C140.** As Fig. C1 but for FSR 1138

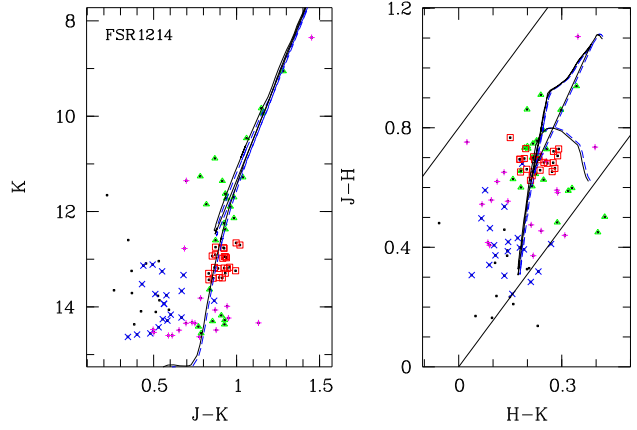


**Figure C143.** As Fig. C1 but for FSR 1214

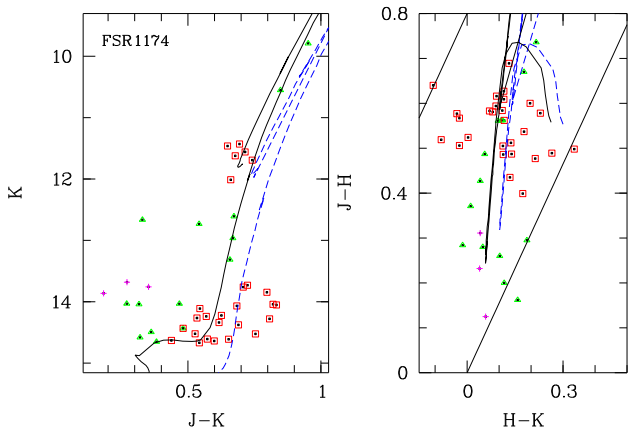


**Figure C141.** As Fig. C1 but for FSR 1174

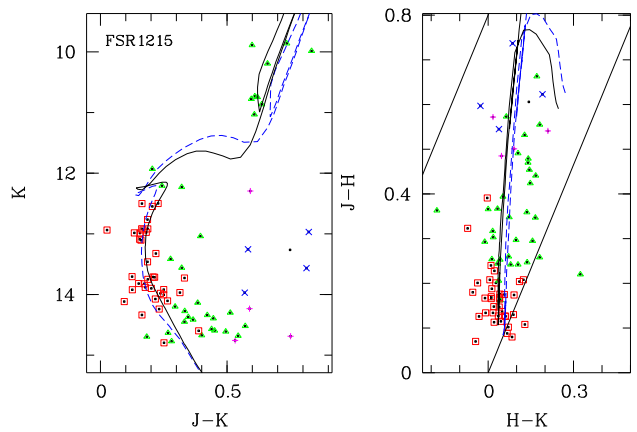


**Figure C144.** As Fig. C1 but for FSR 1215

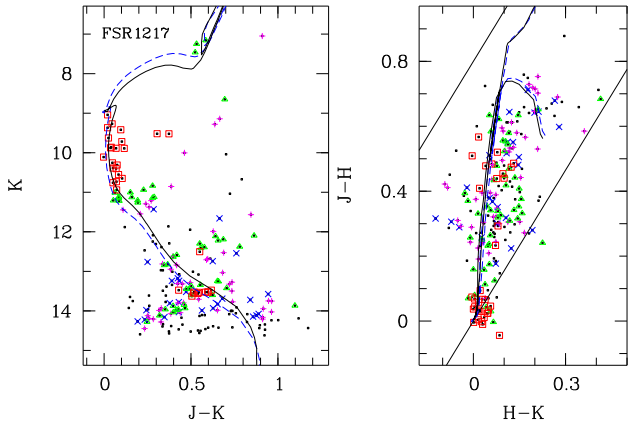


Figure C145. As Fig. C1 but for FSR 1217

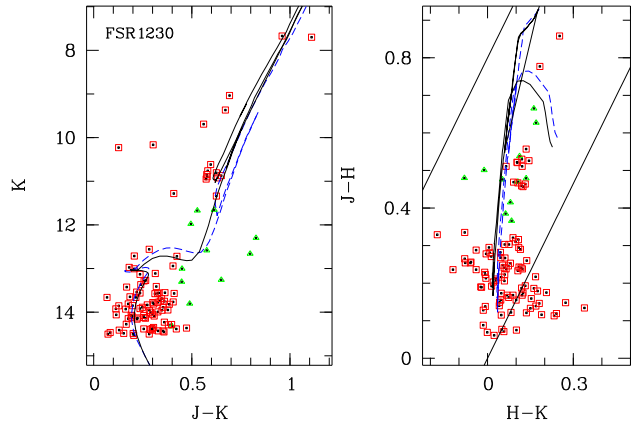


Figure C148. As Fig. C1 but for FSR 1230

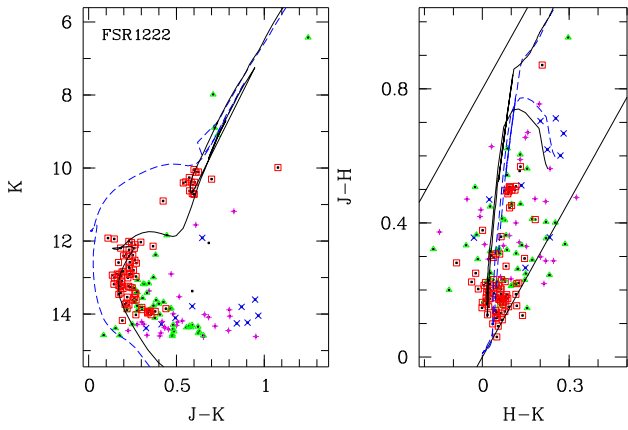


Figure C146. As Fig. C1 but for FSR 1222

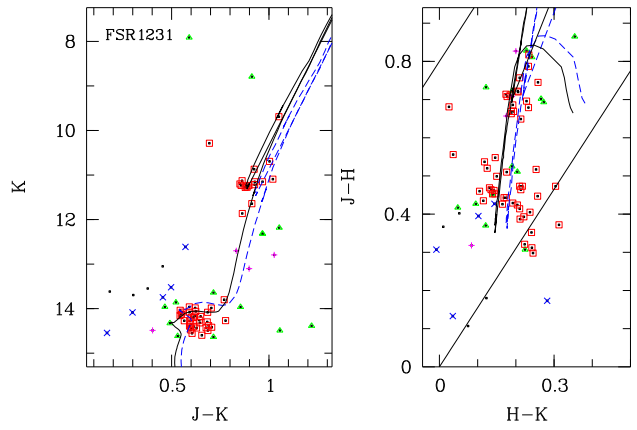


Figure C149. As Fig. C1 but for FSR 1231

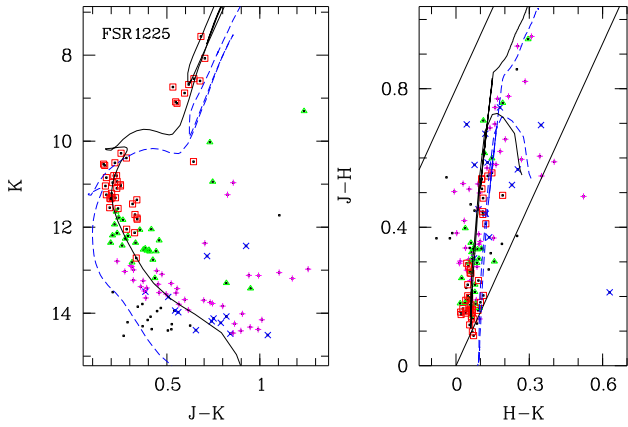


Figure C147. As Fig. C1 but for FSR 1225

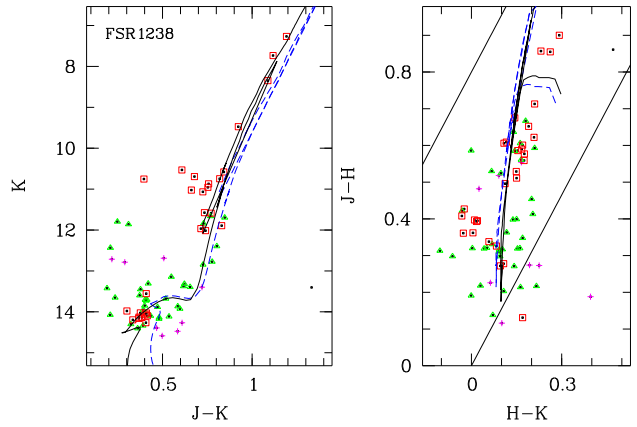
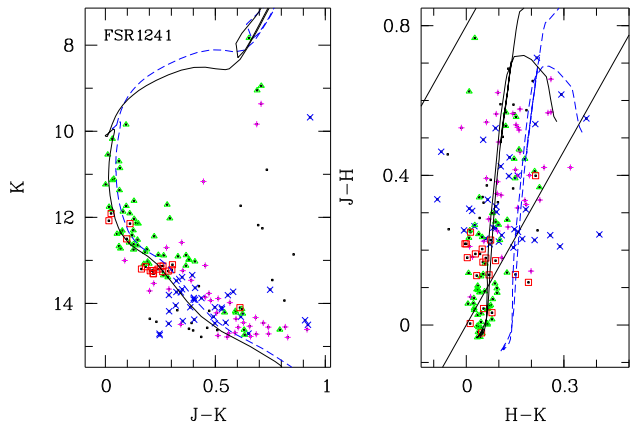
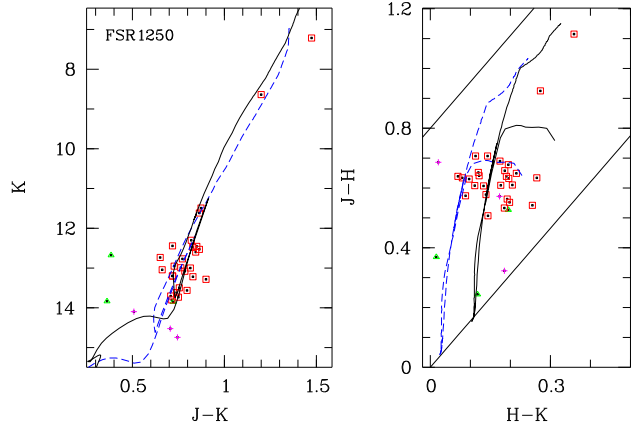


Figure C150. As Fig. C1 but for FSR 1238



**Figure C151.** As Fig. C1 but for FSR 1241



**Figure C154.** As Fig. C1 but for FSR 1250

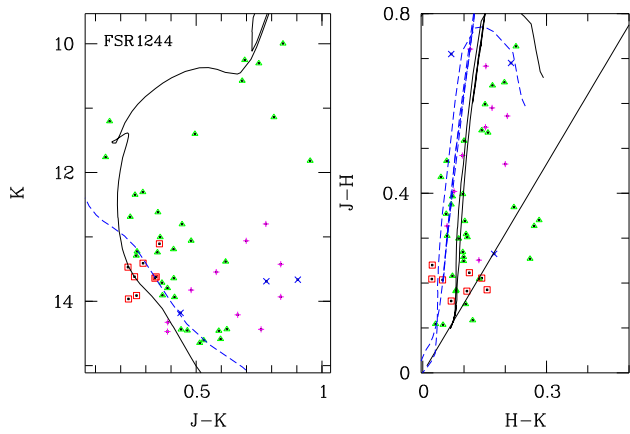


**Figure C152.** As Fig. C1 but for FSR 1244

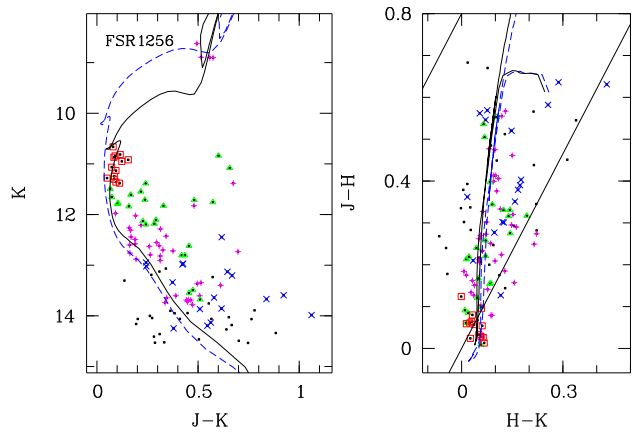


**Figure C155.** As Fig. C1 but for FSR 1256

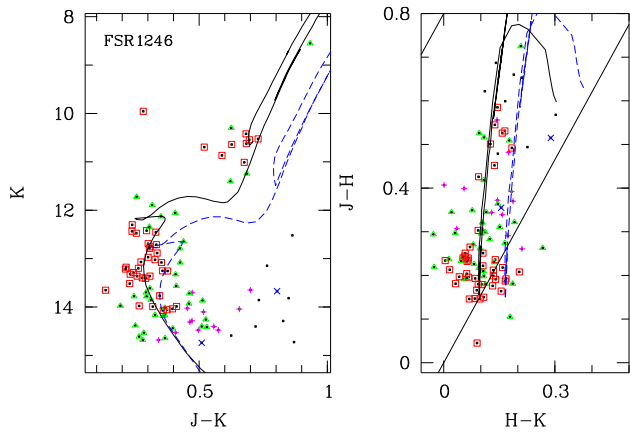


**Figure C153.** As Fig. C1 but for FSR 1246

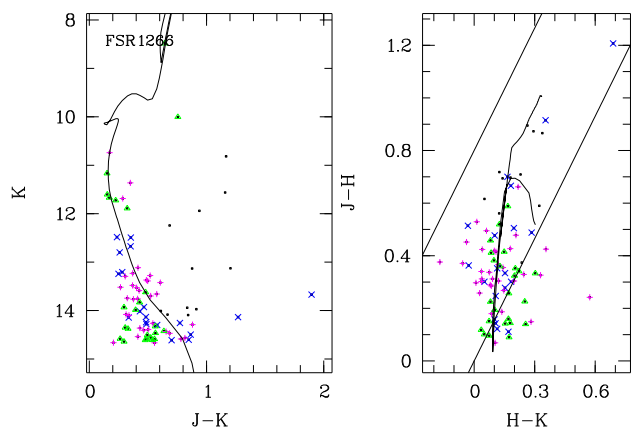


**Figure C156.** As Fig. C1 but for FSR 1266

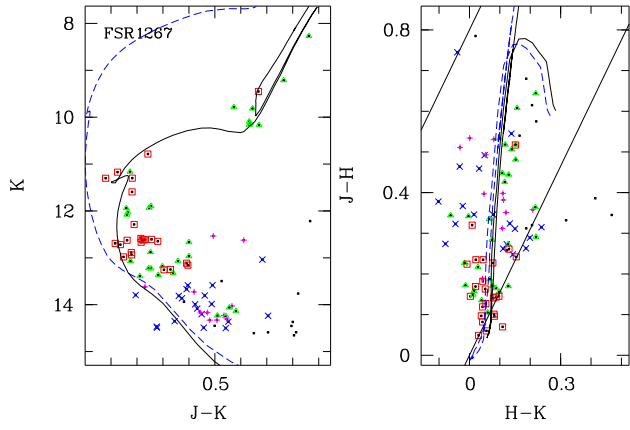


Figure C157. As Fig. C1 but for FSR 1267

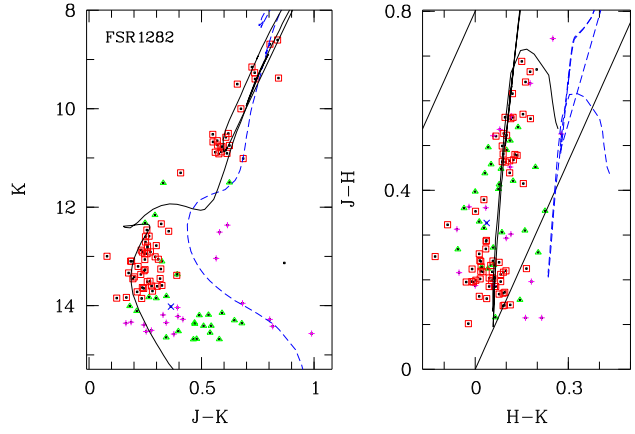


Figure C160. As Fig. C1 but for FSR 1282

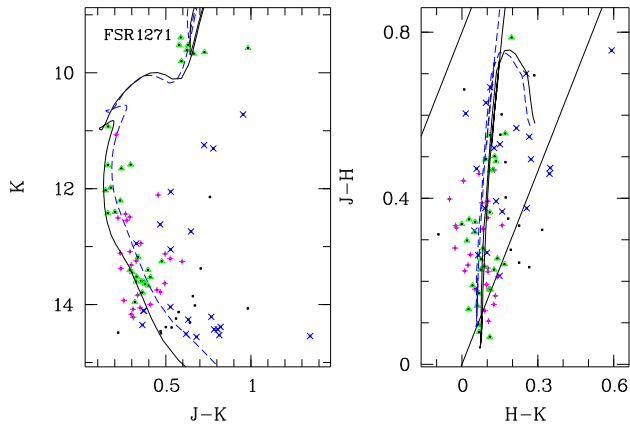


Figure C158. As Fig. C1 but for FSR 1271

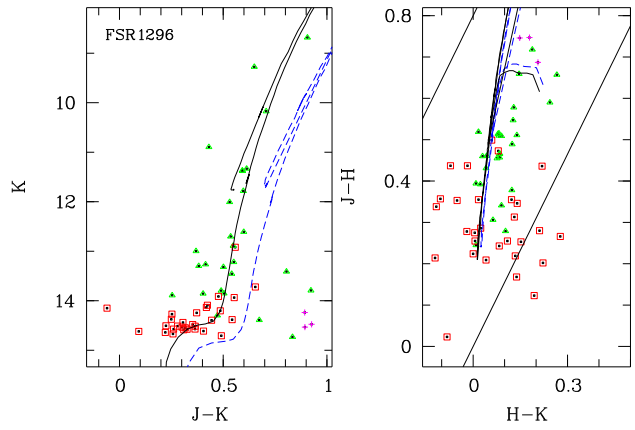


Figure C161. As Fig. C1 but for FSR 1296

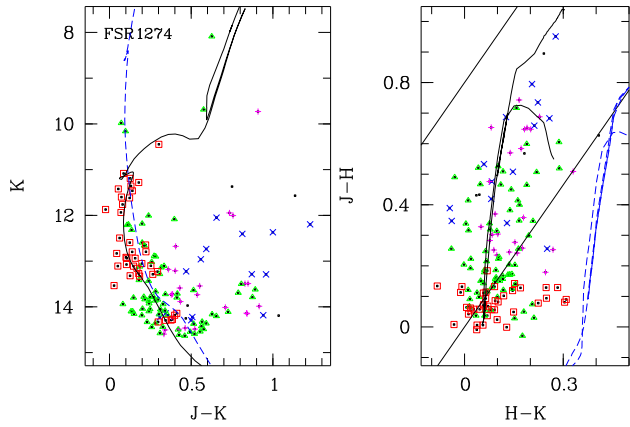


Figure C159. As Fig. C1 but for FSR 1274

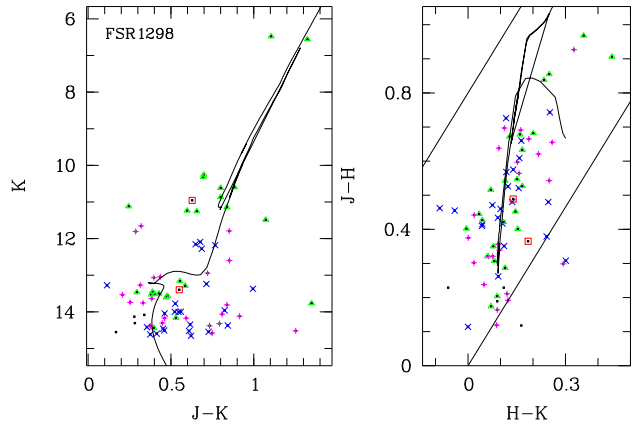
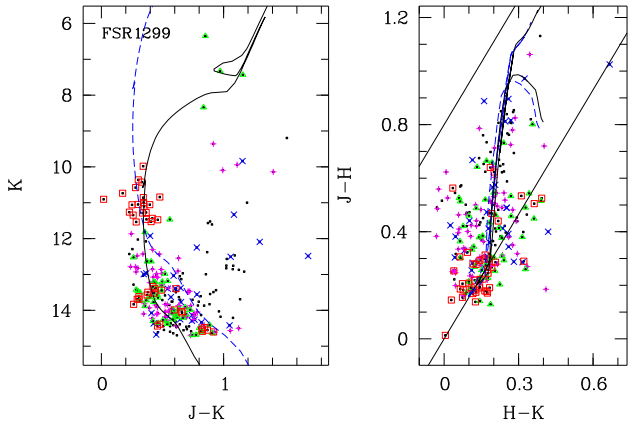
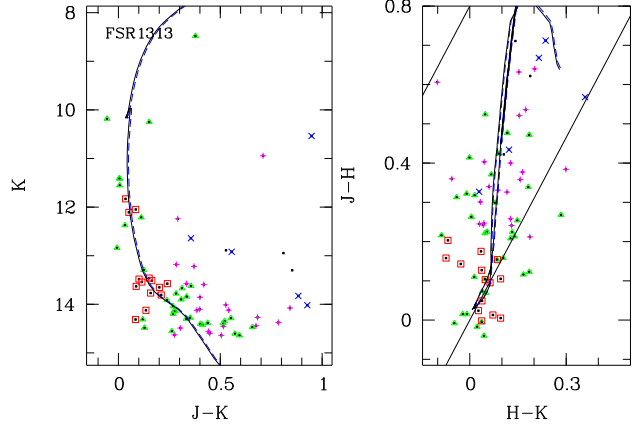


Figure C162. As Fig. C1 but for FSR 1298



**Figure C163.** As Fig. C1 but for FSR 1299



**Figure C166.** As Fig. C1 but for FSR 1313

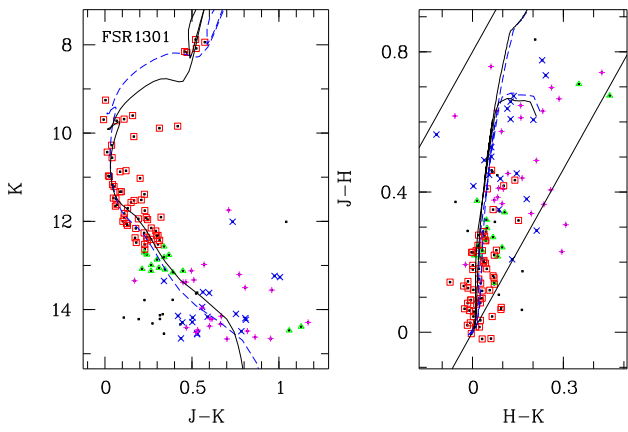


**Figure C164.** As Fig. C1 but for FSR 1301

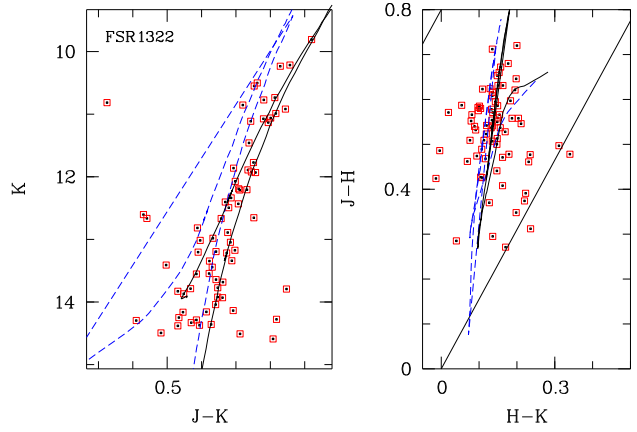


**Figure C167.** As Fig. C1 but for FSR 1322

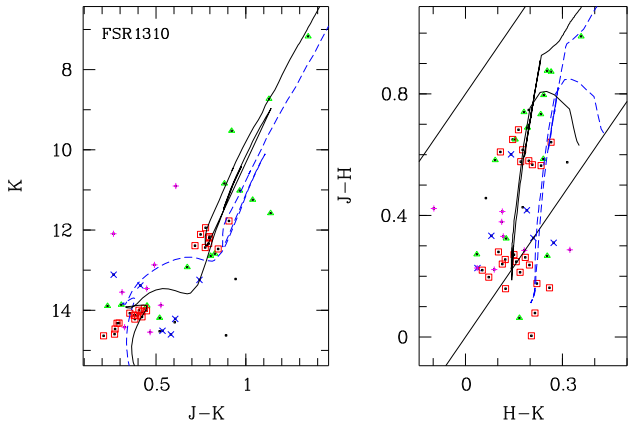


**Figure C165.** As Fig. C1 but for FSR 1310

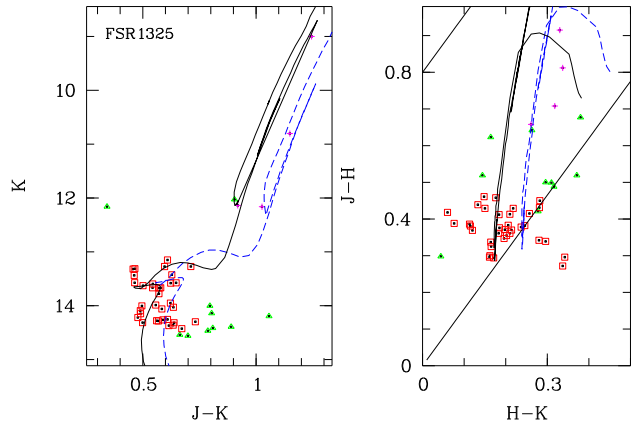


**Figure C168.** As Fig. C1 but for FSR 1325

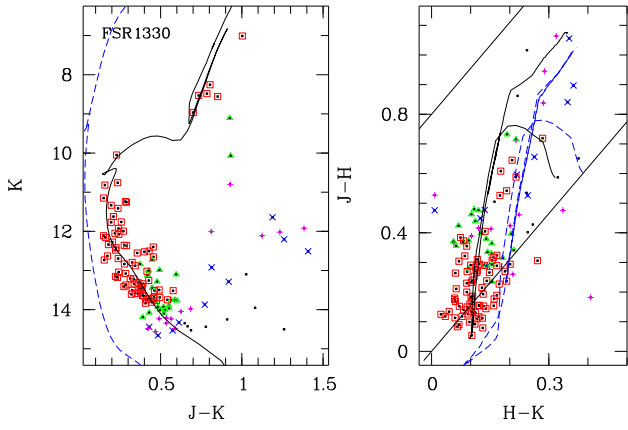


Figure C169. As Fig. C1 but for FSR 1330

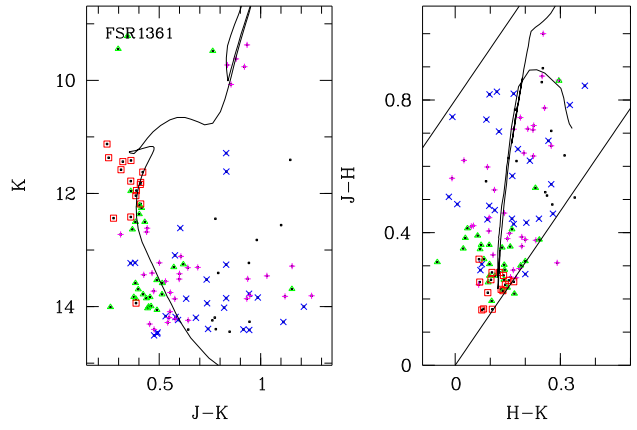


Figure C172. As Fig. C1 but for FSR 1361

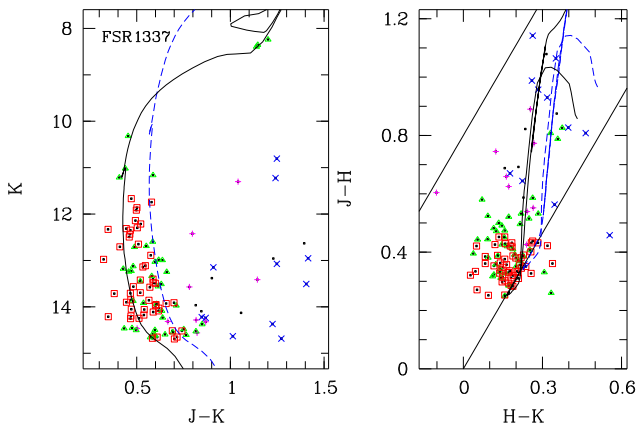


Figure C170. As Fig. C1 but for FSR 1337

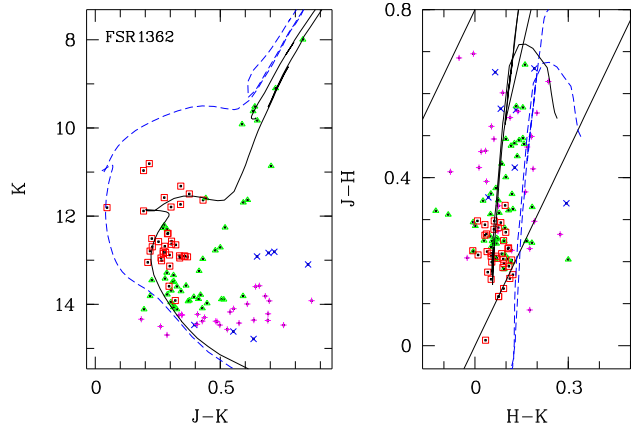


Figure C173. As Fig. C1 but for FSR 1362

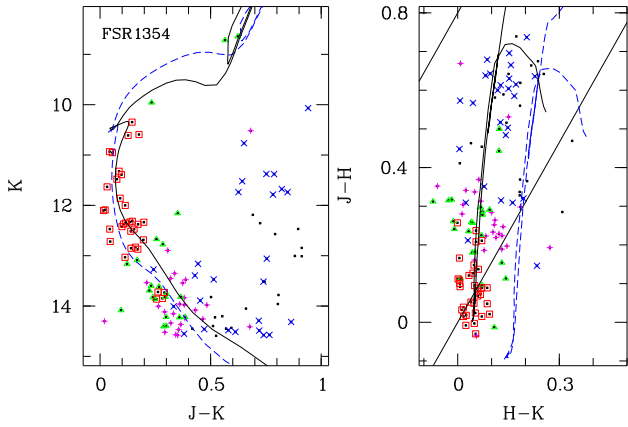


Figure C171. As Fig. C1 but for FSR 1354

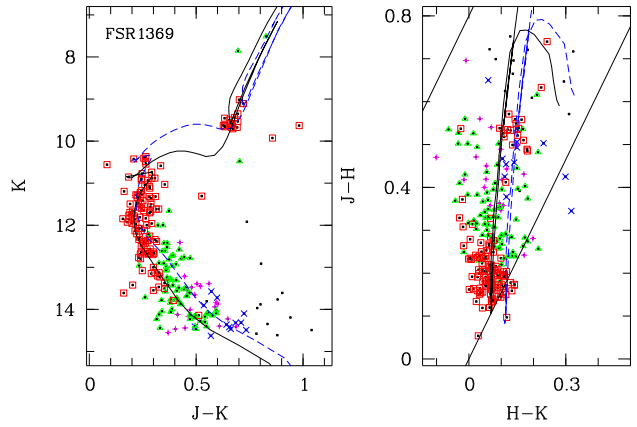
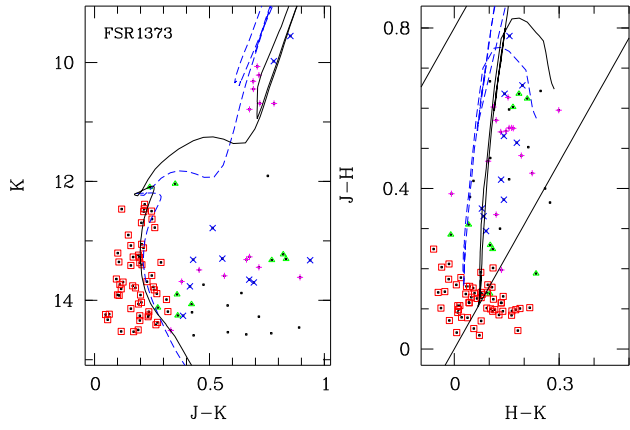
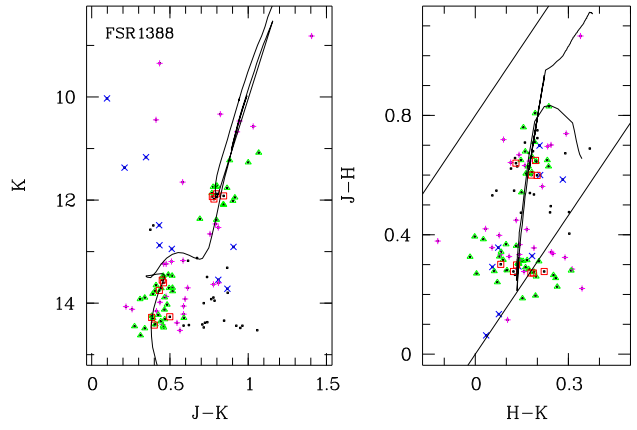


Figure C174. As Fig. C1 but for FSR 1369



**Figure C175.** As Fig. C1 but for FSR 1373



**Figure C178.** As Fig. C1 but for FSR 1388

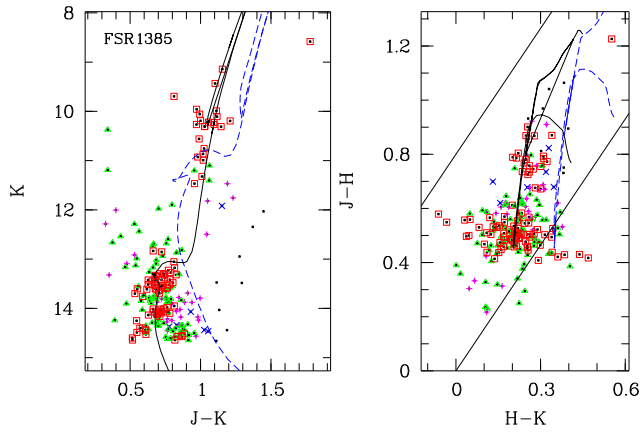


**Figure C176.** As Fig. C1 but for FSR 1385

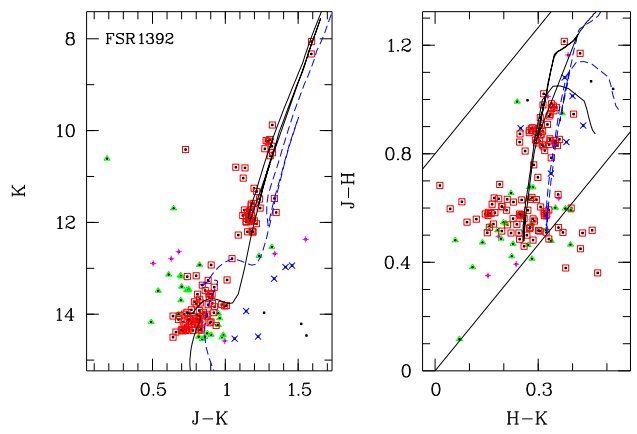


**Figure C179.** As Fig. C1 but for FSR 1392

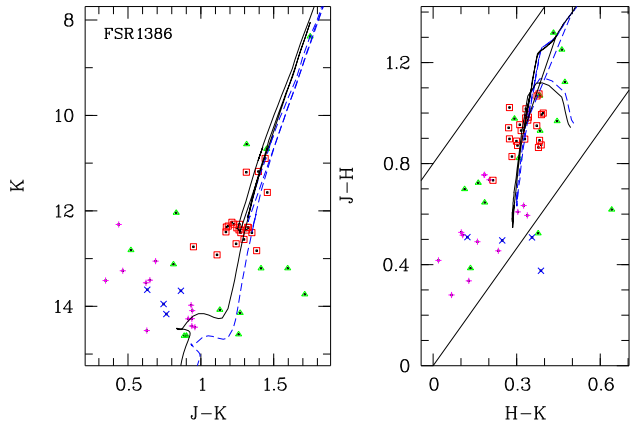


**Figure C177.** As Fig. C1 but for FSR 1386

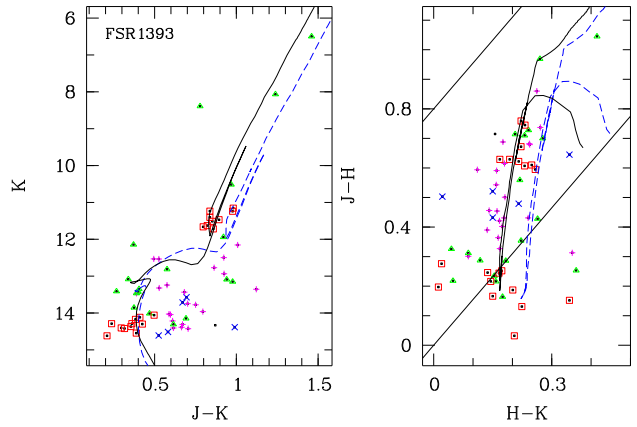


**Figure C180.** As Fig. C1 but for FSR 1393

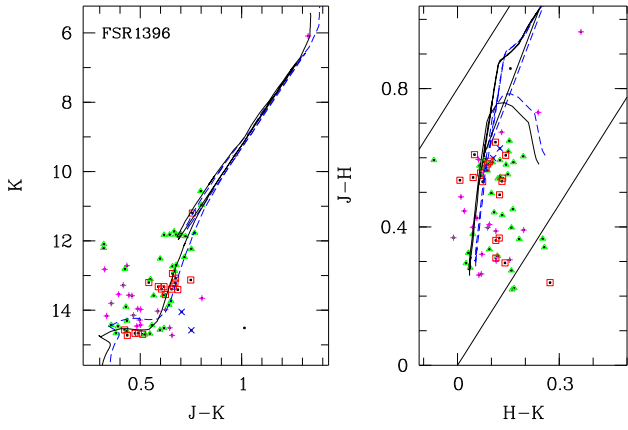


Figure C181. As Fig. C1 but for FSR 1396

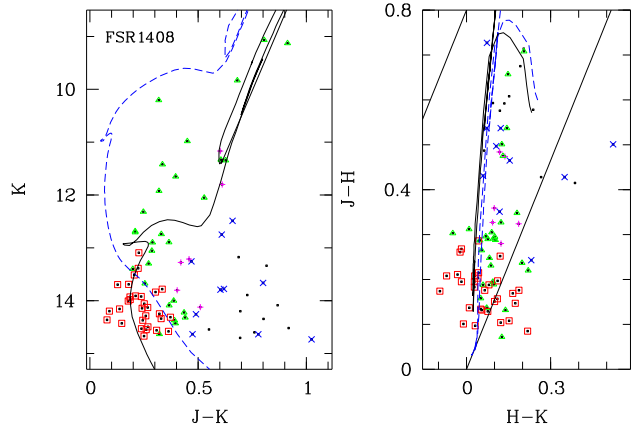


Figure C184. As Fig. C1 but for FSR 1408

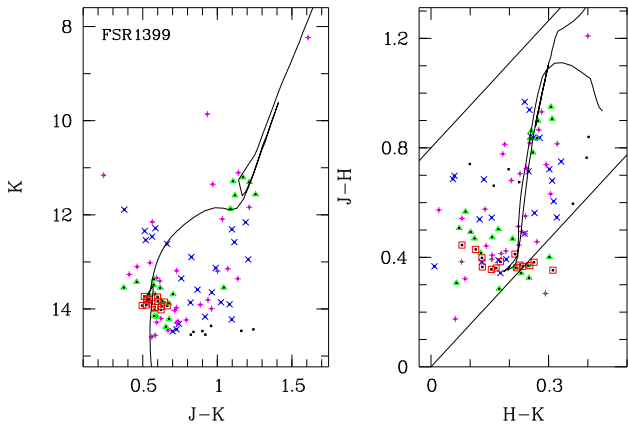


Figure C182. As Fig. C1 but for FSR 1399

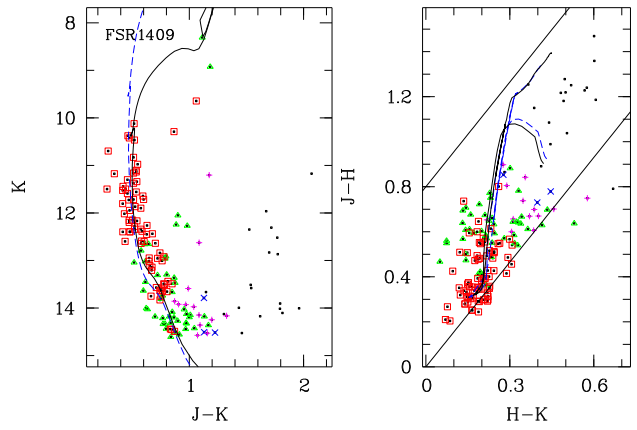


Figure C185. As Fig. C1 but for FSR 1409

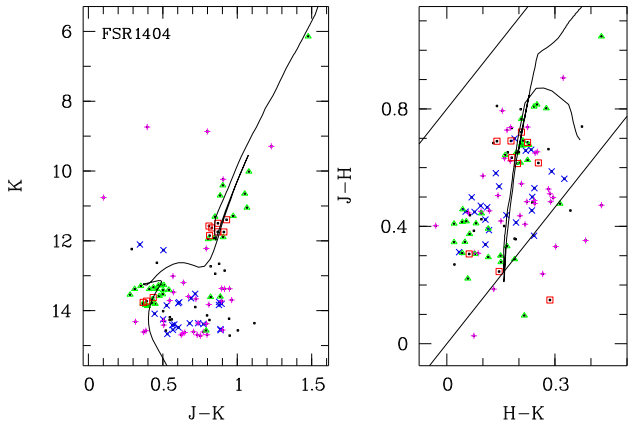


Figure C183. As Fig. C1 but for FSR 1404

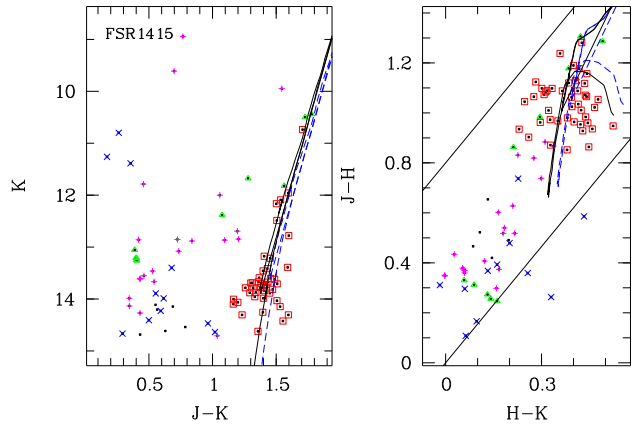
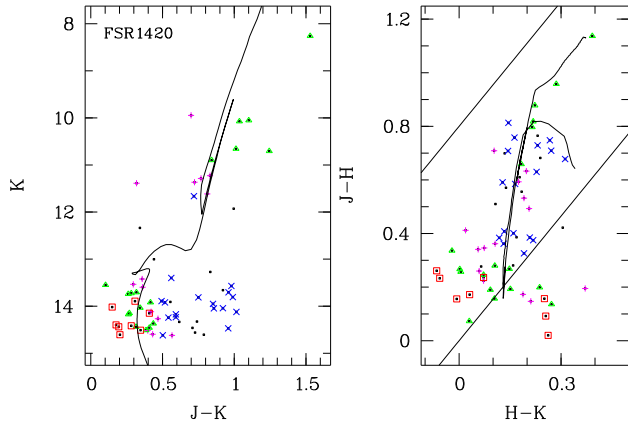
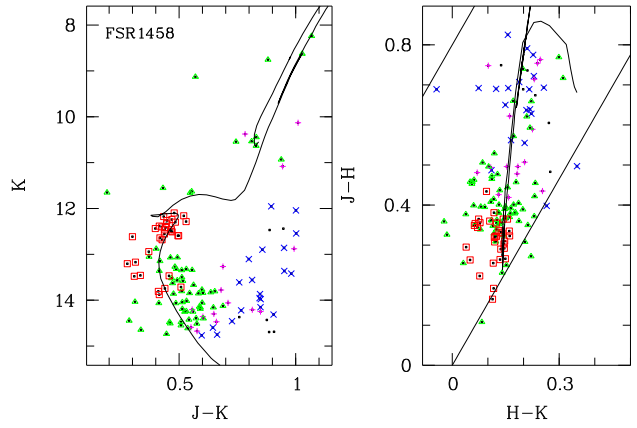


Figure C186. As Fig. C1 but for FSR 1415



**Figure C187.** As Fig. C1 but for FSR 1420



**Figure C190.** As Fig. C1 but for FSR 1458

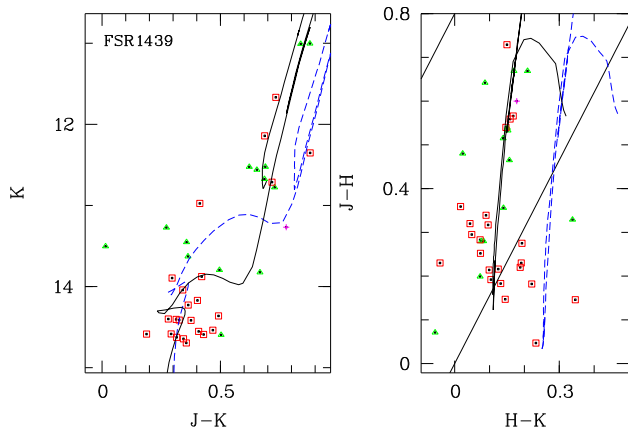


**Figure C188.** As Fig. C1 but for FSR 1439

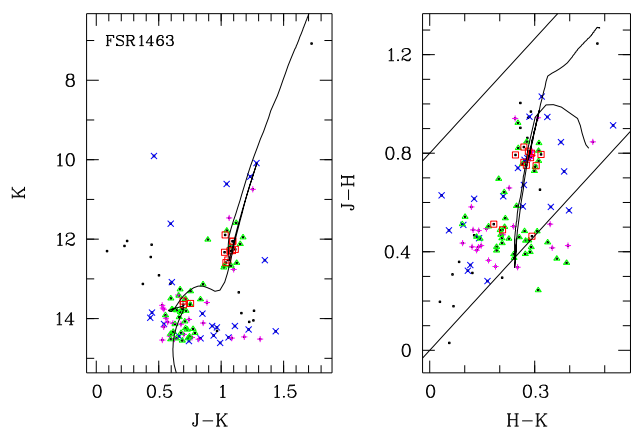


**Figure C191.** As Fig. C1 but for FSR 1463

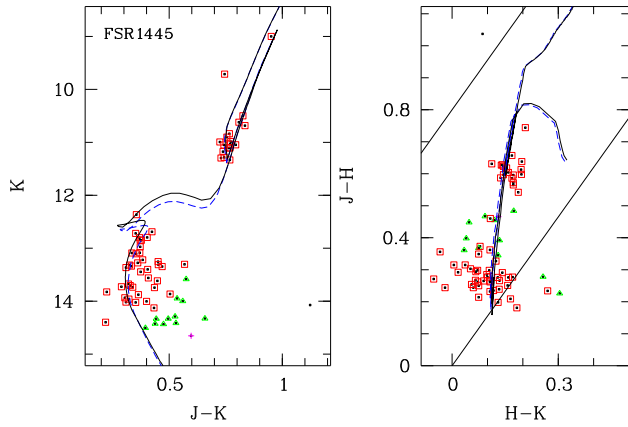


**Figure C189.** As Fig. C1 but for FSR 1445

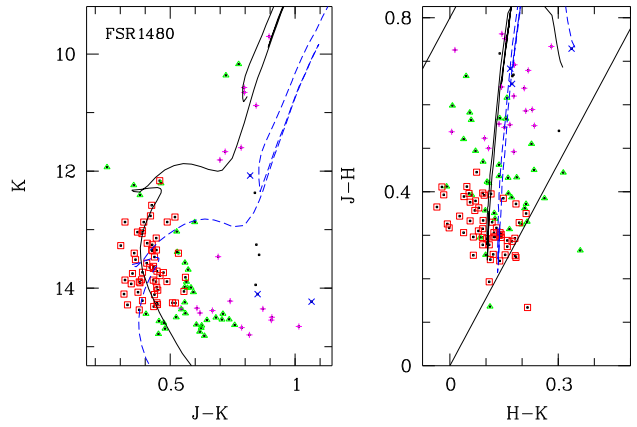


**Figure C192.** As Fig. C1 but for FSR 1480

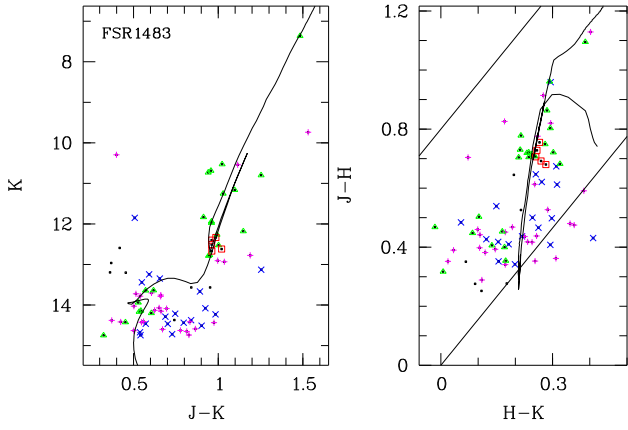


Figure C193. As Fig. C1 but for FSR 1483

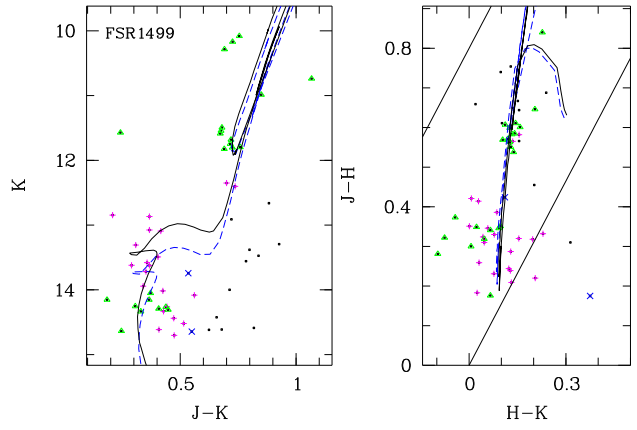


Figure C196. As Fig. C1 but for FSR 1499

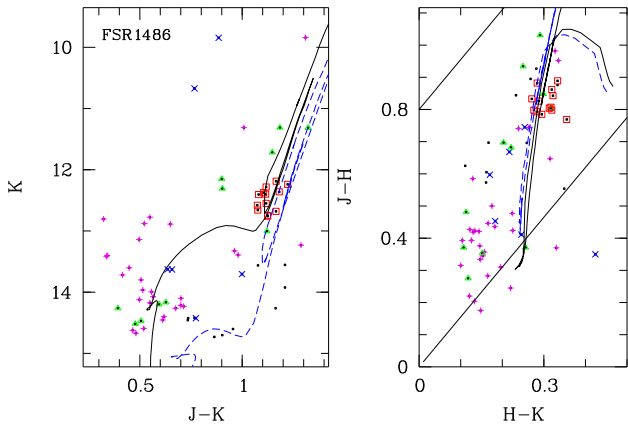


Figure C194. As Fig. C1 but for FSR 1486

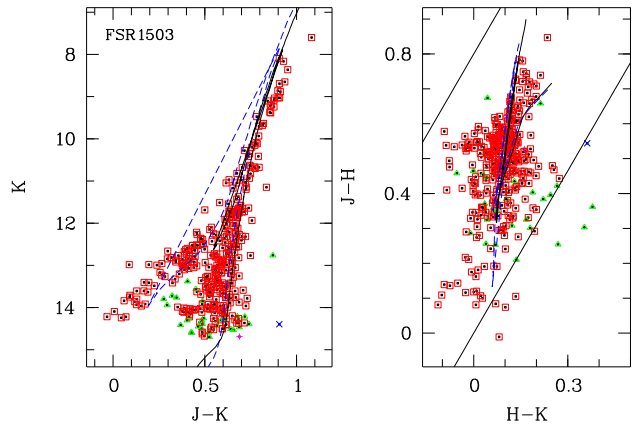


Figure C197. As Fig. C1 but for FSR 1503

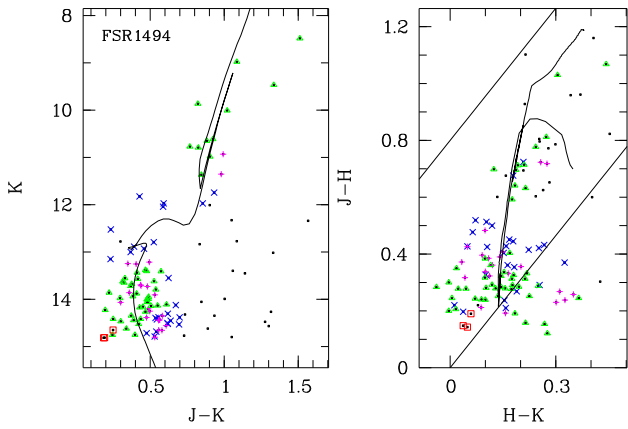


Figure C195. As Fig. C1 but for FSR 1494

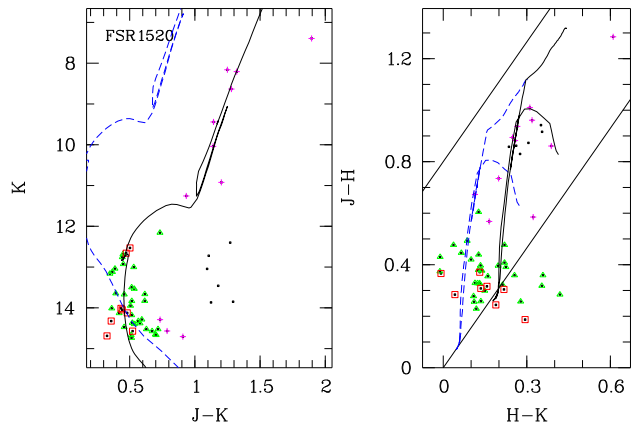
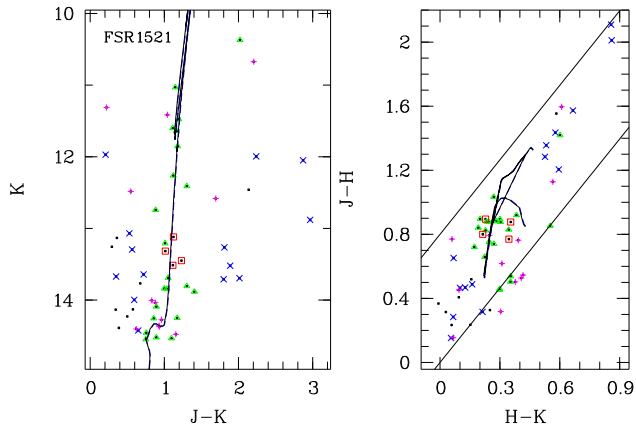
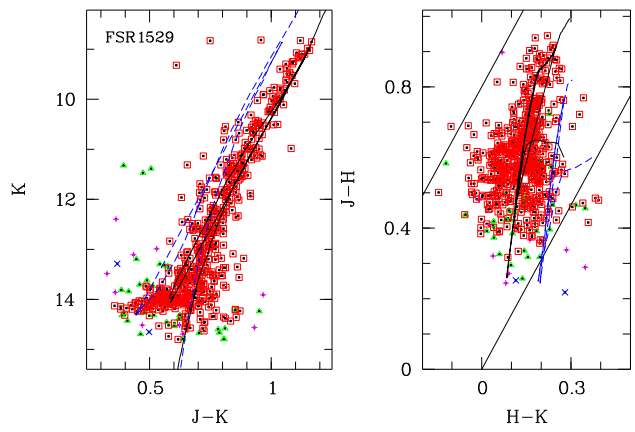


Figure C198. As Fig. C1 but for FSR 1520



**Figure C199.** As Fig. C1 but for FSR 1521



**Figure C202.** As Fig. C1 but for FSR 1529

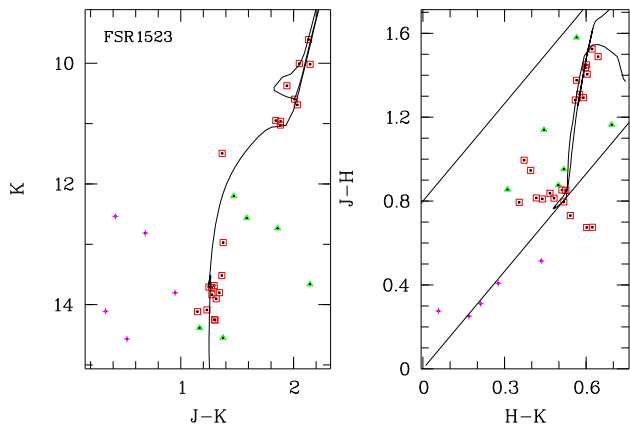


**Figure C200.** As Fig. C1 but for FSR 1523

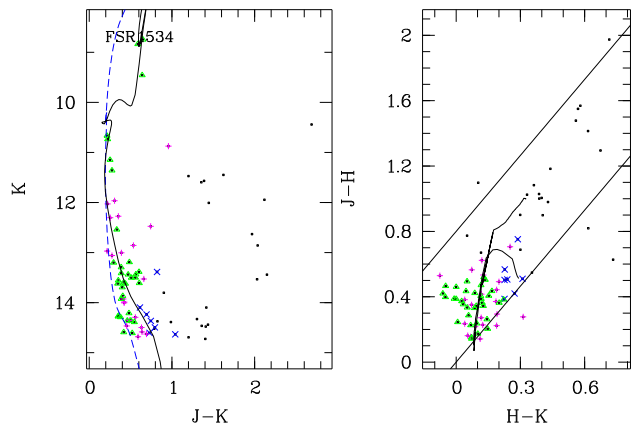


**Figure C203.** As Fig. C1 but for FSR 1534

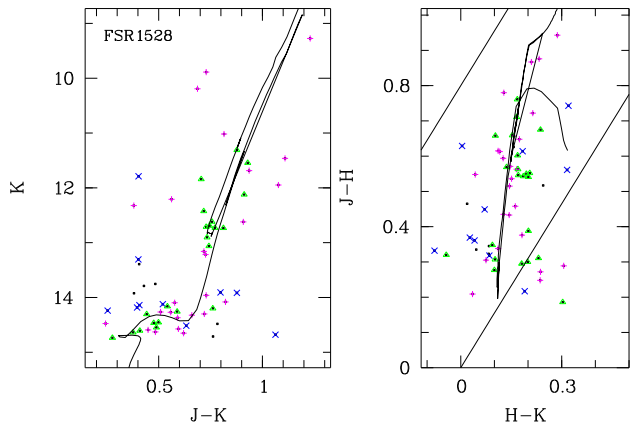


**Figure C201.** As Fig. C1 but for FSR 1528

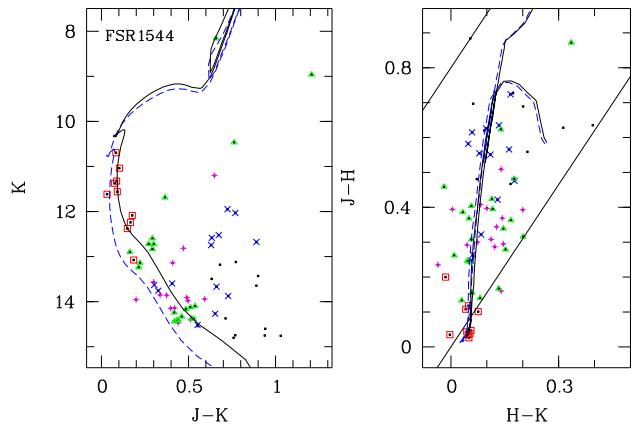


**Figure C204.** As Fig. C1 but for FSR 1544

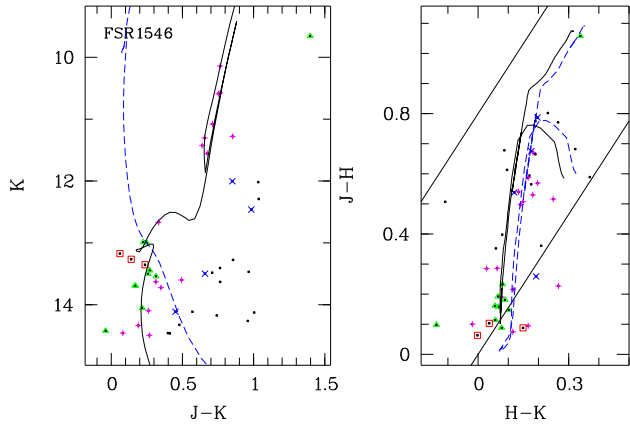


Figure C205. As Fig. C1 but for FSR 1546

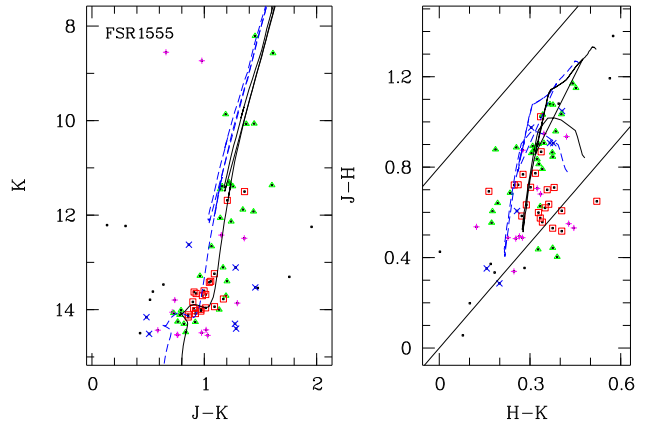


Figure C208. As Fig. C1 but for FSR 1555

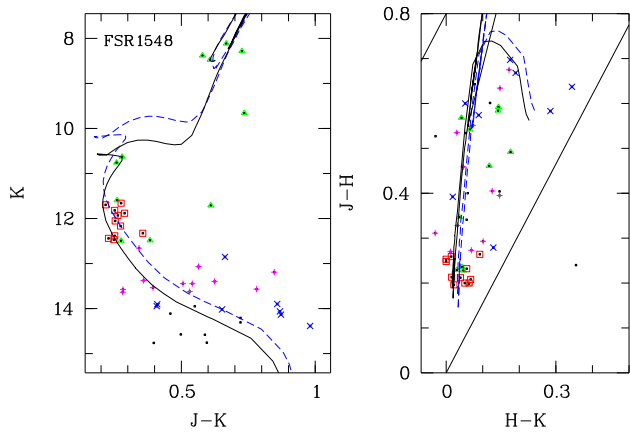


Figure C206. As Fig. C1 but for FSR 1548

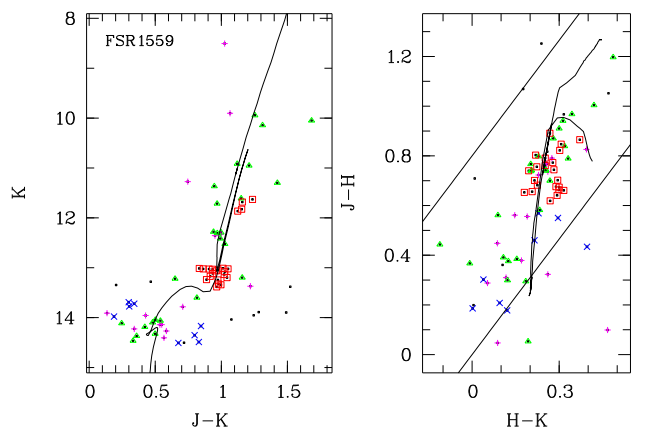


Figure C209. As Fig. C1 but for FSR 1559

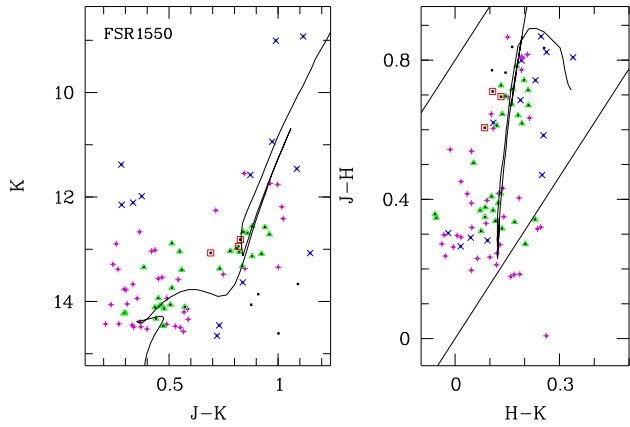


Figure C207. As Fig. C1 but for FSR 1550

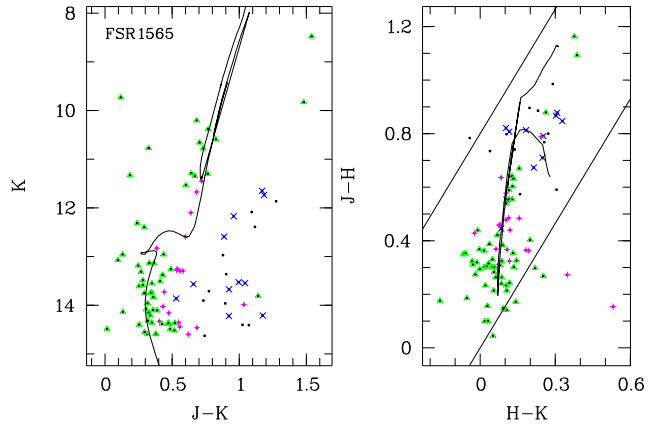


Figure C210. As Fig. C1 but for FSR 1565

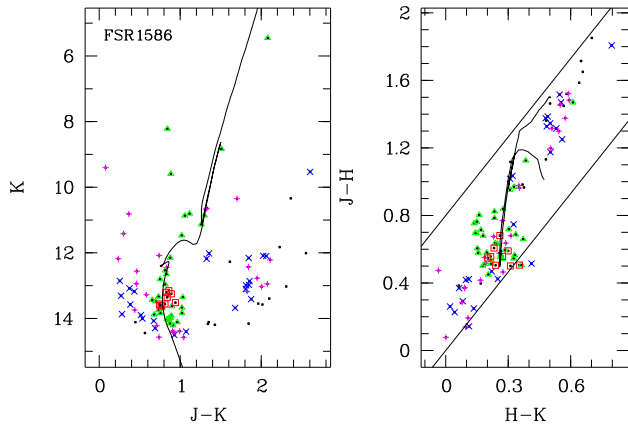


Figure C211. As Fig. C1 but for FSR 1586

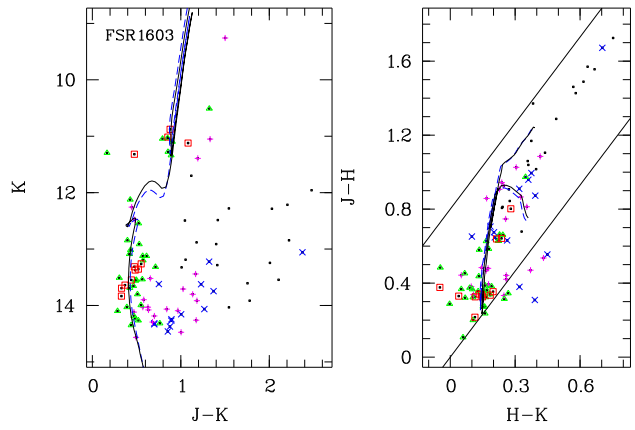


Figure C214. As Fig. C1 but for FSR 1603

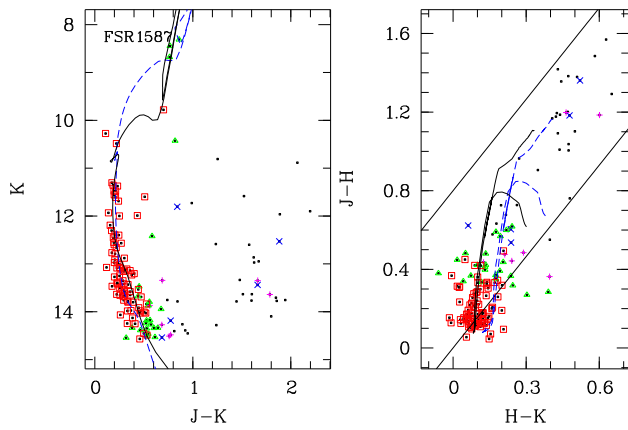


Figure C212. As Fig. C1 but for FSR 1587

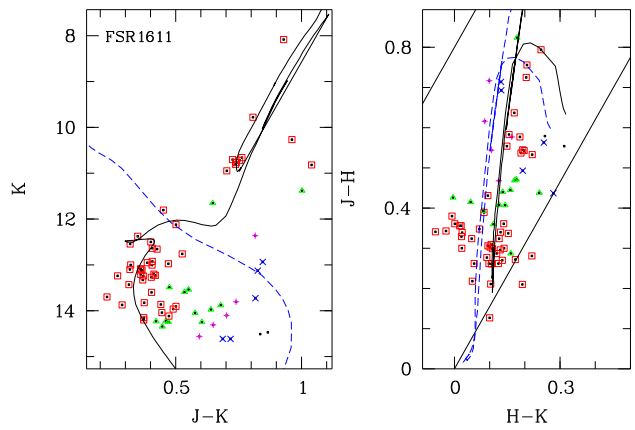


Figure C215. As Fig. C1 but for FSR 1611

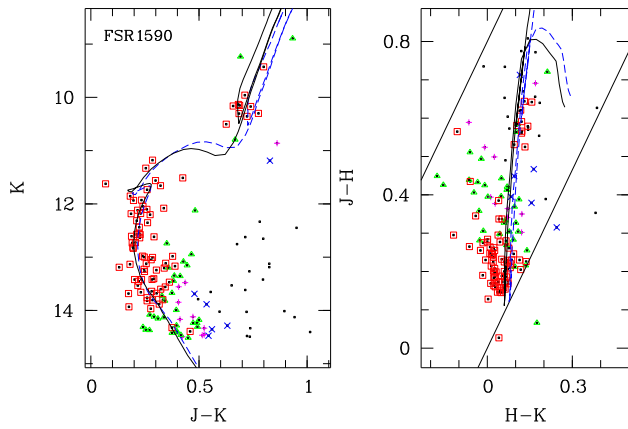


Figure C213. As Fig. C1 but for FSR 1590

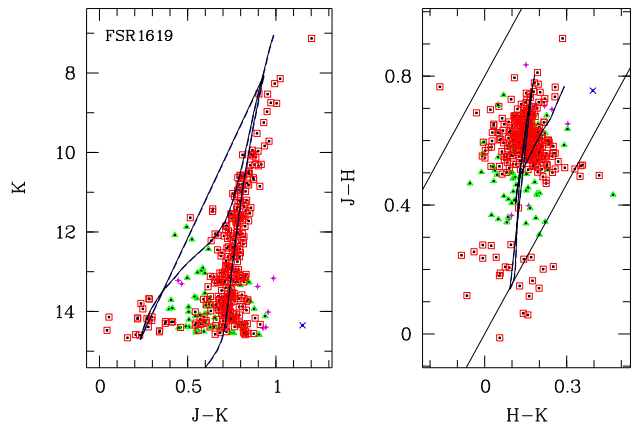


Figure C216. As Fig. C1 but for FSR 1619

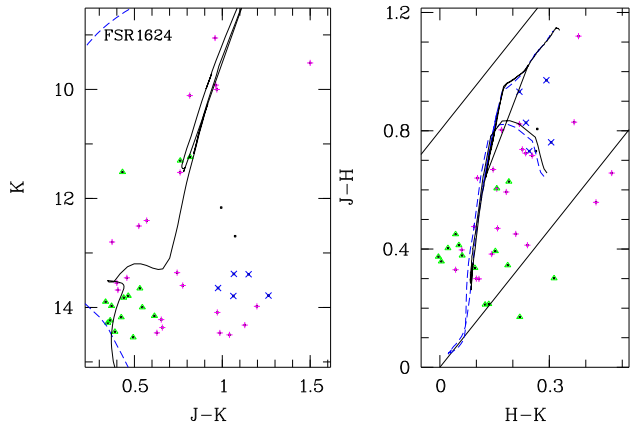


Figure C217. As Fig. C1 but for FSR 1624

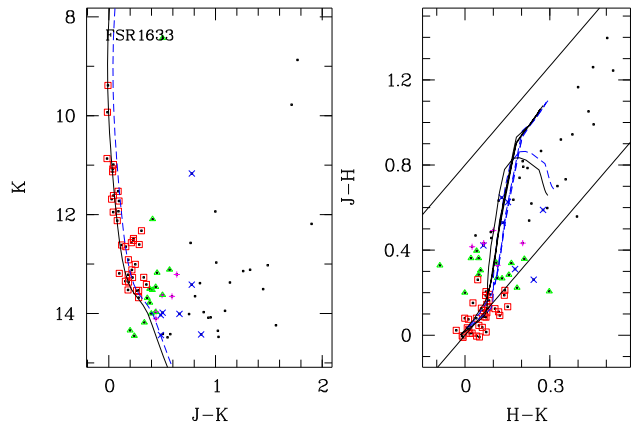


Figure C220. As Fig. C1 but for FSR 1633

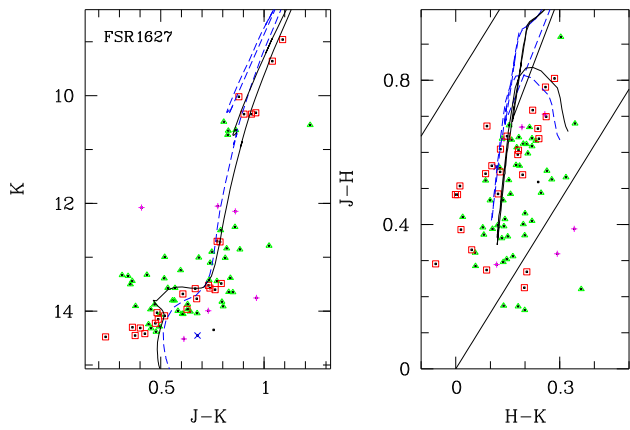


Figure C218. As Fig. C1 but for FSR 1627

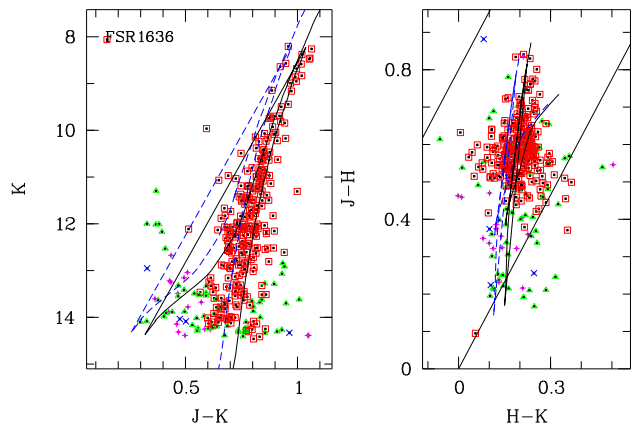


Figure C221. As Fig. C1 but for FSR 1636

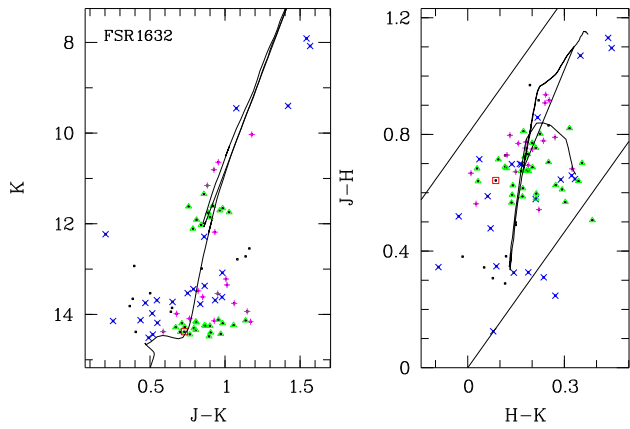


Figure C219. As Fig. C1 but for FSR 1632

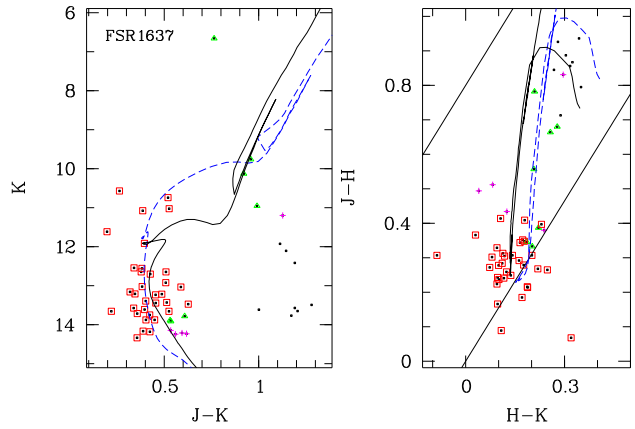


Figure C222. As Fig. C1 but for FSR 1637

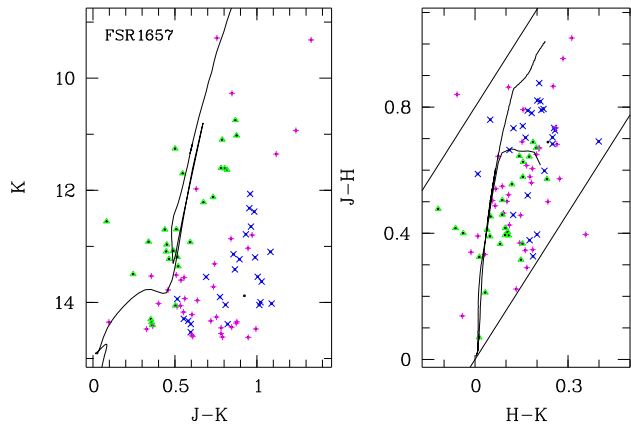


Figure C223. As Fig. C1 but for FSR 1657

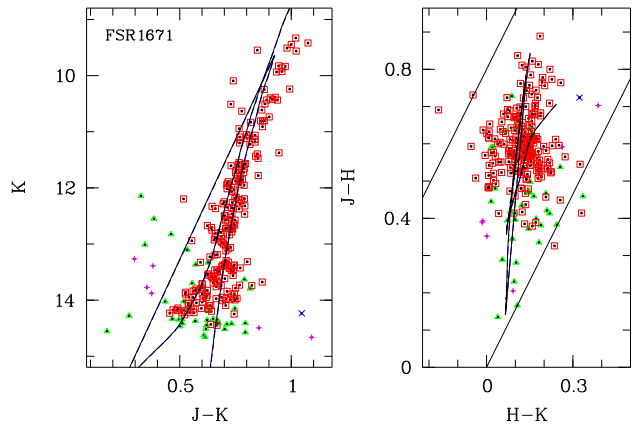


Figure C226. As Fig. C1 but for FSR 1671

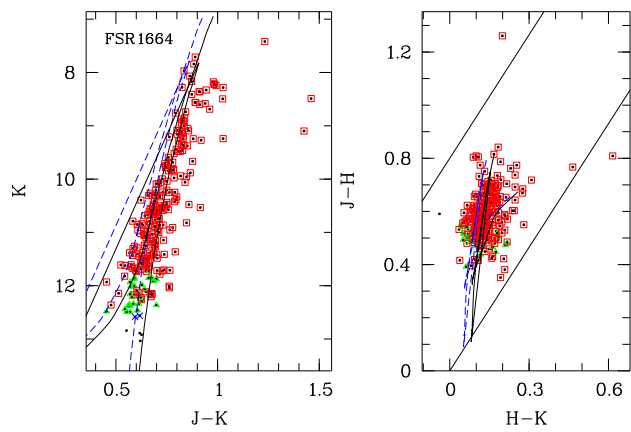


Figure C224. As Fig. C1 but for FSR 1664

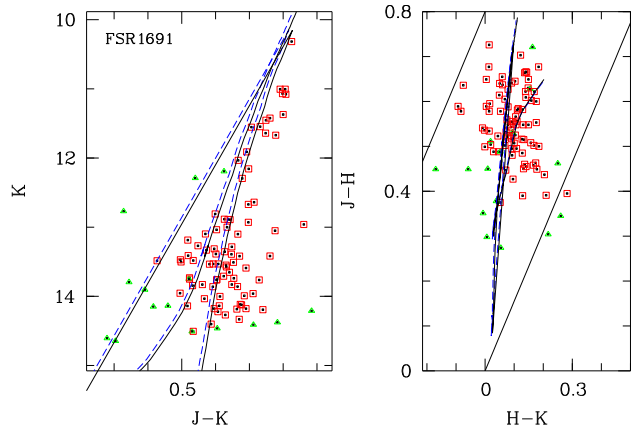


Figure C227. As Fig. C1 but for FSR 1691

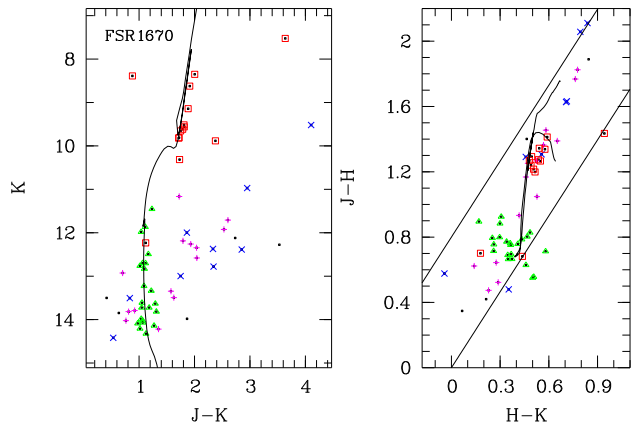


Figure C225. As Fig. C1 but for FSR 1670

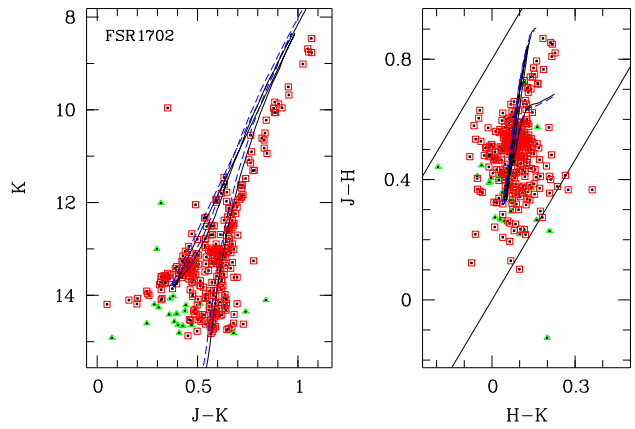


Figure C228. As Fig. C1 but for FSR 1702

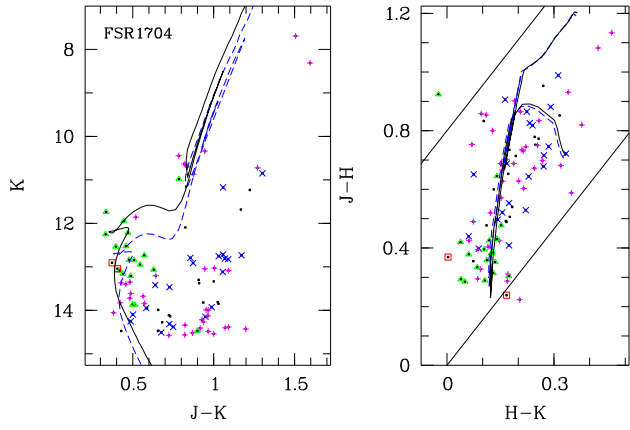


Figure C229. As Fig. C1 but for FSR 1704

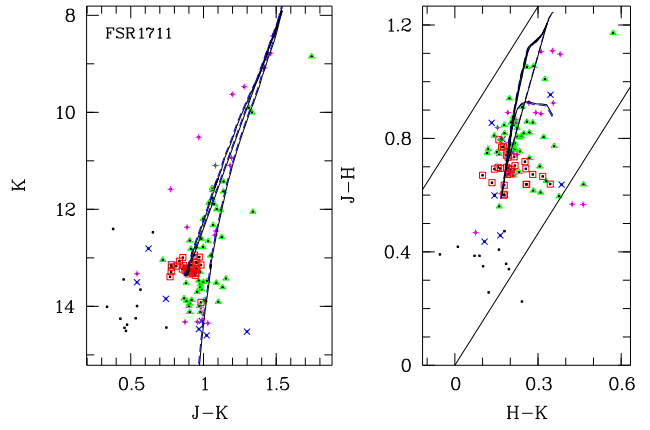


Figure C232. As Fig. C1 but for FSR 1711

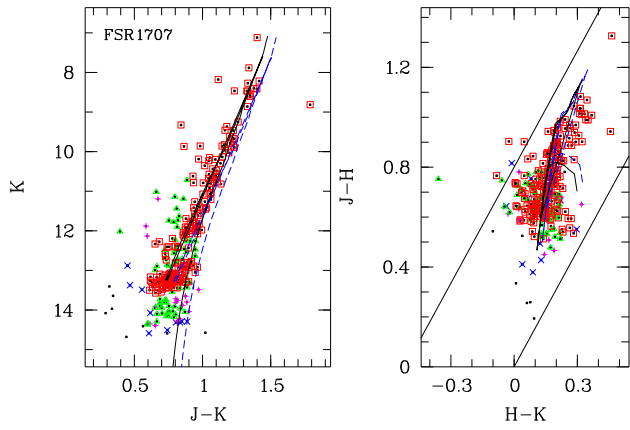


Figure C230. As Fig. C1 but for FSR 1707

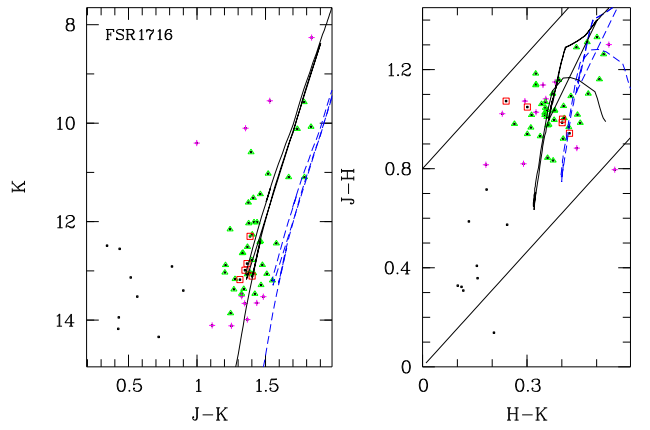


Figure C233. As Fig. C1 but for FSR 1716

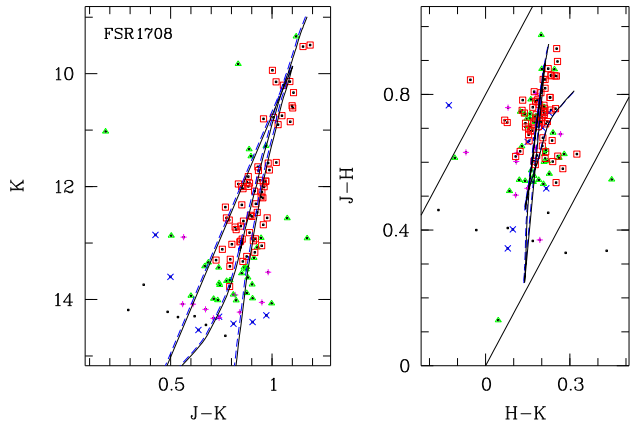


Figure C231. As Fig. C1 but for FSR 1708

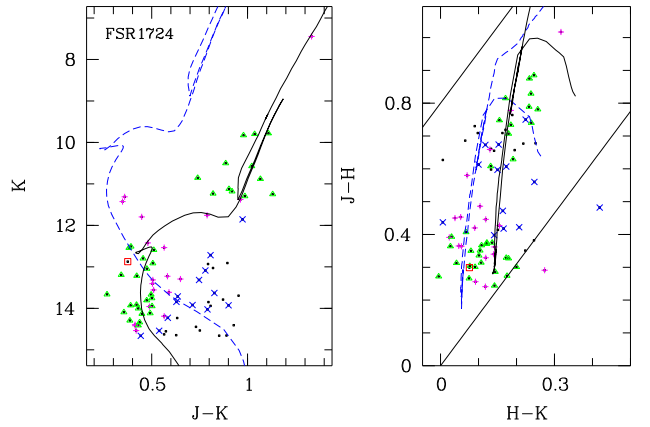
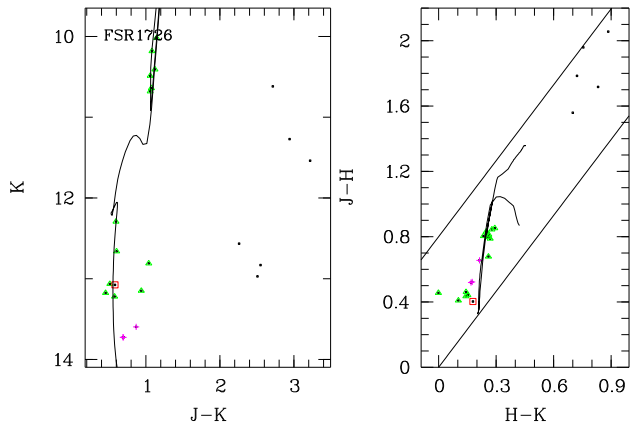
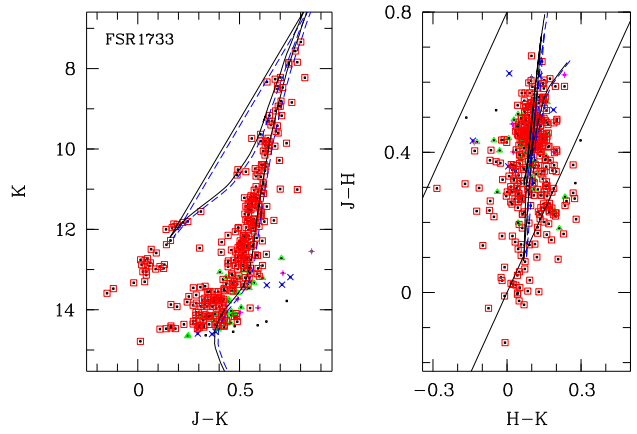


Figure C234. As Fig. C1 but for FSR 1724



**Figure C235.** As Fig. C1 but for FSR 1726



**Figure C238.** As Fig. C1 but for FSR 1733

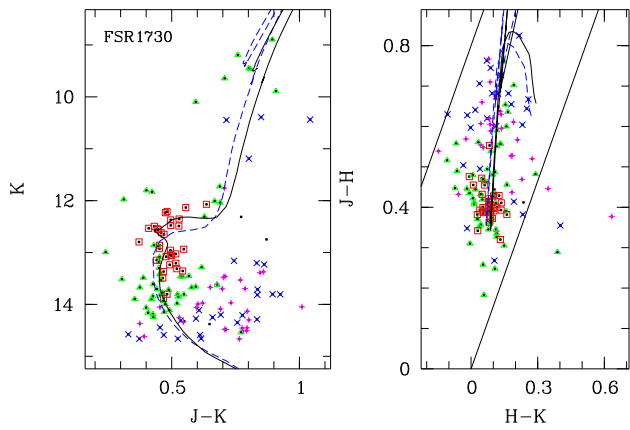


**Figure C236.** As Fig. C1 but for FSR 1730

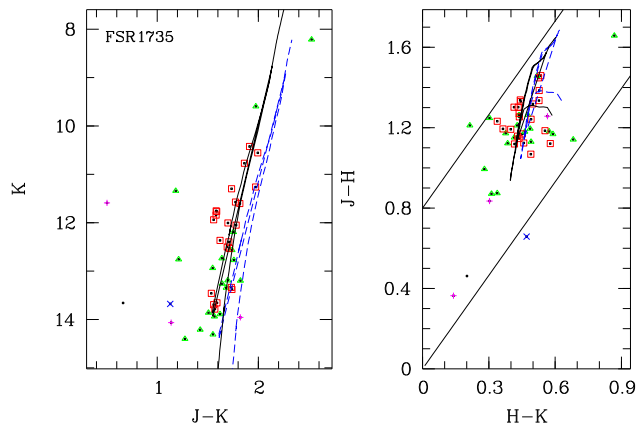


**Figure C239.** As Fig. C1 but for FSR 1735

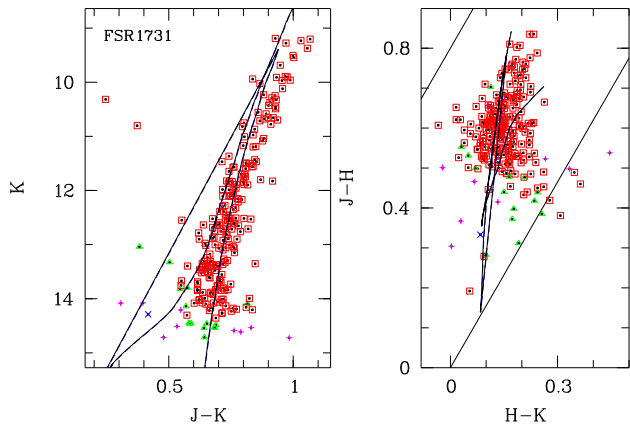


**Figure C237.** As Fig. C1 but for FSR 1731

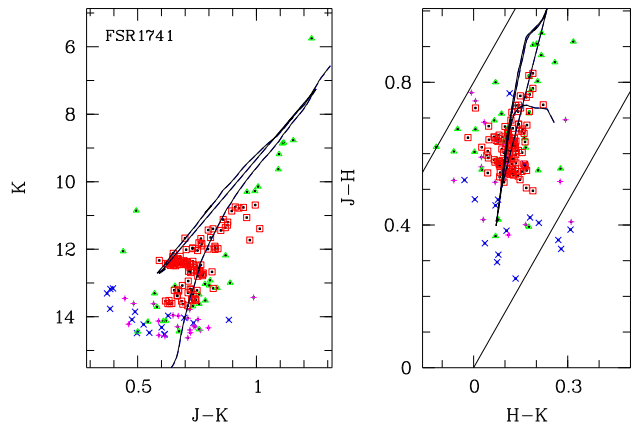


**Figure C240.** As Fig. C1 but for FSR 1741

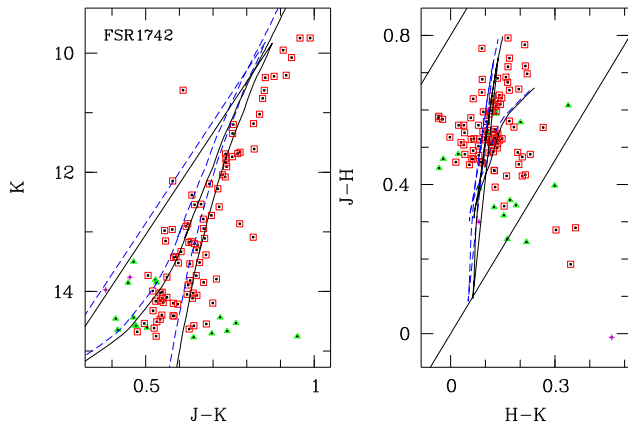


Figure C241. As Fig. C1 but for FSR 1742

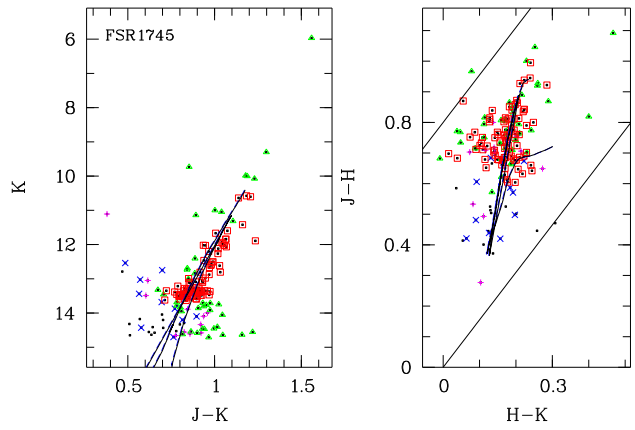


Figure C244. As Fig. C1 but for FSR 1745

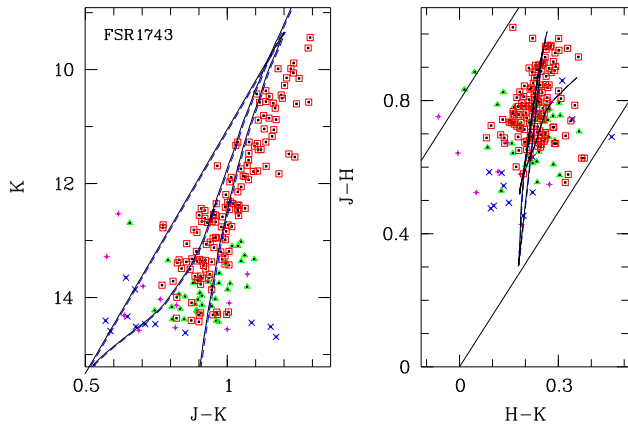


Figure C242. As Fig. C1 but for FSR 1743

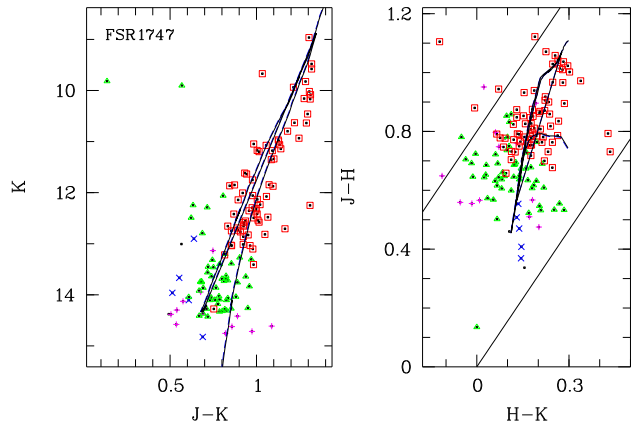


Figure C245. As Fig. C1 but for FSR 1747

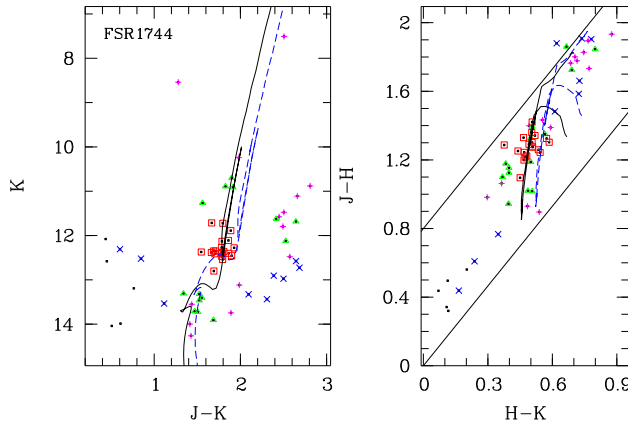


Figure C243. As Fig. C1 but for FSR 1744

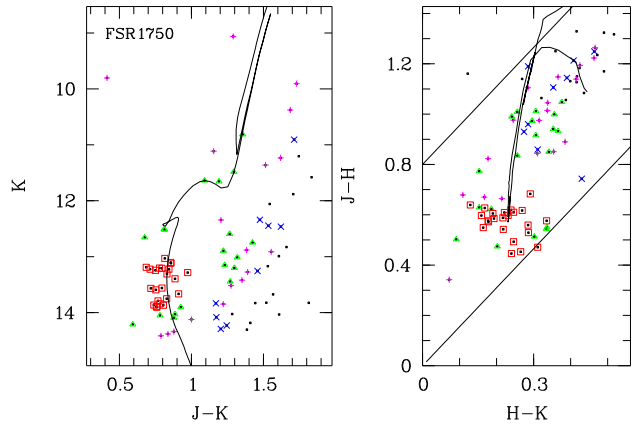


Figure C246. As Fig. C1 but for FSR 1750

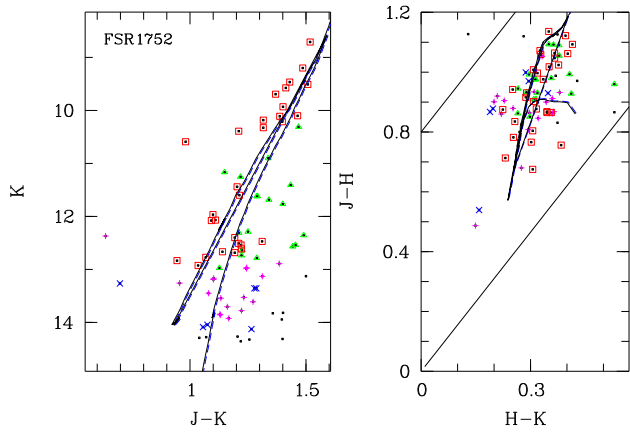


Figure C247. As Fig. C1 but for FSR 1752

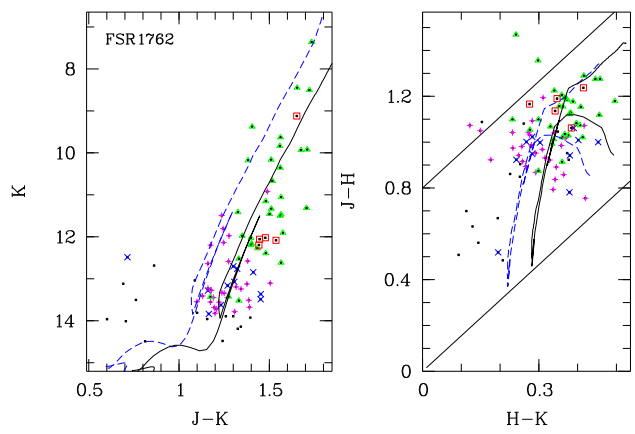


Figure C250. As Fig. C1 but for FSR 1762

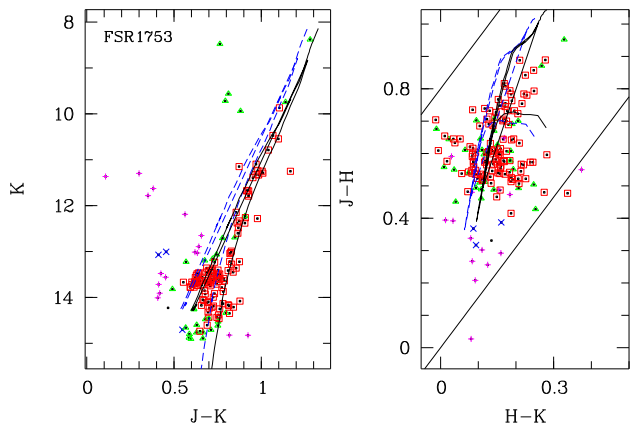


Figure C248. As Fig. C1 but for FSR 1753

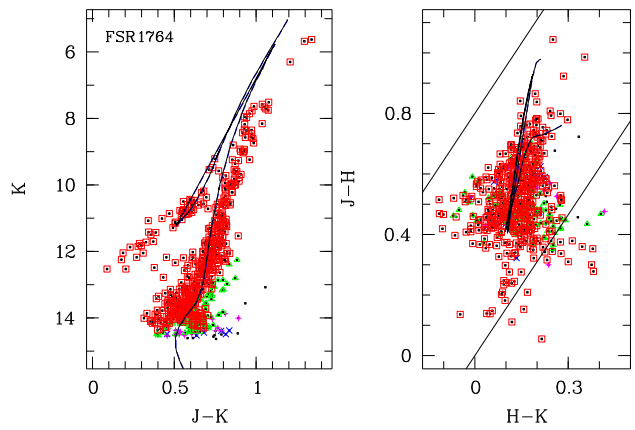


Figure C251. As Fig. C1 but for FSR 1764

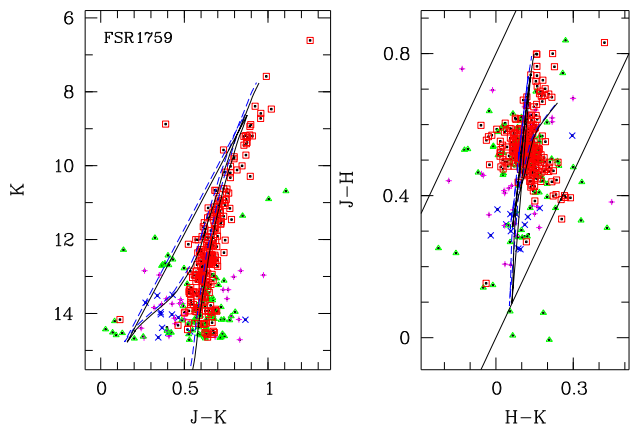


Figure C249. As Fig. C1 but for FSR 1759

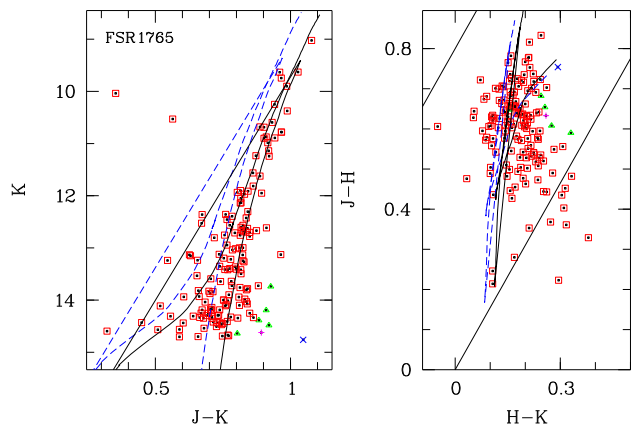


Figure C252. As Fig. C1 but for FSR 1765

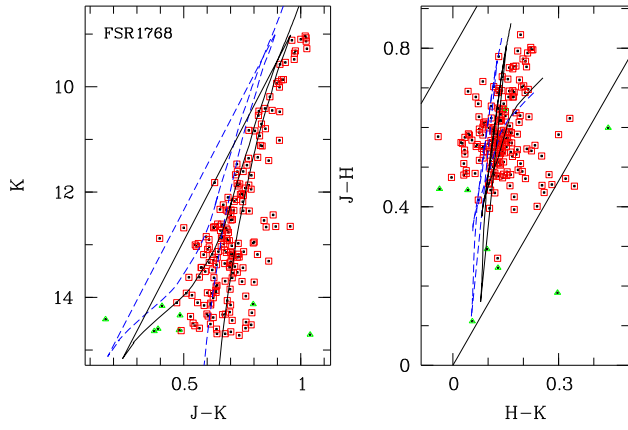


Figure C253. As Fig. C1 but for FSR 1768

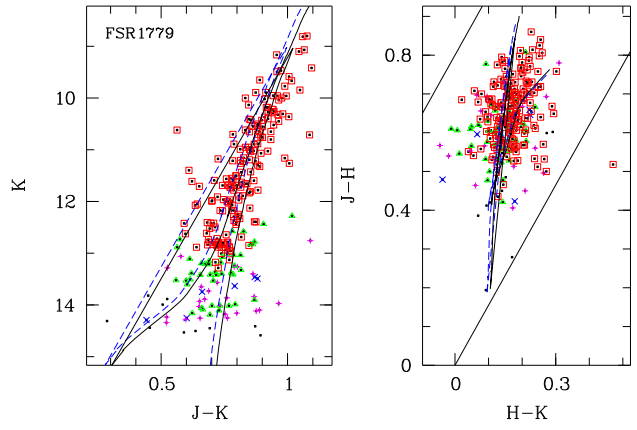


Figure C256. As Fig. C1 but for FSR 1779

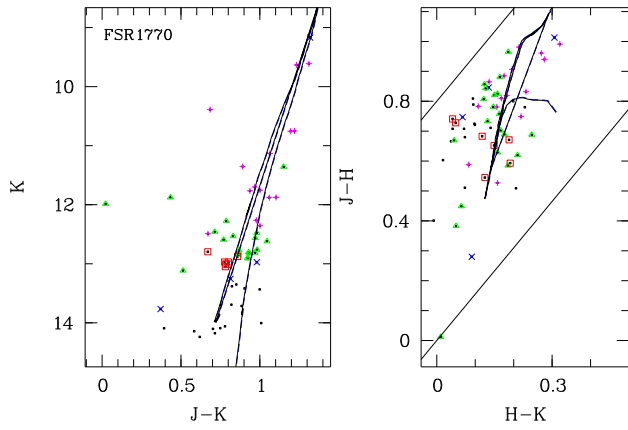


Figure C254. As Fig. C1 but for FSR 1770

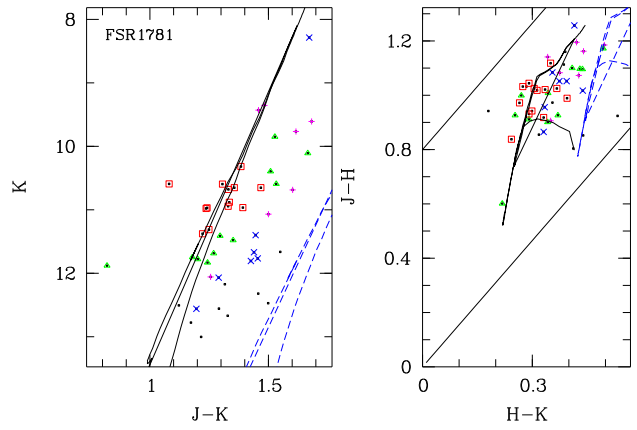


Figure C257. As Fig. C1 but for FSR 1781

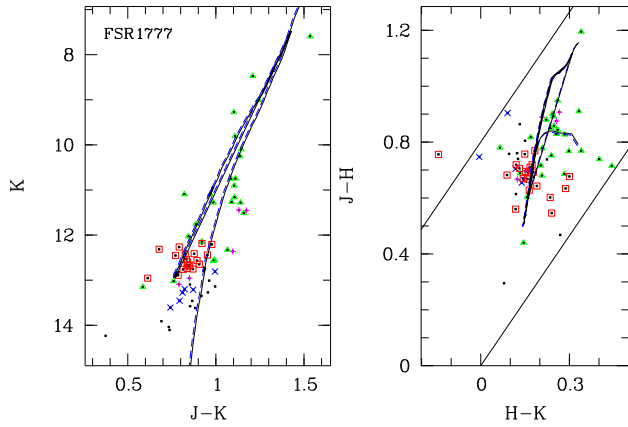


Figure C255. As Fig. C1 but for FSR 1777

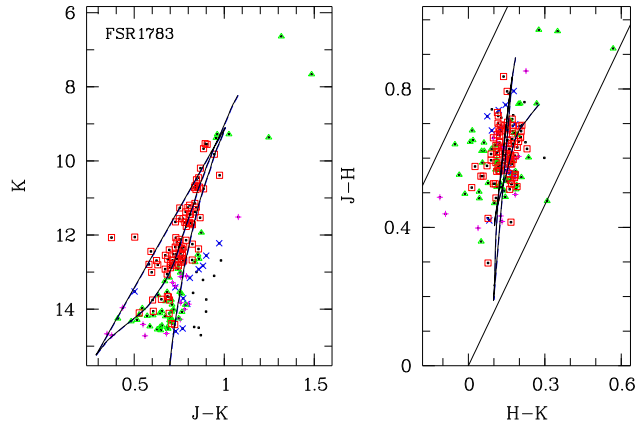
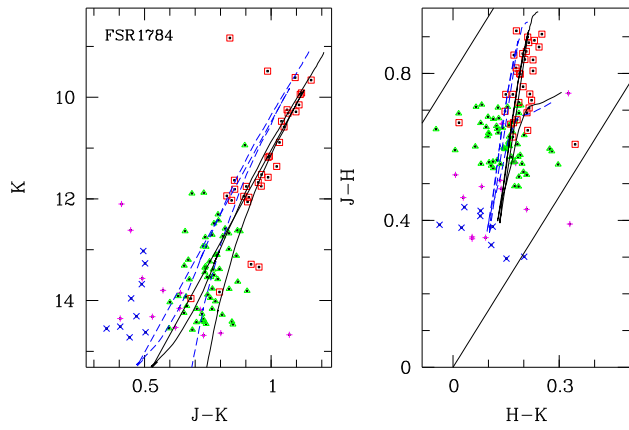
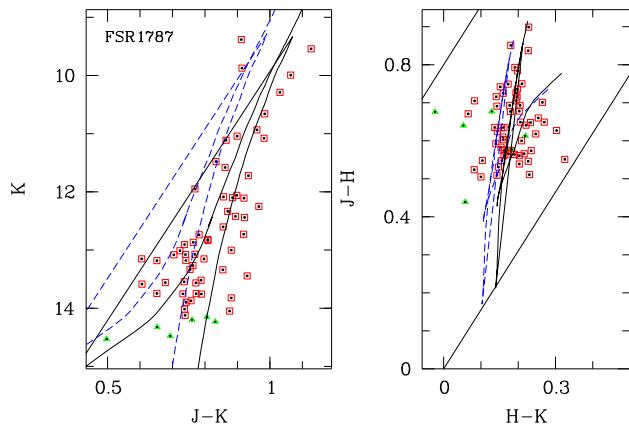


Figure C258. As Fig. C1 but for FSR 1783



**Figure C259.** As Fig. C1 but for FSR 1784



**Figure C260.** As Fig. C1 but for FSR 1787

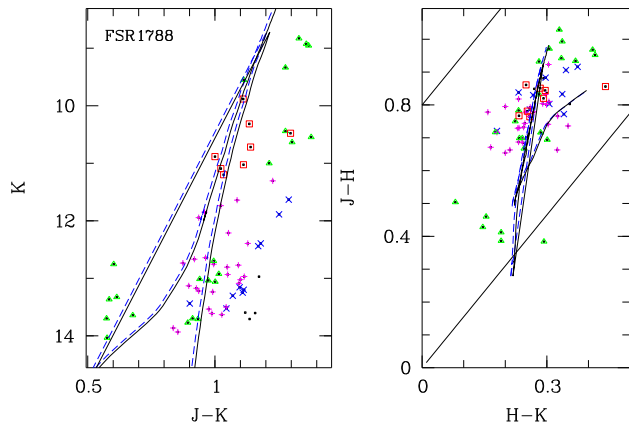


**Figure C261.** As Fig. C1 but for FSR 1788